Analysis of blastomeres of bovine embryos during genome activation by evaluation of single-cell RNA sequencing data

von Ilaria Lavagi

Inaugural-Dissertation zur Erlangung der Doktorwürde
(Dr. rer. biol. vet.)
der Tierärztlichen Fakultät der Ludwig-Maximilians-
Universität München

Analysis of blastomeres of bovine embryos during genome activation by evaluation of single-cell RNA sequencing data

von Ilaria Lavagi

aus Mailand

München 2018

Aus demVeterinärwissenschaftlichen Department der
Tierärztlichen Fakultät der Ludwig-Maximilians-Universität München

Lehrstuhl für Molekulare Tierzucht und Biotechnologie

Arbeit angefertigt unter der Leitung von:
Univ.-Prof. Dr. Eckhard Wolf

Angefertigt im
Laboratorium für Funktionale Genomanalyse (LAFUGA)
Abteilung Genomics
Genzentrum der Ludwig-Maximilians-Universität München

Mentor: Dr. Helmut Blum

Gedruckt mit Genehmigung der Tierärztlichen Fakultät
der
Ludwig-Maximilians-Universität München

Dekan:	Univ.-Prof. Dr. Reinhard K. Straubinger
Berichterstatter:	Univ.-Prof. Dr. Eckhard Wolf
Korreferent/en:	Priv. –Doz. Dr. Wolfram Petzl

Tag der Promotion: 27. Juli 2018

Contents

Abbreviations

rRNA	Ribosomal RNA
EGA	Embryonic Genome Activation
RNA-seq	RNA-sequencing
Dnmts	DNA methyltransferases
TE	Trophectoderm
ICM	Inner Cell Mass
PE	Primitive Endoderm
EP	Pluripotent Epiblast
qPCR	Quantitative Real-Time PCR
WISH	Whole-Mount *in situ* Hybridization
MET	Maternal-to-Embryonic Transition
scRNA	Single-cell sequencing
hpf	Hours Post Fertilization
SCRB-Seq	Single-cell RNA Barcoding and Sequencing
UMIs	Unique Molecular Identifier(s)
DATs	Differentially Abundant Transcript(s)
K	Cluster
SC3	Single-cell Consensus Clustering
M3Drop	Michaelis-Menten Modelling of Dropouts
AUROC	Area under the ROC Curve
GO	Gene Ontology
LDA	Latent Dirichlet Allocation
IVM	*in vitro* Maturation
IVF	*in vitro* Fertilization
COC(s)	Cumulus-Oocyte Complex(es)
MPM	Modified Parker Medium
LH	Luteinising Hormone
FSH	Follicle-Stimulating Hormone
ECS	Estrous Cow Serum
SOF	Synthetic Oviductal Fluid
THP	TALP-HEPES-PVP
ZP	Zona Pellucida
FCS	Foetal Calf Serum

Introduction

Bovine Embryos as Model System

Direct analysis of human embryos is restricted for ethical reasons and in many countries prohibited by specific regulations, such as the "German embryo protection law" in Germany. For this reason, embryos from animal species are used as models for studying early human development. The most widely used organism for this purpose is mouse, as mouse and human embryo implantation are very similar [1]. However, as interactions between the embryo and the corpus luteum are very similar between human and bovine, the bovine animal represents a better model than mouse to study biochemical and maternal and paternal regulatory processes in human [1].

Cell Cleavage and Cell Stage

After fertilization the newly formed zygote starts dividing; cell cleavage is regulated by cell cycle. As blastomeres divide asynchronously from the four-cell stage onwards [2], embryos at the same developmental stage show different numbers of blastomeres, a fact that might be misinterpreted. The third cleavage cycle results into the eight-cell stage embryo, while the fourth cleavage results into 16-cells stage embryos. We refer to the eight-cell stage when the embryo is composed of 5-9 cells (Day 2 *in vitro* post fertilization). Similarly, we define the embryo at the 16-cell stage, when it is made of 13-17 cells (Day 3 *in vitro* post fertilization).

Early Bovine Embryo Development

After fertilization, the zygote undergoes multiple cell divisions. The embryo and its blastomeres change their morphology and function. These changes characterize the different developmental stages [3]. In early embryonic stages, cell polarization is an important event in the transition from zygote to blastocyst, leading to different cell-types [4]. Microvilli, membrane protrusions that increase the surface area, have been studied to model cell polarization. In the 9- to 15-cell bovine embryos two cell-types have been observed. Some cells are uniformly covered with long and short microvilli (non-polar), while others have a single pole of long microvilli (polar). From the 16-cell stage onwards, almost all bovine embryos possessed one or more blastomeres with a single pole of long microvilli (polar) [5]. In addiction to cell polarization, the nucleologenesis and the onset of transcription play a crucial role in yielding different cell-types. The nucleolus is the site of ribosomal RNA (rRNA) synthesis; rRNA is an essential component of ribosomes, required for mRNA translation. At the four-cell stage only a fibrillar center is visible. This is the structure where the enzymes necessary for transcription are located. At the eight-cell stage, a dense fibrillar component is visible in addition to the fibrillar center. The dense fibrillar component carries the unprocessed rRNA transcripts [6]. Interestingly, the starting point for morphogenetic events linked with the onset of transcription was identified at the eight-cell stage [7]. Finally, at the 16-cell stage, the granular component is formed as

the third part of the nucleolus. Here the processed rRNAs are associated with proteins [6].

Embryonic Genome Activation (EGA)

At the time of embryo fertilization, maternal mRNAs and proteins support the development of the embryo. During early stages of embryonic development, the embryo starts gene expression and gradually degrades the maternal products, thus acquiring the control over its own embryonic development. This process is called Embryonic Genome Activation (EGA) and occurs in several waves [8]. The timing of the major EGA is species-specific. In the mouse embryo it takes place at the two-cell stage, while in human and pig embryos it occurs at the four- to eight-cell stage. In bovine embryos the major wave of EGA takes place during eight- to 16-cell stage (reviewed by [9]). In a more recent work based on RNA-sequencing (RNA-seq) data, *de novo* RNA transcripts were identified by (*i*) detection of embryonic transcripts, which are not present in oocytes; (*ii*) detection of transcripts from the paternal allele; and (*iii*) detection of primary transcripts with intronic sequences [10].

Epigenetic Modifications

In early developmental stages the embryo reprograms its genome by epigenetic modifications [11]. The reprogramming consists in the removal of the existing epigenetic marks in the nucleus and their subsequent establishment with a different set of marks. In mammals the most important modifications involve DNA methylation and histone modifications (reviewed by [12]).

The addition of a methyl group to the fifth carbon of the base cytosine is called DNA methylation. This reaction is catalyzed by enzymes named DNA methyltransferases (Dnmts) [11]. Although DNA methylation reprogramming is evolutionary conserved in early embryos of diverse species, species-specific differences can be observed.

In bovine, DNA methylation decreases from the 1-cell stage to the eight- to 16-cell stage, when *de novo* methylation occurs at the eight- to 16-cell stage. In contrast, *de novo* methylation takes place after the blastocyst stage in mouse [13].

DNA is packaged in a structure called chromatin. The nucleosome is the unit of chromatin and it is composed of an octamer of four core histones (which are H3, H4, H2A, H2B proteins) around which DNA is wrapped [14]. These core histones can undergo diverse modifications causing activation or repression of transcription [15].

Di- or tri-methylation of histone H3 at lysine 9 or 4 (H3K9me2 and H3K4me3) were observed in late zygotes and early two-cell stage in mouse, bovine and rabbit embryos, thus suggesting evolutionary conservation among the three species. Interestingly, this developmental stage corresponds to the major EGA in mouse, but not in bovine or rabbit [16].

Lineage Specification at Early Stages of Embryo Development

During compaction, the outer blastomeres of the embryo acquire a polarity and lose pluripotency [17]. This process is the first lineage specification and leads to the formation of trophectoderm (TE) at the blastocyst stage [18]. The inner blastomeres form the inner cell mass (ICM) and are pluripotent cells. Subsequently, a second lineage specification within the ICM cells event takes place. This results in primitive endoderm (PE) cells, an extra-embryonic lineage forming the yolk sac, and pluripotent epiblast (EP) cells. EP cells will give rise to the embryo proper [19].

Although lineage specification has already been investigated with different methods and technologies, timing and mechanisms of this process are not fully understood. In bovine embryos, gene expression of pools of cells from ICM or TE, previously separated by chemical or mechanical methods, has been studied by RNA-seq [20] or quantitative real-time PCR (qPCR) and whole-mount *in situ* hybridization (WISH) [21]. These two studies provided a demonstration that these ICM- and TE-dominant transcripts accompanied the establishment of cell lineage specification [20,21]. Time-lapse microscopy technology was also used to study the relation between the two-cell stage plane and further embryonic-abembryonic axis at the blastocyst stage in bovine. The cells were traced and these were observed to intermingle between the third (results into 8-cell stage embryo) and fourth cleavage (results into 16-cell stage embryo) [22]. Most recently, the mRNA levels of 96 candidate genes were analyzed in single cells from zygote to blastocyst in bovine. Based on the expression patterns, three lineages could be identified at the expanded blastocyst stage [23].

Aims of the Project

Embryo development at early stages is a critical period during embryogenesis. Morphology, genomics, transcriptomics and proteomics have been extensively studied in bovine animal model embryo. However transcriptomics at single-cell level enabling identification of different cell populations at the time of major embryonic genome activation (EGA) has not been investigated yet.

This project will address the questions (*i*) Do the single cells within an embryo show different transcriptome profiles? (*ii*) Do the transcriptome profiles provide evidence for early inclination events during and after the major EGA?

Therefore single-cell RNA-sequencing (RNA-seq) was performed to generate transcriptome profiles of bovine eight- to 16-cell stage embryos. Embryos were produced by *in vitro* fertilization and the developmentally most competent embryos were selected by following their development *in vitro* by time-lapse video microscopy.

This thesis presents a transcriptomic analysis of early bovine development. It reveals a continuity of blastomere development at the time of major EGA.

Publication

Sci Rep. 2018 Mar 6;8(1):4071. doi: 10.1038/s41598-018-22248-2

Single-cell RNA sequencing reveals developmental heterogeneity of blastomeres during major genome activation in bovine embryos

Ilaria Lavagi[1,2], Stefan Krebs[1], Kilian Simmet[3], Andrea Beck[3], Valeri Zakhartchenko[3], Eckhard Wolf[1,3,*], Helmut Blum[1,*]

[1]*Laboratory for Functional Genome Analysis (LAFUGA), Gene Center, LMU Munich, Germany*
[2]*Graduate School of Quantitative Biosciences Munich (QBM), Gene Center, LMU Munich, Germany*
[3]*Chair of Molecular Animal Breeding and Biotechnology, Gene Center and Department of Veterinary Sciences, LMU Munich, Germany*

*equal last author contribution

Correspondence:
Prof. Dr. Eckhard Wolf, Gene Center, LMU Munich, Feodor-Lynen-Str. 25, D-81377 Munich, Germany; Phone +49-89-2180-76800; Email: ewolf@genzentrum.lmu.de
Dr. Helmut Blum, Gene Center, LMU Munich, Feodor-Lynen-Str. 25, D-81377 Munich, Germany; Phone +49-89-2180-76700; Email: blum@genzentrum.lmu.de

Abstract

Embryonic development is initially controlled by maternal RNAs and proteins stored in the oocyte, until gene products gradually generated by the embryo itself take over. Major embryonic genome activation (EGA) in bovine embryos occurs at the eight- to 16-cell stage. Morphological observations, such as size of blastomeres and distribution of microvilli, suggested heterogeneity among individual cells already at this developmental stage. To address cell heterogeneity on the transcriptome level, we performed single-cell RNA sequencing of 161 blastomeres from 14 *in vitro* produced bovine embryos at Day 2 (n=6) and Day 3 (n=8) post fertilization. Complementary DNA libraries were prepared using the Single-Cell RNA-Barcoding and Sequencing protocol and sequenced. Non-supervised clustering of single-cell transcriptome profiles identified six clusters with specific sets of genes. Most embryos were comprised of cells from at least two different clusters. Sorting cells according to their transcriptome profiles resulted in a non-branched pseudo-time line, arguing against major lineage inclination events at this developmental stage. In summary, our study revealed heterogeneity of transcriptome profiles among single cells in bovine Day 2 and Day 3 embryos, suggesting asynchronous blastomere development during the phase of major EGA.

Introduction

During early stages of embryonic development, maternal RNAs and proteins are gradually degraded, while embryonic transcripts are synthesized. This process is called maternal-to-embryonic transition (MET) and involves embryonic genome activation (EGA) (reviewed in) [1]. EGA occurs in distinct waves, which are species-specific. Major EGA occurs at the two-cell stage in mouse embryos, at the four- to eight-cell stage in human and pig embryos, and at the eight- to 16-cell stage in bovine embryos (reviewed in) [2]. Recently, time-lapse microscopy was used to study lineage specification in early bovine embryos by tracing the allocation of blastomeres [3]. In the majority of embryos, cells intermingled between the third and fourth cell cycle, yielding a random allocation pattern. Single-cell RNA sequencing (scRNA-seq) is increasingly used to investigate mechanisms regulating the formation of the three cell lineages (trophectoderm, epiblast and primitive endoderm) during embryo development. The transcriptomes of these cell lineages have already been investigated in mouse [4,5] and human embryos [6,7], and in differentiating human embryonic stem cells [8]. In bovine, the transcriptome of whole embryos has been studied at different developmental stages [9,10]. More recently, transcript profiling of single embryonic cells for a set of candidate genes has been performed for different stages from zygote to blastocyst [11,12], providing new insight into lineage specification events in bovine embryos. However, holistic single-cell transcriptome analysis has not been performed in bovine embryos during major EGA (eight-cell to 16-cell stage) yet. Our study applied scRNA-seq on these developmental stages to provide a refined view into the timing of major EGA, developmental heterogeneity, and potential early lineage inclination events in bovine embryos.

Results

Selection of developmentally competent *in vitro* produced embryos. The kinetics of early embryo development *in vitro* is strongly associated with the potential to form a blastocyst and to establish pregnancy [13]. Therefore, we studied a total of 541 bovine embryos for 168 hours after fertilization by time-lapse microscopy. The timing and duration of the first, second and third cleavages and their effects on blastocyst rate were analysed in order to select embryos with high developmental potential. The highest blastocyst rate (75%) was detected, when the first embryonic cleavage occurred between 25.6 and 27.1 hours post fertilization (hpf). The optimal time ranges for the second and third cleavages were 33.4 to 36.2 hpf and 41.6 to 43.7 hpf, respectively. The optimal duration of the two-cell stage was 7.7 to 8.6 hours, resulting in blastocyst rates of 77 to 81% (Supplementary Fig. S1) [14]. For the present study, six Day 2 and eight Day 3 embryos were selected to fit most closely into the optimal developmental kinetics (Table 1). Single cells were prepared and processed for

sequencing. In total, six to 9 cells per Day 2 embryo and 13 to 17 cells per Day 3 embryo were analysed.

Embryo designation	1st cleavage (hpf)	2nd cleavage (hpf)	3rd cleavage (hpf)	Embryo collection (hpf)	Total cell number
Day2-E1	25:45	33:51	41:15	44:00	8*
Day2-E2	27:01	34:06	42:50	44:00	9
Day2-E3	27:01	34:26	39:45	44:00	9
Day2-E4	27:11	35:11	42:10	45:00	8
Day2-E5	27:35	34:25	45:25	45:30	8
Day2-E6	27:45	37:3	45:04	45:04	6
Day3-E1	29:18	38:45	47:07	67:00	15
Day3-E2	26:08	34:23	41:17	67:00	16
Day3-E3	27:48	35:53	44:02	67:00	16
Day3-E4	25:53	33:45	40:47	67:00	13
Day3-E5	29:56	37:16	45:20	69:00	17
Day3-E6	29:51	37:31	45:15	69:00	14
Day3-E7	27:15	36:20	44:15	71:00	16
Day3-E8	25:35	33:45	39:56	71:00	16

Table 1. Cleavage timing, embryo collection time and number of cells in Day 2 and Day 3 embryos used for single-cell transcriptome profiling. *In vitro* developing embryos were observed by time-lapse microscopy, and embryos with high developmental potential were selected based on the timing (hours post fertilization; hpf; shown as hours:minutes) of the first three cleavage divisions. * = 1 cell was lost during the cell collection.

Filtering and Quality Control of RNA-Seq Data. Transcriptome profiles of 170 single cells were generated by Single-Cell RNA Barcoding and Sequencing (SCRB-Seq) [15]. On average, 1,896,797 reads per library were obtained. Subsequently, the unique molecular identifiers (UMI) were counted as a measure for the complexity of the sequencing libraries and used for further analyses to exclude PCR duplicates. On

average, 45,000 UMI per library were obtained. The numbers of generated reads, UMI and detected genes per library are reported in Supplementary Table S1. Sequencing data of nine cells were excluded from further analyses because their UMI count was below the empirical threshold of 2,000 (Supplementary Fig. S2). In total, 10,772 genes were captured by combining the transcriptome profiles of 161 cells. Saturation plots are shown in Supplementary Fig. S3-S5.

Cluster Analysis of Single-Cell Transcriptome Profiles. In order to search for cell populations present in sampled embryos, cluster analyses were performed with two different unsupervised tools for single-cell sequencing data sets. For the SC3 R package tool [16], the number of clusters for calculation of the consensus matrix was set to six. This value had been obtained using the Tracy-Widom theory on random matrices to estimate the optimal number of clusters k [17]. The SC3 pipeline was used to cluster the single cells, and 2,494 differentially abundant transcripts (DAT; $p < 0.01$) were identified (Supplementary Table S2). Figure 1 shows the assignment of the 161 cells to the six clusters and plots the colour-coded abundance levels of the 50 most significant DAT sorted according to their p-value. Most embryos were comprised of cells from at least two different clusters. Three clusters (K1, K5 and K6) contained cells of both Day 2 and Day 3 embryos, the other three clusters (K2, K3 and K4) exclusively cells from Day 3 embryos (Table 2).
In order to study the influence of dropouts (zero read counts for certain genes, due to failure of reverse transcription or low read counts) on the clustering and number of DAT, the dataset was analysed with the M3Drop R package tool [18]. This tool identified only 15 genes not affected by dropout (Fig. 2), which were a subset of the 2,494 DAT identified by the SC3 approach (Supplementary Fig. S6).

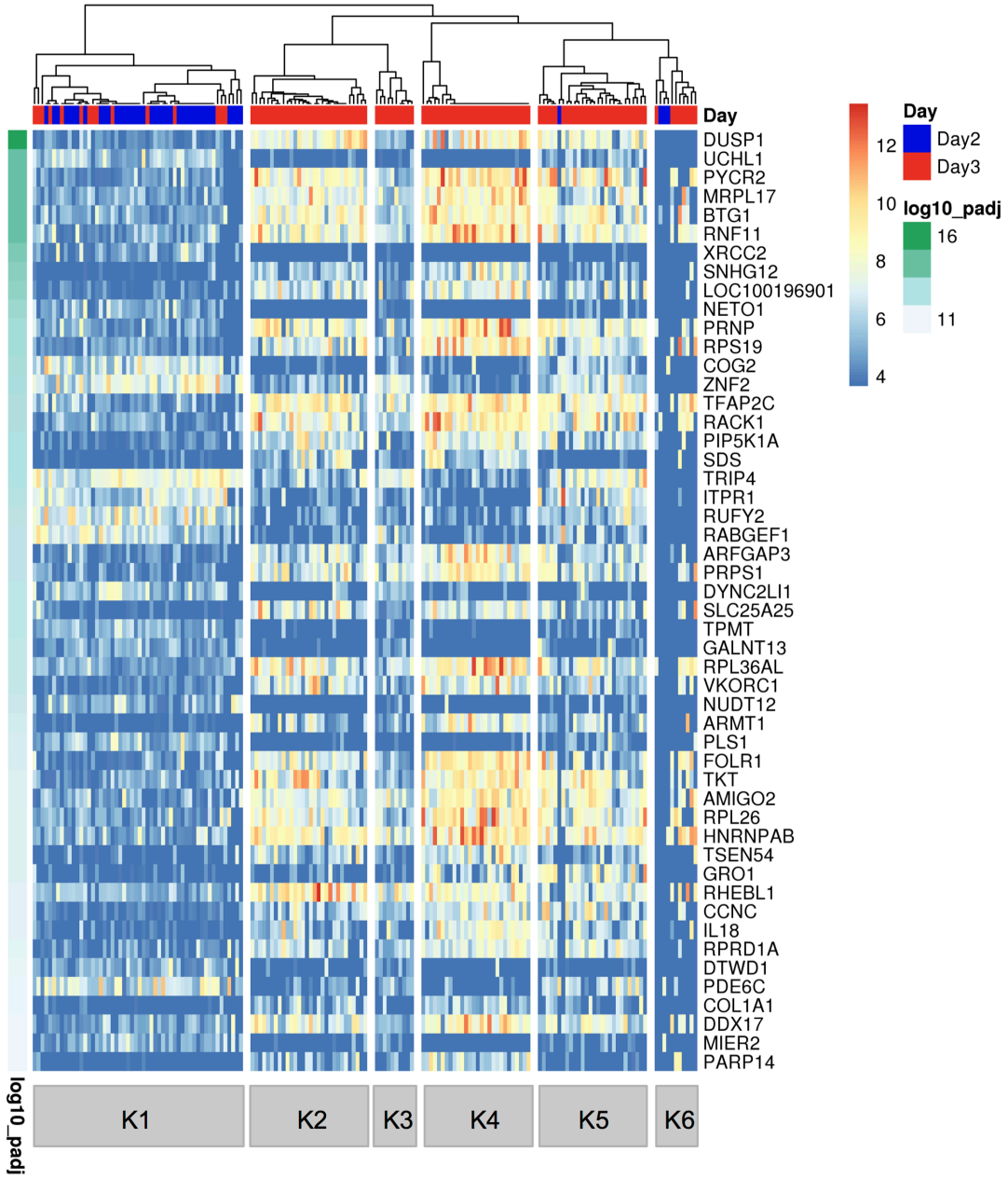

Figure 1. Single-cell Consensus Clustering (SC3). Single-cell transcriptome profiles of 161 blastomeres from six Day 2 embryos and eight Day 3 embryos were analysed with the SC3 tool [16]. Differentially abundant transcripts (DATs) were identified with the non-parametric Kruskal-Wallis test. DATs were clustered with a pre-set number of six clusters and the results for the 50 top genes are shown. The adjusted p-value is shown on the left. A blue or red colour label in the embryo ID row indicates blastomeres collected from Day 2 or Day 3 embryos, respectively.

Embryo designation	K 1	K 2	K 3	K 4	K 5	K 6	No. cells not analyzed	No. embryo cells
Day2-E1	4	-	-	-	-	2	2	8
Day2-E2	9	-	-	-	-	-	-	9
Day2-E3	7	-	-	-	-	-	2	9
Day2-E4	6	-	-	-	-	1	1	8
Day2-E5	7	-	-	-	1	-	-	8
Day2-E6	6	-	-	-	-	-	-	6
Day3-E1	13	-	-	-	-	1	1	15
Day3-E2	14	-	-	-	-	-	2	16
Day3-E3	2	-	-	-	13	1	-	16
Day3-E4	-	-	-	11	-	2	-	13
Day3-E5	-	6	9	-	-	2	-	17
Day3-E6	-	13	1	-	-	-	-	14
Day3-E7	-	11	-	3	-	1	1	16
Day3-E8	-	-	-	14	-	1	1	16

Table 2. Distribution of the cells collected from Day 2 and Day 3 bovine embryos through the clusters identified by the SC3 tool. The original number of cells in each embryo is reported in the last column. Some cells were lost at the time of collection or filtered out because of low quality of their transcriptome; the number of these cells is reported in the penultimate column.

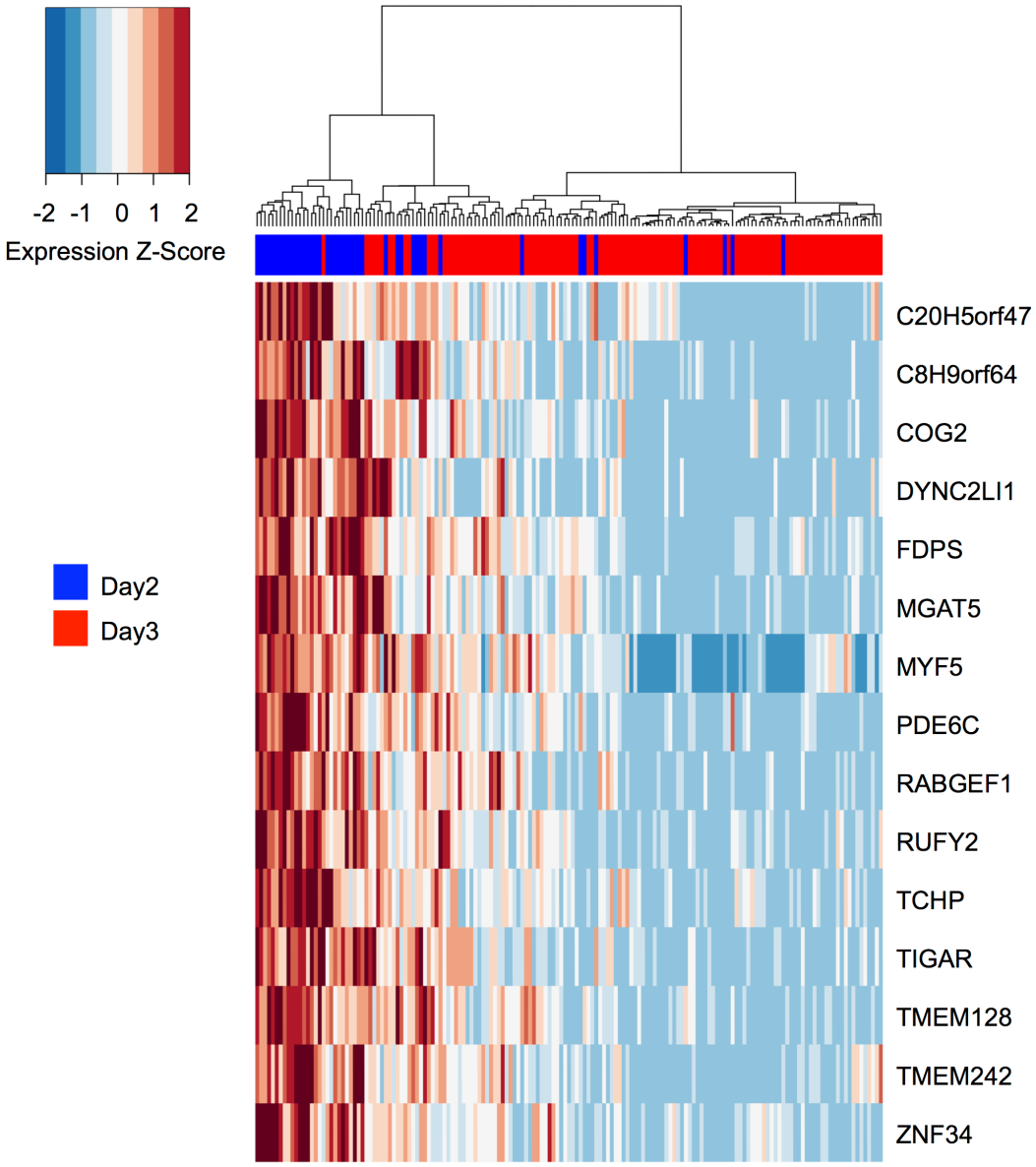

Figure 2. Michaelis-Menten Modelling of Dropouts (M3Drop). The single-cell transcriptome dataset of 161 blastomeres from six Day 2 and eight Day 3 embryos was analysed with the M3Drop tool [18]. Genes with detectable levels of transcripts in all blastomeres (genes not affected by dropouts; n = 15) were identified with the Z-test and hierarchical clustering was performed only on these genes. Expression values are displayed as Z-scores of log2 transformed expression data (adding a pseudo-count of 1). A blue colour label in the embryo ID row marks cells collected from Day 2 embryos; cells from Day 3 embryos are marked in red. Note that cells cluster independently of embryo age.

Cluster Specific Marker Genes. Cluster specific marker genes were identified using the SC3 pipeline [16]. Threshold criteria were: adjusted p-value < 0.01; area under the ROC curve (AUROC) > 0.85. In cluster K1, 12 marker genes were identified. These genes encode proteins belonging to diverse protein classes, such as serine/cysteine protease, membrane traffic protein, and DNA strand-pairing protein hydrolase. In cluster K2, *RHEBL1*, a gene involved in TORC1 signalling [19], was found. Cluster K3 showed no statistically significant marker genes. In cluster K4, 88 cluster specific marker genes were identified. One of them, *NANOG*, is involved in the maintenance of pluripotency [20]. Another marker gene of cluster K4 was *FOLR1*, which is expressed in murine embryos from the two-cell stage [21]. Several other K4 marker genes encode 40 S (*RPS19*, *RPS27*, *RPS29*, *RPS4Y1*) or 60 S (*RPL37*, *RPL38*) ribosomal proteins. Another interesting candidate among the K4 marker genes was *KLF5* that is involved in self-renewal of mouse embryonic stem cells [22]. The other marker genes encode proteins belonging to different functional classes, such as kinases, transcription factors, proteins involved in membrane trafficking, and translation initiation factors. Cluster K5 showed the chemokine coding gene *CXCL1* (also known as *GRO1*) as cluster specific gene. Cluster K6 showed no statistically significant marker genes (Supplementary Table S3).

Gene Set Enrichment Analysis of the Cluster Specific Genes. Gene set enrichment analysis was performed for the cluster specific genes by using the ClueGO [25] plugin of Cytoscape. This tool was used with the downloadable *Bos taurus* genome, and a p-value <0.01 was set for filtering the pathways. Statistically significant gene ontology (GO) terms were only found in cluster K4, where "ribosome biogenesis", "ribosome assembly", "ribosomal large subunit biogenesis", "nucleobase biosynthetic process", "translational elongation" and "cellular amino acid biosynthetic process" were over-represented (Supplementary Table S4).

Biological Pseudo-Order and Identification of Gene Topics. The R package CellTree [24] was used to order the cells according to their developmental stage. CellTree identifies cells that are good representatives of major steps in development and uses them to construct a backbone of big circles sorted according to developmental progress (biological pseudo-time line). All other cells are aligned as smaller circles branching from the most similar representative cell. Big and small circles constitute a backbone tree. Based on the overall pseudo-time line, embryos were sorted from top to bottom according to the median position of their cells (Fig. 3a).

All single cells from Day 2 embryos were located in the left third of the backbone tree, whereas the cells from Day 3 embryos were found over the whole length of the backbone tree except for the first circle. Cells of some embryos were concentrated on two major circles (e.g. Day2-E3 or Day2-E6), while cells of other embryos were distributed over a broad range of circles (e.g. Day3-E3 or Day3-E2).

CellTree assumes that transcriptomes of cells contain a mixture of "topics" with per-topic gene distributions. It uses a Bayesian mixture model – the Latent Dirichlet

Allocation (LDA) – to identify different topics. In our dataset, we identified six different topics present along the developmental pseudo-time line (Fig. 3b). Topic 1 was the most prominent, but was nearly absent in the penultimate phase of the pseudo-time line. Topic 2 was absent in the early phase, but predominantly present in the penultimate phase of the pseudo-time line. Topic 3 dominated the middle of the developmental pseudo-time line. Topics 4, 5 and 6 were less prominent and mainly observed in the first phase of the pseudo-time line. The biological roles of the six topics were also analysed by the CellTree tool. Gene set enrichment analysis was performed based on the org.Bt.eg.db genome-wide annotation with GO mapping [25] and Bonferroni's correction. The following GO terms were over-represented: Topic 1: "translation", "cell division"; Topic 2: "translation", "regulation of translational initiation", "mRNA splicing, via spliceosome", "cytoplasmic translation", "rRNA processing", "spliceosomal complex assembly", "negative regulation of mRNA splicing, via splicing", "cell division", "regulation of alternative mRNA splicing, via spliceosome"; Topic 3: "translation"; Topic 4: "ATP synthesis coupled proton transport"; Topic 5: "mitochondrial translational elongation"; and Topic 6: "organic hydroxyl compound transport" (Supplementary Table S5).

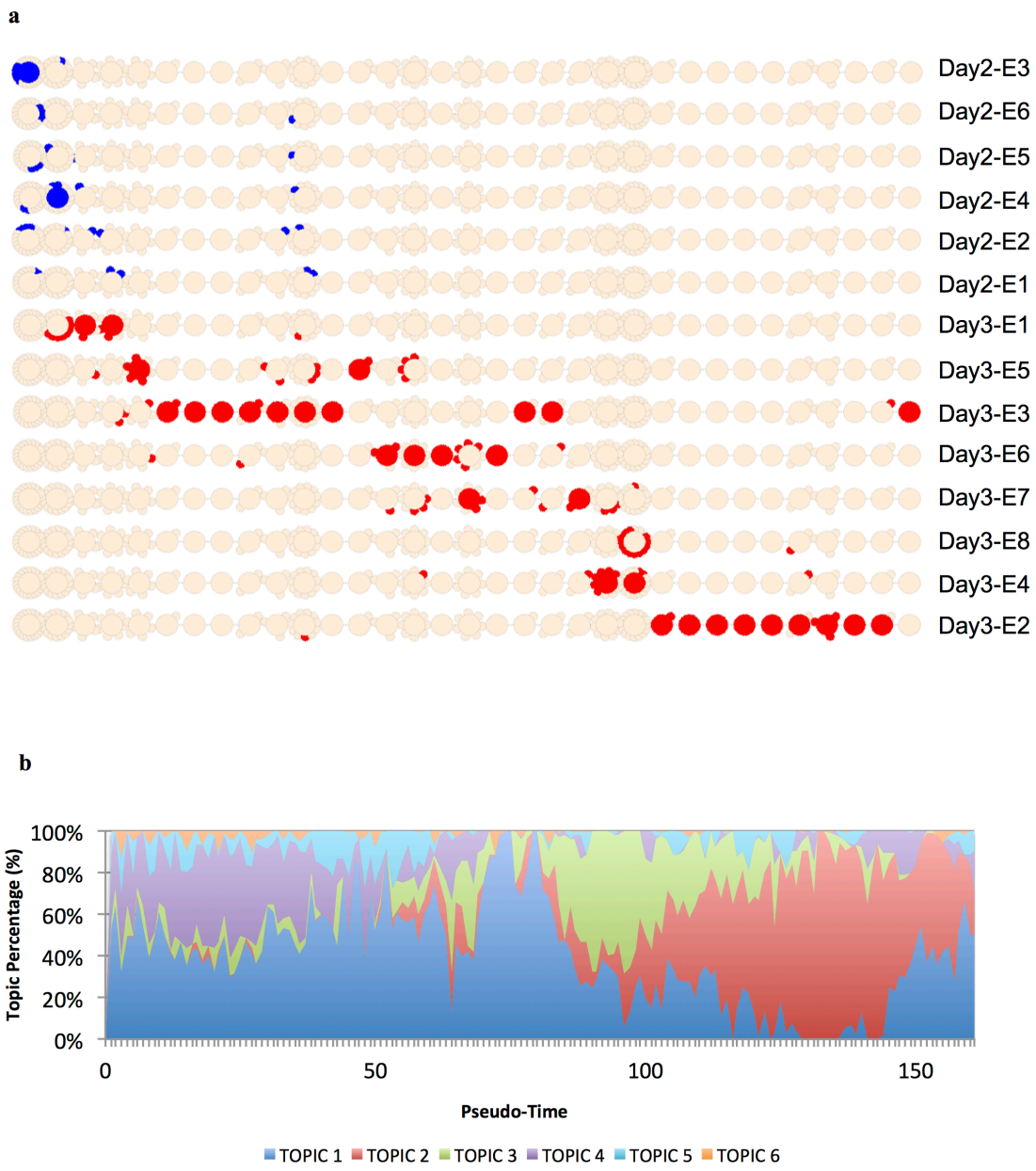

Figure 3. Biological pseudo-time. The single-cell transcriptome dataset of 161 blastomeres from six Day 2 and eight Day 3 embryos was analysed with the CellTree tool [24]. **(a) Backbone tree.** A backbone tree is built by computing a matrix of pairwise distances. This shows the hierarchical relationship between all blastomere transcriptome profiles and aligns the blastomeres in a pseudo-time line. The backbone trees of individual embryos are sorted according to the median position of their cells. Blastomeres from Day 2 embryos are coloured in blue, blastomeres from Day 3 embryos in red. **(b) Identification of latent groups of genes (topics), which characterise the steps of the development.** The number and distribution of topics along the pseudo-time line was obtained by using the Latent Dirichlet Allocation (LDA). To each topic, gene ontology terms were associated. Topic 1 = "translation", "cell division"; Topic 2 = "translation", "regulation of translational initiation", "mRNA splicing, via spliceosome", "cytoplasmic translation", "rRNA processing", "spliceosomal complex assembly", "negative regulation of mRNA splicing, via splicing", "cell division", "regulation of alternative mRNA splicing, via spliceosome"; Topic 3 = "translation"; Topic 4 = "ATP synthesis coupled proton transport"; Topic 5 = "mitochondrial translational elongation"; Topic 6 = "organic hydroxyl compound transport".

Major Embryonic Genome Activation (EGA) at the Single-Cell Level. In order to investigate when major EGA occurs in each blastomere, we analysed transcript levels of 129 genes that are actively transcribed at the eight-cell stage and whose mRNA is not present in earlier embryonic stages or oocytes [10]. In our dataset, transcripts of only 20 of these genes were detected. Each of these genes showed a unique expression pattern in blastomeres along the pseudo-time line (Supplementary Fig. S7) and blastomeres of individual embryos showed different transcript abundances. Interestingly, five Day 2 embryos and two Day 3 embryos had one blastomere each without UMI counts for any of these genes 20 genes.

Analysis of Candidate Genes Inducing or Reflecting Cell Fate Decisions. In order to study potential early cell lineage inclination events, we investigated the abundance of transcripts of genes known to be involved in early cell fate decisions. For each cell – ordered according to the pseudo-time line – the UMI counts for selected genes provided by the Drop-Seq pipeline were plotted (Fig. 4, 5).

The transcription factor POU5F1/OCT4 is involved in maintaining cell pluripotency of the inner cell mass in mouse embryos [26]. In bovine embryos, mRNA expression of *POU5F1/OCT4* was found in both the ICM and TE at the late blastocyst stage [27], and its knockout was observed to be lethal at the second lineage differentiation in bovine embryos [28]. The homeobox gene *CDX2* regulates multiple trophoblast genes in bovine blastocysts [29], but - in contrast to the situation in mouse embryos - CDX2 does not suppress *POU5F1/OCT4* expression [30], but only down-regulates its level [29]. *NANOG* and *GATA6* are two key genes involved during the second lineage segregation in epiblast or primitive endoderm, respectively (reviewed in) [31]. *NANOG* transcripts were first observed at the eight-cell stage in the bovine embryo [10], and its expression is required for the bovine embryonic development [28]. *GATA6* was observed to have acquired a species-specific ability to control trophoblast-specific gene expression in ruminant ungulates [32].

In our study, *POU5F1*/*OCT4* transcripts were detected in more than 70% of the cells from Day 2 embryos and in about 50% of the cells from Day 3 embryos. *CDX2* transcripts were also detected in about 53% of the Day 2 blastomeres, but in a markedly lower proportion (12%) of the Day 3 blastomeres, although the positive cells contained relatively high levels of *CDX2* mRNA. *NANOG* transcripts were found in roughly 20% of the cells aligned in the first half of the pseudo-time line, and in a higher proportion (55%) and at higher levels in the more advanced half of the cells. *GATA6* mRNA was not detected in our dataset.

In addition to these key genes regulating the specification of the first embryonic cell lineages, we investigated additional candidate genes relevant for the maintenance of pluripotency or early differentiation events. UMI counts of the proto-oncogene *MYC*, which contributes to the selection of the epiblast cell pool [33], were found in only one cell of Day 2 embryos, but in about half of the cells from Day 3 embryos. The proportion of *MYC* expressing blastomeres in individual Day 3 embryos ranged from

13% (2/15) to 100% (14/14). Transcripts of Krüppel like factor 4 (*KLF4*), which was observed to prevent differentiation of mouse ES cells and to regulate the expression of *Nanog* [34], but not to be essential for early development [35], were found in nearly all cells of Day 2 and Day 3 embryos with increasing abundance towards the end of the pseudo-time line. Similarly, transcripts of Sal-like 4 (*SALL4*), which is important for cell fate decision and required to maintain pluripotency of the inner cell mass in early mouse embryos [36], were found in nearly all cells of Day 2 and Day 3 embryos, in various levels of abundance. Transcripts of Sal-like 1 (*SALL1*) were found in all embryos except for one Day 3 embryo, but only in a proportion of the blastomeres. In mouse ES cells, SALL1 is expressed in a differentiation-dependent manner and physically interacts with NANOG and SOX2 to regulate transcription [37]. Transcripts of *FOSL1*, which is required for development of the trophoblast lineage [38], were detected in nearly all cells of the first third of the pseudo-time lime. In more advanced stages, the UMI count as well as the number of cells with detectable levels of *FOSL1* transcripts declined.

Moreover, we looked specifically at genes that were described to be predominantly expressed in either ICM or TE of bovine blastocysts [39] and intersected this gene set with transcripts not detected before the eight-cell stage to exclude carry-over of maternal transcripts [10]. The intersection contained the predominantly ICM-expressed protocadherin-10 (*PCDH10*) gene. In our data set, *PCDH10* transcripts were found in 30 blastomeres of seven Day 3 embryos at the advanced end of the pseudo-time line (Fig. 5).

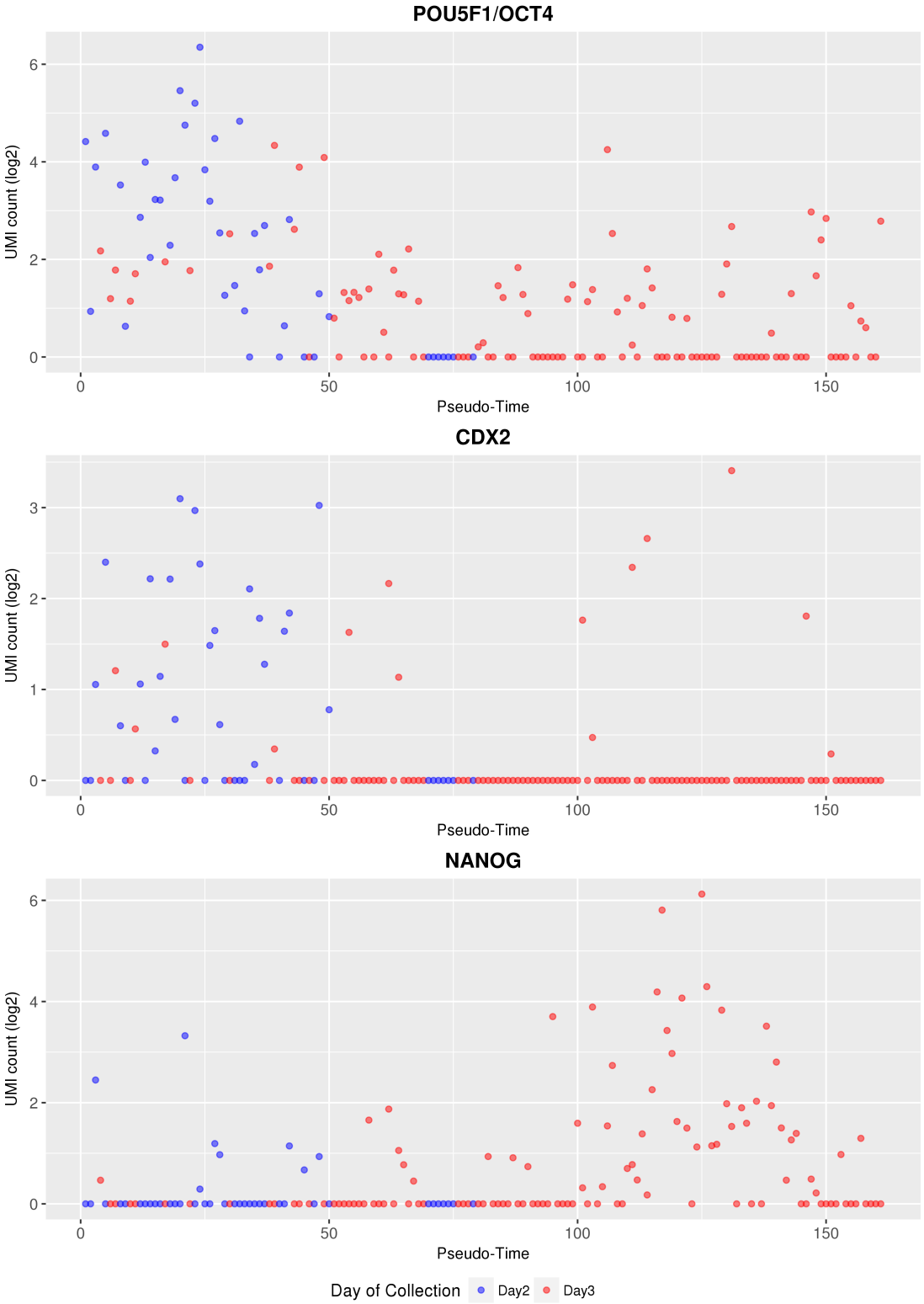

Figure 4. Changes in the transcript abundance of *POU5F1*/*OCT4*, *CDX2,* and *NANOG* along the pseudo-time line. Cells from Day 2 embryos are shown as blue symbols, cells from Day 3 embryos as red symbols.

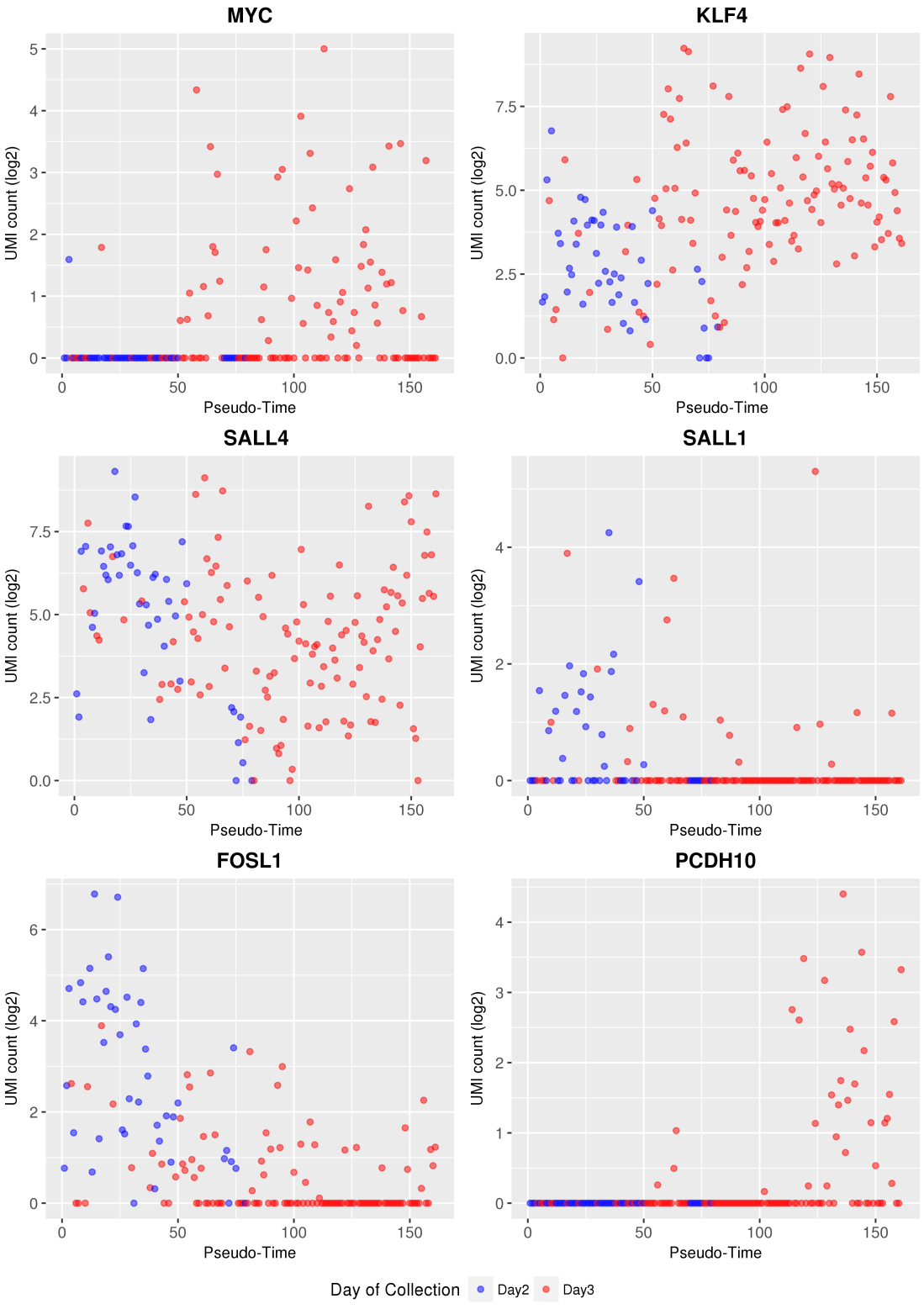

Figure 5. Changes in the transcript abundance of *MYC*, *KLF4*, *SALL4*, *SALL1*, *FOSL1*, and *PCDH10* as development proceeds. The UMI values of these genes are shown along the pseudo-time line. Cells from Day 2 embryos are shown as blue symbols, cells from Day 3 embryos as red symbols.

Discussion

Single-cell RNA sequencing enables the study of heterogeneity in cell populations and paves a way for unprecedented analyses of developmental processes. Our study provides a comprehensive insight into developmental heterogeneity of blastomeres in bovine embryos at the time of major EGA (eight- to 16-cell stage). Previous studies of these developmental stages were performed with pools or individual bovine embryos [9,10], while individual cells have not been analysed yet. In the present study, we used the SCRB-Seq approach to study the transcriptome of individual blastomeres derived from Day 2 and Day 3 embryos. The analysis itself destroys the embryos and therefore the developmental potential of the dissected embryo remains uncertain. A correlation between a combination of kinetic and morphological parameters and the rate of successful blastocyst formation was previously described for *in vitro*-fertilized human embryos [40]. A similar study described a novel system for selection of bovine IVF blastocysts for transfer to recipient animals by tracing the development of individual embryos with time-lapse cinematography and analysing embryo metabolism. This approach includes several kinetic and morphological prognostic factors that span from the zygote to the blastocyst stage and facilitate prediction of pregnancy success [13]. In the present study, we followed the development of 541 embryos by time-lapse microscopy in order to find parameters predictive for blastocyst formation. We found strong correlations between the timing of the first, second and third cleavages and the blastocyst formation rate [14]. These parameters were subsequently used for selecting developmentally competent embryos and excluding their low-grade counterparts.

SCRB-Seq [15], a sophisticated procedure to construct 3′ specific UMI containing libraries from single cells, was used to sequence the transcriptomes of blastomeres of the selected embryos. cDNA reads were mapped to the bovine reference genome btau7 with the STAR tool [41]. Subsequently, data were normalized without using exogenous spike-ins, because technical variations do not affect spike-ins and endogenous transcripts uniformly, thus causing poorly normalized data [42]. We used UMI count [43] instead of read count in order exclude duplicates originating from PCR amplification. Genes involved in the cell cycle [44] were not excluded from our analysis as the variation between cells is largely explained by the sum of log expression values over all genes in a cell, rather than by cell cycle stage [45].

Transcriptome data were used to cluster the cells and sort them along a pseudo-time line (from position 1 to position 161).

The clustering tool SC3 [16] identified six different clusters, and three of them contained cells from both Day 2 and Day 3 embryos. This finding indicates that at least some blastomeres of an embryo develop asynchronously. The number of 2,494 DAT hints to enormous changes of the transcriptome in that developmental period. This order of magnitude is comparable to the number of 2,940 DAT described by Graf et al. [10] when comparing pools of ten eight-cell and 16-cell embryos. In addition to the DAT, the SC3 tool identified cluster specific markers genes. *FOLR1, NANOG* and *KLF5* were revealed as marker genes specific for cluster K4. In a previous

study [10], transcripts of the first two genes were not detected before the eight-cell stage, while *KLF5* transcripts are already present in the oocyte and embryonic transcription of this gene was detected at the four-cell stage. In contrast, transcripts of *RHBL1* (marker gene of cluster K2) and *CXCL1* (marker gene of cluster K5) were not detected in the previous study by Graf et al. [10]. Collectively, the results of this analysis suggest the presence of six different cell populations in early bovine embryos (Day 2 to Day 3). These cell populations are characterised by specific transcriptome signatures and comprise blastomeres of different embryos.

It is known that so-called dropouts (zero read counts for certain genes, due to failure of reverse transcription or low read counts) hamper single-cell transcriptome analyses. The clustering tool M3Drop [18] focuses on genes not affected by dropouts, but cannot distinguish between technically caused dropouts and mRNA-species that naturally occur only in a certain proportion of the blastomeres. In our dataset, the M3Drop tool identified 15 genes unaffected by dropouts and clustered the cells based on these genes. In line with the clusters generated by the SC3 tool, some clusters contained cells from both Day 2 and Day 3 embryos.

In addition, the CellTree tool [24] was used to sort cells based on their transcriptome in a time line (called "pseudo-time line") and to build, based on the obtained time line, a backbone tree. Within the timeline, blastomeres of some embryos (e.g. Day 2-E3: 9 cells) were located either in close vicinity or distributed over a broad range (e.g. Day 3-E3: 16 cells). This finding hints to an asynchronous development of blastomeres within an embryo. The linear structure of the backbone tree suggests that the first lineage differentiation towards ICM and TE has not occurred yet or is ongoing but below the detection level of single-cell RNA sequencing. Along the obtained pseudo-time line, different over-represented GO terms were identified. Their order suggested an orchestrated process of early development, starting with the GO terms "translation" and "cell division". The GO term "cell division" then gradually disappeared, while the GO term "translation" and later also GO terms related to "RNA processing" became more prominent.

In order to study major EGA at the single-cell level, we investigated the abundance of 129 different transcripts that were first detected at the eight-cell stage in pooled embryos [10], and detected 20 of these transcript species in our single-cell study. Five Day 2 embryos and two Day 3 embryos did not have detectable levels of any of these transcripts. This suggests that the timing of major EGA is neither synchronous among different embryos of the same stage nor among all blastomeres of one embryo.

Among the genes not transcribed before the eight-cell stage was *NANOG* that is involved in preventing differentiation of pluripotent cells. *NANOG* transcripts were detected in only 19% (8/43) of the Day 2 blastomeres, but in 43% (51/118) of the Day 3 blastomeres, reflecting a gradual and asynchronous activation of this gene in individual blastomeres. In contrast, *POU5F1*/*OCT4* and *CDX2* transcripts were revealed in 74% and 53% of the Day 2 blastomeres, while these proportions decreased to 50% and 12% in the Day 3 blastomeres, respectively. This is most likely due to degradation of maternal RNA that is apparently more pronounced for *CDX2* than for *POU5F1*/*OCT4*. The relatively high mRNA levels of *CDX2* in a proportion

of the Day 3 blastomeres may hint to lineage inclination towards trophectoderm, although this was not evident from the backbone tree generated by the CellTree tool. An alternative explanation would be impaired maternal RNA degradation in a proportion of the blastomeres. Transcripts of the primitive endoderm marker gene *GATA6* were not detected in our study.

Transcripts of *MYC* that is involved in selecting the epiblast cell pool are already present in the oocyte [10], but were detected in only one blastomere from a Day 2 embryo and in ~45% of the Day 3 blastomeres. This suggests rapid degradation of maternal *MYC* transcripts and embryonic activation of *MYC* towards the end of major EGA in about half of the blastomeres.

KLF4 (necessary for preventing differentiation) and *SALL4* (involved in maintenance of pluripotency) are also present in oocytes and are thus detected before the eight-cell stage [10]. In the present study, blastomeres located at the end of the pseudo-time line showed higher transcript abundance of *KLF4,* suggesting increased embryonic transcription of this gene. The abundance levels of *SALL4* transcripts were high at the beginning and at the end of the pseudo-time line, but lower in the middle. This finding hints to initial degradation of maternal *SALL4* transcripts followed by active embryonic transcription of *SALL4*.

Embryonic transcription of *SALL1* (involved in pluripotency) and *FOSL1* (involved in TE development) is known to start at the 16-cell stage, although maternal transcripts of these genes were detected at earlier stages [10]. This explains the higher abundance of transcripts of the *SALL1* and *FOSL1* at the beginning of the pseudo-time line. Compared to *FOSL1*, the abundance of *SALL1* transcripts was on average lower and detected in a smaller proportion of blastomeres. Blastomeres with detectable levels of both transcripts were frequently found at the beginning of the pseudo-time line. Interestingly, in mouse embryonic stem cells, over-expression of the *Sall1* gene was observed to positively regulate the *Nanog* expression and thus prevent differentiation [37]. *FOSL1* is known to be important for invasive placentation, e.g. in human and mouse [46]. In our study of bovine embryos, the abundance of *FOSL1* transcripts was highest at the beginning and decreased towards the end of the pseudo-time line, which may be related to the late implantation and non-invasive, synepitheliochorial placentation in ruminants.

As an approach to detect potential early lineage inclination events in Day 2 to Day 3 embryos, we analysed genes that are known to be predominantly expressed in the ICM or TE of bovine blastocysts [39]. From this gene set, we selected the predominantly ICM-expressed protocadherin-10 (*PCDH10*) gene since its transcripts were not detected before the eight-cell stage [10], thus avoiding confounding effects of maternal transcripts. *PCDH10* transcripts were detected in 30 blastomeres of 7 Day 3 embryos at the advanced end of the pseudo-time line, raising the possibility that these blastomeres may be determined towards ICM. However, the non-branched backbone tree revealed by the CellTree analysis of our data set argues against major lineage inclination events at the developmental stages investigated. Elegant aggregation experiments of labelled TE cells with blastomeres from 8-cell embryos revealed that TE cells can contribute to the ICM and its derivatives [30], arguing against early lineage

commitment in bovine embryos. In contrast, early lineage commitment and its relation to cell allocation have been observed in mouse embryos (reviewed in) [47,48], thus underscoring the need for comparative embryological studies.

In summary, our study revealed heterogeneity of transcriptome profiles among single cells in bovine Day 2 and Day 3 embryos, suggesting asynchronous blastomere development during the phase of major embryonic genome activation.

Material and Methods

In vivo procedures were conducted according to the German Animal Welfare Act (Tierschutzgesetz). Bull semen was donated by Bayern Genetik GmbH, Grub, Germany. Estrous cow serum was donated by BFZF GmbH, Oberschleißheim, Germany. Bovine ovaries were obtained from a slaughterhouse (Münchner Schlachthof Betriebs GmbH, Munich, Germany). *In vitro* produced embryos were obtained from an EU approved bovine embryo collection and production centre at the Chair for Molecular Animal Breeding and Biotechnology of the LMU Munich (Moorversuchsgut Badersfeld, Oberschleißheim, Germany; approval number DE ETR 006 EWG).

***In vitro* embryo production and single cell collection.** Embryos were produced *in vitro* according to a standard procedure including *in vitro* maturation (IVM) and fertilization (IVF) [49]. Briefly, follicles from slaughterhouse ovaries were aspirated and obtained cumulus-oocyte complexes (COCs) were matured for 23 hours in modified Parker medium (MPM) supplemented with luteinising hormone (LH), follicle-stimulating hormone (FSH), and 5% estrous cow serum (ECS). Matured COCs were co-incubated with sperm selected by the swim-up method after thawing. For IVM and IVF, COCs were incubated at 39°C in a maximum humidified atmosphere of 5% CO_2 in air. After 20 hours of co-incubation, presumptive zygotes were vortexed to remove remaining cumulus cells and transferred to synthetic oviductal fluid (SOF) supplemented with 5% ECS, 400 µl BME, 100 µl MEM under mineral oil and cultured at 5% CO_2, 5% O_2, 90% N_2 and 39°C in humidified air. At the time of collection (Table 1), embryos were transferred to drops of TALP-HEPES-PVP (THP) [50] under oil for handling outside the incubator. All embryo manipulations were performed on a heated microscope plate set to 36 °C. The zona pellucida (ZP) was removed by treatment with 5 mg/ml pronase (Sigma Aldrich) for 1 min. Enzyme reaction was stopped by washing embryos in THP supplemented with 10% foetal calf serum (FCS) and dissolved ZP was completely removed by gentle pipetting. Embryos were incubated in drops of PBS without Mg^{2+} and Ca^{2+} supplemented with 4 mg/ml polyvinylpyrrolidone under oil for 5-10 minutes and blastomeres were subsequently disaggregated by gentle pipetting [51]. Single cells were transferred individually to 0.5 µl drops of lysis buffer (Buffer A of Prelude Direct Lysis Module, NuGEN) under mineral oil, collected in a 384-well plate, and stored at -80 °C.

Timing of early cleavages as a predictive parameter for blastocyst formation. A total of n = 541 zygotes generated by *in vitro* fertilization as described before were transferred into an embryo monitoring system (Primo Vision, Vitrolife, Gothenburg, Sweden) and images were recorded every 5 minutes for 168 hours and analysed with Primo Vision Analyzer software. Timing of the first, second and third cleavage, i.e. development until eight-cell stage, was evaluated and correlated to the formation of a blastocyst with logistic regression analysis. Statistical analysis were performed with SPSS 18.00 and p-values less than 0.05 were considered as significant [14].

Single-cell RNA-seq library preparations. Sequencing libraries were constructed according to the Single-Cell RNA Barcoding and Sequencing (SCRB-Seq) protocol [15]. Briefly, the 384-well plate containing the lysed blastomeres was thawed and an RT master mix supplemented with 0.1 µl of diluted ($1:10^6$) ERCC RNA Spike-In Mix (Life Technologies) was added to each well. A polyT anchor containing a cell barcodes (6 nt) and the Unique Molecular Identifiers (UMIs; 10 nt) was used to prime cDNA synthesis in a template switching reaction with Maxima H Minus Reverse Transcriptase (Thermo Scientific). After cDNA synthesis, samples were pooled and unused barcode primers were removed by digestion with exonuclease I (New England Biolabs). Full-length cDNA amplification was performed with the KAPA HiFi HotStart polymerase (KAPA Biosystems). Nextera XT libraries were constructed from 1 ng of pre-amplified cDNA according to the instruction of the manufacturer and finally amplified with a custom P5 primer (IDT). The libraries were sequenced paired-end with 16 cycles to decode cell barcodes and UMI from read 1 and 50 cycles for read 2 to sequence the cDNA fragment.

Basic Data Processing and Sequence Alignment. SCRB-Seq libraries were demultiplexed based on Nextera barcodes and cell barcodes. All reads were mapped to Bos tau7 (UCSC) and ERCC spike-in reference. Alignments were calculated using STAR 2.5.2b with default parameters. UMI tables were generated using the published Drop-seq pipeline [52].

Data Filtering and Normalization. Cells with less than 2,000 UMI were removed (Supplementary Fig. S2). Genes that showed no expression more than 10% of the cells were removed. Data were then normalized to account for differences in efficiency of transcript recovery between wells: gene specific UMI counts were divided by the total number of UMI counts per blastomere and then multiplied by the median of total UMI counts across all blastomeres.

Clustering Analysis. Two unsupervised hierarchical clustering analyses were performed on the filtered and normalized data. In order to investigate the transcript in single cells, Single-Cell Consensus Clustering (SC3) version 1.4.2, R package [16] was used. The required number of clusters was calculated after testing the significance of the eigenvalues of the matrix of covariance, by using the Tracy-Widom test [17]. The default parameters were used. A second hierarchical clustering tool was used that excludes gene affected by dropouts. The Michaelis-Menten Model (M3Drop) R package [18] relies on the Michaelis-Menten equation to model the relationship between the frequencies of dropouts and the expression level of genes. Significant outliers from the Michaelis-Menten equation are identified after performing a Z-test between the estimated K (mean expression level required for a gene to be detected in 50% of the cells) and the fitted K_M (FDR = 1%, p = 0.05). The significant outliers, also called differentially expressed genes, are the genes not affected by drop-outs and are then

used for identifying cell sub-populations by using Ward's hierarchical clustering. The default parameters were used.

Biological Pseudo-Time. In order to align the blastomeres according to their developmental progress, rather than by the time they were collected, we used the R package CellTree [24] on the log2(UMI+1) transformed data. Briefly, CellTree assumes that cells belong to a temporal continuum and assigns each cell a biological "pseudo-time" to form a "pseudo-time line" along which they can be ordered. This is performed by computing a matrix of pairwise distances (chi-square distance) and assuming that intragroup variance increases as development proceeds. According to such order, CellTree produces tree structures showing the hierarchical relationship between single-cell samples. It identifies groups of genes (called "topics"), by using the Bayesian mixture model - the Latent Dirichlet Allocation (LDA), and the topic-associated gene ontology terms.

Acknowledgements

This work was supported – in part – by the Bayerische Forschungsstiftung and by LMU Munich. I.L. was supported by a DFG fellowship through QBM. We cordially thank Christoph Ziegenhain and Wolfgang Enard from the Department of Biology at the Biozentrum (LMU) for the excellent technical support for the single-cell sequencing technology.

Author Contribution

E.W., H.B and S.K. designed the study. A.B. studied the parameters for identifying good quality embryos. V.Z. trained K.S. on general embryo manipulation. K.S. produced and disaggregated the embryos. S.K. collected the single cells, prepared the cDNA libraries and sequenced them. I.L. analysed the data and wrote the paper. All authors approved the final version of the manuscript.

Supplementary Information

Supplementary Tables

Library Name	No. Reads	% Kept reads after filtering	No. Uniquely mapped reads	No. UMI	No. Genes Detected	All UMI
E1.1_p3	4.309.219	89%	2.617.309	135.584	7.081	1.529.101
E1.2_p3	3.053.922	90%	2.056.708	94.401	6.536	1.207.649
E1.3_p3	88.737	87%	47.586	3.230	1.666	23.673
E1.4_p3	67.384	83%	28.105	1.501	997	8.783
E1.5_p3	80.205	85%	41.752	3.019	1.605	20.148
E1.6_p3	548.917	88%	186.014	14.445	3.847	101.070
E1.7_p3	7.874.226	90%	4.707.109	224.445	7.675	2.835.856
E14.1_p3	12.610.686	90%	8.084.065	362.668	8.308	4.244.672
E14.2_p3	249.717	86%	120.012	8.800	3.045	51.591
E14.3_p3	3.501.574	90%	2.102.756	115.550	7.028	1.126.286
E14.4_p3	2.412.252	90%	1.482.867	69.337	6.330	757.771
E14.5_p3	2.577.675	91%	1.315.563	75.167	6.537	698.945
E14.6_p3	1.888.132	90%	1.232.652	60.590	6.033	721.484
E14.7_p3	3.528.126	91%	2.309.520	106.574	6.929	1.207.219
E14.8_p3	4.520.663	90%	2.642.867	122.157	7.181	1.376.819
E14.9_p3	352.989	88%	169.544	12.803	3.700	83.270
E16.1_p3	6.772.236	90%	4.232.149	193.714	7.568	2.264.002
E16.2_p3	4.167.351	89%	2.500.150	118.750	7.056	1.350.425
E16.3_p3	40.178	78%	17.930	615	481	2.413
E16.4_p3	2.649.490	90%	1.266.674	76.074	6.528	667.004
E16.5_p3	17.830	85%	9.177	52	48	141
E16.6_p3	3.612.133	91%	2.224.111	115.331	6.969	1.225.211
E16.7_p3	4.679.685	90%	2.616.788	147.803	7.377	1.363.480
E16.8_p3	2.357.782	90%	1.302.557	75.886	6.505	691.882
E16.9_p3	1.241.578	89%	755.650	41.019	5.597	400.440
E11.1_p3	1.367.911	88%	796.982	54.145	5.869	440.236
E11.2_p3	3.483.479	91%	2.212.214	111.307	6.665	1.278.410
E11.3_p3	1.834.149	90%	1.190.849	58.345	5.765	655.806
E11.4_p3	8.352.228	90%	5.188.133	238.601	7.601	3.000.471
E11.5_p3	4.364.058	90%	2.891.704	130.121	6.954	1.642.287
E11.6_p3	31.107	85%	18.447	261	216	1.045
E11.7_p3	100.289	84%	50.032	2.666	1.419	15.293
E11.8_p3	2.392.645	90%	1.564.471	71.512	6.024	848.358

E14.1_p2	5.423.343	90%	3.577.154	189.025	7.390	2.006.453
E14.2_p2	5.278.511	89%	3.211.369	157.273	7.427	1.725.599
E14.3_p2	1.752.728	90%	1.137.290	56.431	6.035	589.384
E14.4_p2	1.803.850	90%	1.163.582	71.983	6.333	601.206
E14.5_p2	1.861.393	89%	1.181.417	65.054	6.243	613.073
E14.6_p2	4.584.879	89%	3.105.469	140.255	7.279	1.667.861
E14.7_p2	2.986.164	90%	1.900.664	107.522	6.966	1.060.522
E14.8_p2	210.133	90%	84.180	5.029	2.274	14.808
E15.1_p2	388.988	82%	149.687	23.892	4.639	62.059
E15.2_p2	6.540.522	91%	4.130.170	156.960	7.343	2.348.421
E15.3_p2	5.306.400	90%	3.477.480	139.949	7.177	1.977.386
E15.4_p2	232.592	88%	126.840	7.275	2.691	59.799
E15.5_p2	1.087.197	90%	682.145	35.909	5.240	358.261
E15.6_p2	2.140.465	90%	1.415.147	81.403	6.552	812.163
E2.1_p1	2.017.591	91%	1.301.448	76.616	6.452	698.734
E2.2_p1	1.438.567	91%	1.009.960	43.309	5.348	585.032
E2.3_p1	1.530.360	91%	1.021.546	48.109	5.693	549.746
E2.4_p1	2.394.571	89%	1.573.168	61.729	5.925	908.156
E2.5_p1	1.194.954	91%	715.114	33.663	5.070	372.875
E2.6_p1	1.041.759	91%	693.928	29.184	4.866	360.359
E2.7_p1	1.349.760	90%	934.746	49.264	5.683	500.989
E2.8_p1	7.580	77%	3.600	131	106	462
E2.9_p1	1.687.878	90%	1.030.766	61.780	6.063	527.843
E2.10_p1	1.806.208	91%	1.160.519	46.836	5.648	611.734
E2.11_p1	1.785.101	90%	1.226.962	54.151	5.730	705.344
E2.12_p1	87.483	88%	46.516	2.101	1.274	19.796
E2.13_p1	870.011	89%	532.522	25.916	4.605	272.246
E2.14_p1	1.394.605	90%	883.201	43.669	5.395	490.327
E2.15_p1	1.232.789	91%	783.593	32.377	5.064	394.694
E3.1_p1	484.659	88%	301.101	19.806	4.316	143.636
E3.2_p1	856.134	89%	410.829	21.090	4.383	173.911
E3.3_p1	63.987	88%	36.701	2.794	1.601	10.888
E3.4_p1	80.521	90%	11.188	17	15	18
E3.5_p1	845.288	88%	482.586	27.858	4.886	212.247
E3.6_p1	1.553.963	89%	1.058.614	38.977	5.308	459.240
E3.7_p1	620.395	89%	427.105	14.349	3.535	149.818
E3.8_p1	528.305	88%	307.432	15.121	3.842	143.592
E3.9_p1	426.958	87%	281.918	12.473	3.478	117.755
E3.10_p1	1.237.362	89%	729.772	30.439	5.113	256.207
E3.11_p1	742.877	89%	439.513	24.431	4.608	187.921
E3.12_p1	448.514	89%	261.059	17.415	4.071	120.318
E3.13_p1	989.028	90%	598.738	27.275	4.870	213.488

E3.14_p1	525.728	89%	279.837	19.880	4.336	112.326
E3.15_p1	44.312	86%	22.804	1.608	1.100	4.095
E3.16_p1	721.139	90%	363.933	27.384	4.928	134.324
E10.1_p1	678.898	91%	428.182	26.960	4.818	189.882
E10.2_p1	135.710	86%	69.621	6.504	2.710	29.734
E10.3_p1	450.136	90%	274.323	15.936	3.973	126.464
E10.4_p1	872.973	90%	523.998	43.565	5.657	230.927
E10.5_p1	456.202	90%	285.617	17.719	4.025	149.398
E10.6_p1	381.453	91%	226.686	15.954	3.973	100.629
E10.7_p1	934.996	90%	551.167	30.459	5.009	250.204
E10.8_p1	855.873	91%	565.245	32.500	5.065	255.466
E10.9_p1	603.654	90%	355.595	22.487	4.545	152.345
E10.10_p1	1.159.038	90%	728.391	48.477	5.685	326.292
E10.11_p1	276.785	89%	179.612	9.443	2.961	85.648
E10.12_p1	1.115.059	90%	723.902	33.903	5.113	314.641
E10.13_p1	711.883	91%	489.964	23.969	4.224	267.040
E10.14_p1	540.288	89%	256.378	23.578	4.650	98.472
E10.15_p1	1.055.395	90%	671.050	30.536	4.936	307.538
E10.16_p1	504.032	88%	73.522	5.543	2.015	29.192
E16.1_p1	978.007	87%	633.021	16.849	3.365	357.514
E16.2_p1	263.699	92%	50.136	3.472	1.781	19.789
E16.3_p1	1.962.716	91%	1.005.093	23.364	4.255	432.581
E16.4_p1	3.551.203	90%	2.348.935	48.907	5.375	1.138.934
E16.5_p1	1.730.919	91%	1.057.360	23.695	4.159	528.138
E16.6_p1	2.057.572	88%	1.100.607	27.582	4.377	576.931
E16.7_p1	1.410.131	90%	823.233	20.479	3.750	393.791
E16.8_p1	1.547.770	89%	1.009.226	16.546	3.479	346.615
E16.9_p1	3.278.847	89%	2.115.466	21.560	4.029	499.113
E16.10_p1	2.353.477	91%	1.273.060	49.694	5.251	1.101.034
E16.11_p1	5.352.561	91%	3.782.308	30.466	4.656	592.325
E16.12_p1	126.296	88%	66.982	59.744	5.597	1.657.147
E16.13_p1	2.547.637	92%	1.482.645	2.454	1.337	31.906
E6.1_p3	3.313.306	92%	2.150.788	32.716	5.024	823.510
E6.2_p3	583.519	90%	378.301	45.381	5.569	1.169.480
E6.3_p3	2.100.105	91%	1.305.781	8.492	2.616	188.154
E6.4_p3	2.479.727	92%	1.600.455	25.255	4.464	685.815
E6.5_p3	3.079.072	92%	1.808.938	34.583	5.080	847.247
E6.6_p3	630.145	90%	404.914	41.288	5.341	975.402
E6.7_p3	2.961.826	92%	1.982.352	8.565	2.634	200.862
E6.8_p3	1.062.727	91%	555.389	41.374	5.323	1.109.401
E6.9_p3	2.657.791	91%	1.330.700	16.169	3.790	281.977
E6.10_p3	230.403	90%	144.143	32.160	4.902	724.045

E6.11_p3	915.062	90%	585.769	3.418	1.524	70.076
E6.12_p3	202.696	89%	119.715	15.307	3.644	305.049
E6.13_p3	1.824.904	92%	1.209.171	2.924	1.306	53.800
E6.14_p3	1.063.553	91%	431.226	22.301	4.283	600.025
E6.15_p3	2.859.582	91%	1.945.259	11.750	3.339	226.671
E6.16_p3	1.050.413	91%	547.533	40.572	5.280	1.087.451
E6.17_p3	2.078.362	91%	1.234.388	12.049	3.289	275.806
E13.1_p3	972.669	90%	594.197	23.187	4.256	582.905
E13.2_p3	2.951.080	92%	1.918.743	12.871	3.403	283.369
E13.3_p3	2.013.883	90%	1.201.116	29.662	4.675	772.380
E13.4_p3	3.617.751	91%	2.579.678	22.733	4.163	558.663
E13.5_p3	2.372.234	91%	1.718.379	42.413	5.039	1.240.214
E13.6_p3	681.274	90%	405.259	24.742	4.148	705.386
E13.7_p3	1.762.899	89%	1.236.018	11.054	3.190	190.909
E13.8_p3	4.024.786	91%	2.792.992	24.503	4.372	576.064
E13.9_p3	3.348.857	91%	2.391.799	42.248	5.172	1.226.338
E13.10_p3	3.211.189	91%	2.363.796	36.518	4.828	1.083.887
E13.11_p3	3.114.785	92%	2.035.993	36.888	4.987	1.142.351
E13.12_p3	9.530.527	91%	6.860.570	31.623	4.583	925.047
E13.13_p3	1.673.906	90%	1.171.403	111.463	6.701	3.310.101
E13.14_p3	1.527.381	91%	940.115	20.368	3.853	570.780
E6.1_p2	458.157	90%	324.448	21.557	4.107	418.933
E6.2_p2	544.509	87%	358.015	5.513	1.991	142.990
E6.3_p2	2.156.427	90%	1.448.085	8.154	2.253	177.198
E6.4_p2	19.459	85%	12.502	24.784	4.150	604.287
E6.5_p2	1.820.218	89%	1.131.162	209	165	3.544
E6.6_p2	711.367	89%	459.833	23.777	4.302	534.044
E6.7_p2	1.059.032	90%	728.727	9.834	2.759	210.865
E6.8_p2	1.753.787	89%	1.116.952	11.908	3.004	338.414
E6.9_p2	1.400.226	89%	923.803	32.188	4.938	498.505
E6.10_p2	1.798.549	90%	1.103.207	18.695	3.807	431.391
E6.11_p2	3.138.766	91%	2.277.734	26.017	4.493	448.929
E6.12_p2	1.176.448	89%	795.060	34.686	4.767	1.033.905
E6.13_p2	1.810.894	89%	1.073.477	15.574	3.584	386.426
E6.14_p2	3.535.062	89%	2.304.901	21.489	4.161	519.083
E6.15_p2	1.272.423	88%	755.965	42.258	5.315	914.185
E6.16_p2	1.082.173	87%	624.189	22.028	3.855	409.371
E7.1_p2	1.587.929	89%	1.032.524	16.790	3.497	322.032
E7.2_p2	1.485.246	87%	832.310	24.650	3.969	480.199
E7.3_p2	60.025	85%	36.780	22.632	3.621	469.965
E7.4_p2	268.611	89%	55.051	958	614	14.859
E7.5_p2	1.448.848	87%	905.615	2.928	1.575	18.495

E7.6_p2	2.578.354	89%	1.650.081	23.001	3.974	430.839
E7.7_p2	2.994.008	89%	1.790.120	33.598	4.422	755.616
E7.8_p2	2.337.832	88%	1.335.756	33.096	4.271	765.655
E7.9_p2	1.088.741	87%	692.077	33.586	4.206	745.095
E7.10_p2	841.510	86%	511.576	20.540	3.954	308.329
E7.11_p2	1.778.504	89%	1.152.046	18.256	3.707	254.304
E7.12_p2	2.548.699	89%	1.721.453	33.107	4.681	576.902
E7.13_p2	1.765.228	88%	1.101.797	36.242	4.571	788.034
E7.14_p2	3.000.717	90%	2.065.209	31.731	4.504	565.914
E7.15_p2	1.246.208	89%	748.377	40.442	5.037	922.306
E7.16_p2	1.163.853	90%	685.734	27.805	4.376	365.664

Supplementary Table S1. Row count. Information on the count of generated reads, uniquely mapped reads, unique molecular identifiers (UMIs), molecular identifiers (MIs), and detected genes.

Gene	sc3_6_markers_clusts	padj
DUSP1	4	3,19163E-17
UCHL1	1	3,46226E-15
PYCR2	4	3,6645E-15
MRPL17	4	3,69048E-15
BTG1	4	4,19081E-15
RNF11	4	4,49954E-15
XRCC2	1	1,48411E-14
SNHG12	4	3,15744E-14
LOC100196901	4	3,70682E-14
NETO1	1	9,00088E-14
PRNP	4	1,67764E-13
RPS19	4	1,75244E-13
COG2	1	1,91013E-13
ZNF2	1	2,18468E-13
TFAP2C	4	2,65079E-13
RACK1	4	2,80186E-13
PIP5K1A	4	3,69806E-13
SDS	4	3,70259E-13
TRIP4	1	4,26628E-13
ITPR1	5	5,12539E-13
RUFY2	1	6,73613E-13
RABGEF1	1	7,47336E-13
ARFGAP3	4	7,53523E-13

PRPS1	4	7,74517E-13
DYNC2LI1	3	8,85953E-13
SLC25A25	4	9,1132E-13
TPMT	1	9,80319E-13
GALNT13	1	1,11108E-12
RPL36AL	4	1,13246E-12
VKORC1	4	1,64992E-12
NUDT12	1	2,08732E-12
ARMT1	4	4,39041E-12
PLS1	1	4,67168E-12
FOLR1	4	5,56843E-12
TKT	4	7,98055E-12
AMIGO2	4	8,70221E-12
RPL26	4	9,06242E-12
HNRNPAB	4	9,50205E-12
TSEN54	4	9,50988E-12
GRO1	5	9,63135E-12
RHEBL1	2	1,4103E-11
CCNC	4	1,43501E-11
IL18	4	1,47224E-11
RPRD1A	4	1,66394E-11
DTWD1	1	2,19515E-11
PDE6C	1	2,33296E-11
COL1A1	4	2,6209E-11
DDX17	4	2,71957E-11
MIER2	1	2,95389E-11
PARP14	4	3,07252E-11
KDELC1	5	3,1476E-11
ERICH1	4	3,15137E-11
TIGAR	1	3,25596E-11
HAX1	4	3,4073E-11
LOC782781	4	4,24316E-11
C1H3orf58	4	4,78934E-11
PRR5	4	5,71604E-11
CCDC126	4	6,09051E-11
C1D	4	6,4692E-11
C8H9orf64	1	6,70047E-11
CEPT1	1	7,40371E-11
ANK3	1	7,47493E-11
CDV3	4	8,17086E-11
RASA1	1	8,61917E-11
PNP	4	8,78953E-11

DIABLO	4	1,06967E-10
F3	1	1,26512E-10
TMEM128	1	1,43898E-10
SNAPC1	4	1,47879E-10
SLC35D1	1	1,49719E-10
DPP4	1	1,5061E-10
TYW3	4	1,53583E-10
PSMA4	1	1,84571E-10
USP13	1	1,85677E-10
TIMM10B	4	2,07667E-10
ACAA1	1	2,09553E-10
ITM2B	4	2,16148E-10
YTHDF2	4	2,2118E-10
CREM	3	2,31335E-10
RSRP1	2	2,63661E-10
FAM207A	4	2,6939E-10
DNAJB9	4	2,79571E-10
INTS12	1	2,83159E-10
HIST1H2BD	4	2,85355E-10
TDH	4	2,98791E-10
SLC33A1	4	3,39143E-10
C29H11orf84	3	4,11135E-10
INPP1	1	4,12673E-10
RAP1A	1	5,01104E-10
FDPS	1	5,02972E-10
RWDD1	1	5,0301E-10
LEPROTL1	1	5,12055E-10
PPIL1	4	5,30125E-10
EXOSC1	4	5,48554E-10
RPS4Y1	4	6,01448E-10
CEP57L1	1	6,60645E-10
MPLKIP	4	6,60696E-10
IFT43	1	6,79212E-10
SNHG3	2	7,06082E-10
PQBP1	1	7,46609E-10
XRCC4	1	8,11396E-10
ZNF197	1	8,54631E-10
COX7A1	3	8,63411E-10
ANAPC5	1	8,71282E-10
ALAS1	1	8,91176E-10
ENDOV	1	9,46649E-10
CCDC85A	1	9,55386E-10

FASTKD3	1	1,02304E-09
MOB4	1	1,03737E-09
MYF5	1	1,26352E-09
RAB27B	1	1,30194E-09
ZNF75A	1	1,36245E-09
DGCR8	1	1,40902E-09
ARF4	1	1,43948E-09
LARS	1	1,55185E-09
NFYA	5	1,68622E-09
ZCCHC10	4	1,77536E-09
GART	4	1,89748E-09
MAP4K1	3	2,06387E-09
DESI2	4	2,11214E-09
RPS27	4	2,11679E-09
PDGFRA	4	2,19896E-09
IMP3	4	2,26836E-09
CD52	1	2,29483E-09
ENKD1	1	2,46527E-09
NOL11	4	2,6475E-09
PALB2	1	2,65143E-09
SLC35A3	1	2,67465E-09
RMDN3	1	2,81426E-09
ISG20L2	4	2,92537E-09
FBXL12	4	3,08325E-09
TBCA	1	3,11569E-09
ZNF330	1	3,20866E-09
MTHFD1L	4	3,24844E-09
TAF1D	4	3,81957E-09
CKAP5	1	3,97094E-09
ASZ1	1	4,07974E-09
MACROD1	1	4,21481E-09
POLR1C	4	4,38991E-09
EIF6	4	4,44851E-09
LGALS3	3	4,49756E-09
CBX3	4	4,49799E-09
SPESP1	1	4,81327E-09
ADI1	1	5,0669E-09
DCAF8	1	5,07549E-09
C8H4orf27	1	5,08988E-09
ZBTB9	4	5,12411E-09
ZFAND2B	4	5,32943E-09
TFDP2	1	5,60791E-09

EIF1AD	4	5,62308E-09
TMEM159	3	5,71454E-09
NOP16	4	6,2815E-09
ZNF879	1	6,31823E-09
CMC2	4	6,48633E-09
FAM89A	4	6,76758E-09
TMEM42	3	6,83483E-09
DSCC1	1	7,0952E-09
ATF7IP	4	7,34295E-09
ICA1	1	7,66567E-09
RCBTB1	1	7,86037E-09
LXN	4	8,21383E-09
DEPDC7	1	8,30102E-09
TGS1	4	8,40025E-09
PLA2G4A	1	8,42859E-09
DNAJA4	1	9,18969E-09
UQCC3	4	9,20551E-09
RMDN1	3	9,43449E-09
C3H1orf52	4	9,61933E-09
NME7	1	9,94759E-09
GPALPP1	1	1,00354E-08
GLRX2	2	1,04394E-08
ADHFE1	1	1,04959E-08
BORA	1	1,0629E-08
TCEB2	4	1,07568E-08
TMEM196	1	1,0771E-08
ARHGAP24	1	1,08472E-08
MGAT5	1	1,12336E-08
PUS7	4	1,15242E-08
LHX2	3	1,17527E-08
ZNF266	1	1,18925E-08
PIR	1	1,1968E-08
PRDM14	4	1,19687E-08
TMEM38B	1	1,21973E-08
RPL38	4	1,22444E-08
GLT8D1	1	1,26168E-08
GOLIM4	1	1,27811E-08
WRAP53	4	1,29403E-08
VPS45	1	1,3006E-08
NFU1	1	1,32353E-08
LARP4	4	1,32872E-08
COPB2	1	1,32906E-08

NLRP9	1	1,36909E-08
PEX5L	1	1,41165E-08
MFN2	1	1,46858E-08
LOC530773	3	1,50399E-08
ING1	4	1,53541E-08
ABCA1	1	1,53985E-08
TSPAN14	1	1,54826E-08
BRDT	4	1,5578E-08
ELP4	1	1,5696E-08
CLK1	4	1,59391E-08
GNPDA2	1	1,60016E-08
CHMP7	1	1,6118E-08
APBB1IP	1	1,61675E-08
C2CD5	1	1,64053E-08
ETV6	1	1,66813E-08
HIPK3	4	1,70586E-08
LDHC	1	1,70614E-08
SNAI1	2	1,71212E-08
ZNF133	1	1,92423E-08
BMPR1A	1	1,92831E-08
BMP4	4	1,93364E-08
FAM214B	4	1,95836E-08
CCSER1	1	1,97239E-08
BET1	1	1,98614E-08
TTC32	1	1,98821E-08
IFNGR1	1	2,01183E-08
RPH3AL	1	2,1126E-08
FAM175A	3	2,1706E-08
CLCN3	1	2,24827E-08
VANGL1	3	2,34614E-08
LOC538702	1	2,44114E-08
EFCAB7	1	2,54399E-08
ITGA4	1	2,59645E-08
AGPAT5	4	2,67182E-08
GCDH	1	2,8028E-08
HEXIM1	4	2,83701E-08
SAMD12	3	2,86603E-08
LIMK2	1	2,90128E-08
GNPNAT1	1	2,92014E-08
ACOT9	1	2,97939E-08
CADPS	1	3,01728E-08
CDKN2C	4	3,04157E-08

SMIM8	1	3,12319E-08
MTMR6	1	3,25492E-08
IPMK	4	3,35338E-08
TTC14	4	3,38309E-08
AIFM1	1	3,39759E-08
NANOG	4	3,43914E-08
OSTF1	1	3,4533E-08
GMPPA	1	3,51447E-08
DEF6	1	3,53058E-08
DHX9	4	3,69638E-08
PSTPIP1	1	3,94178E-08
CCNL1	5	3,96771E-08
HTATIP2	1	3,97208E-08
SLC27A1	4	3,97596E-08
SDF2	4	3,97883E-08
STK16	1	4,03451E-08
PRIMPOL	1	4,19026E-08
SDSL	1	4,21746E-08
WDR41	1	4,22941E-08
LIAS	1	4,42739E-08
TRIM23	1	4,45806E-08
RNF144B	1	4,51131E-08
EXOC6	1	4,56677E-08
VPS16	1	4,63143E-08
LPPR1	1	4,63236E-08
DISP3	1	4,65133E-08
NDUFC1	1	4,68752E-08
KLF3	4	4,78944E-08
FBXO38	1	4,90218E-08
MNF1	1	5,04428E-08
PPM1H	1	5,1051E-08
ZNF746	3	5,16426E-08
UACA	1	5,16845E-08
PBRM1	5	5,22857E-08
NAA11	4	5,37618E-08
MAD1L1	1	5,57693E-08
ECE2	4	5,60028E-08
TMEM41B	4	5,72233E-08
AP5S1	1	5,72836E-08
ABCB7	1	5,80744E-08
ZNF408	4	6,27171E-08
CNDP1	1	6,30996E-08

ARL14EPL	3	6,64328E-08
SEPT4	1	6,71677E-08
MED23	1	6,76048E-08
MRPL42	1	6,77048E-08
ZWILCH	1	6,83961E-08
NDUFB2	4	6,87129E-08
C23H6orf62	4	6,92059E-08
RAB7B	3	6,94937E-08
ATXN7L3	4	7,18276E-08
DAG1	3	7,19543E-08
GMPS	1	7,20854E-08
GOPC	1	7,27207E-08
PICK1	1	7,46989E-08
ZSCAN12	1	7,50106E-08
MKLN1	1	7,5481E-08
NFXL1	1	7,81534E-08
MKRN1	4	7,82952E-08
SLC1A1	1	7,92608E-08
OXSM	3	8,05007E-08
AACS	3	8,29841E-08
CXCL3	5	8,31593E-08
MT3	3	8,35287E-08
PHF5A	4	8,82837E-08
LIPE	1	8,86413E-08
MGA	4	8,86413E-08
GNB5	1	9,12954E-08
ANAPC13	1	9,31696E-08
KRR1	4	9,33508E-08
NNT	3	9,34465E-08
HACL1	1	9,87804E-08
BRF2	4	1,00833E-07
CDKAL1	1	1,02613E-07
RAB3IP	1	1,03452E-07
KCTD20	4	1,07114E-07
ME1	1	1,08382E-07
SNHG4	4	1,11707E-07
CCDC86	4	1,11941E-07
PSMA1	4	1,12878E-07
MPHOSPH6	1	1,15002E-07
MCFD2	1	1,21147E-07
KLF5	4	1,22365E-07
GADD45GIP1	1	1,25923E-07

RANBP2	4	1,29326E-07
C4H7orf57	1	1,29667E-07
SLC6A20	3	1,32324E-07
JUP	4	1,34127E-07
MED4	1	1,34988E-07
HUWE1	4	1,35782E-07
G3BP2	5	1,36603E-07
UBASH3B	1	1,42506E-07
MRPL38	1	1,42532E-07
UCK2	4	1,49289E-07
MCPH1	1	1,49296E-07
NQO1	1	1,49438E-07
DPH5	1	1,50008E-07
DAPL1	1	1,50798E-07
HERC3	1	1,5363E-07
SLC25A51	1	1,55429E-07
EGR4	1	1,55772E-07
MTMR1	1	1,56745E-07
ATP9B	1	1,56827E-07
IMPACT	4	1,56827E-07
ASPSCR1	1	1,58179E-07
SNRPB	4	1,58989E-07
SESTD1	1	1,60745E-07
CD3G	1	1,61182E-07
CBX1	1	1,62879E-07
MNS1	1	1,63357E-07
TFCP2	1	1,64009E-07
THEM4	1	1,64507E-07
CEP120	1	1,66286E-07
GJA4	1	1,66949E-07
STK25	1	1,69647E-07
CCDC172	1	1,6992E-07
CCNL2	4	1,71981E-07
RPS9	4	1,72533E-07
VIMP	4	1,73295E-07
NLRP5	1	1,77011E-07
CERS3	3	1,81777E-07
LYPLAL1	1	1,82473E-07
C3H1orf228	1	1,85123E-07
BBS2	1	1,8914E-07
RAB31	1	1,89575E-07
LRRC8C	1	1,93125E-07

FAM216A	1	1,98055E-07
COTL1	4	1,98418E-07
THBS4	1	1,99177E-07
ZMAT5	4	2,00116E-07
PSMD5	1	2,00679E-07
LRRC1	1	2,1202E-07
PTTG1IP	1	2,18208E-07
MKRN2	1	2,18309E-07
DPYSL2	4	2,18671E-07
ANKRD16	1	2,19575E-07
CRLS1	1	2,20763E-07
IPO7	4	2,20763E-07
FRA10AC1	1	2,21084E-07
VDAC3	3	2,27973E-07
NDEL1	1	2,30481E-07
MAPK1	1	2,30587E-07
GPR158	1	2,3126E-07
SCO1	4	2,31621E-07
SMAD1	1	2,33137E-07
EWSR1	4	2,33579E-07
EEF2KMT	3	2,33919E-07
LRRC40	4	2,34432E-07
PGM2L1	1	2,35481E-07
PRKCH	1	2,35718E-07
PRICKLE1	1	2,38277E-07
PRDM6	1	2,44217E-07
GRHPR	1	2,44862E-07
TMEM223	4	2,47354E-07
CUTC	1	2,47526E-07
KIAA0922	1	2,50076E-07
PITX2	4	2,52829E-07
TEX261	3	2,56322E-07
DIAPH2	1	2,58336E-07
WDR34	1	2,66635E-07
RPL10A	4	2,66934E-07
STK39	1	2,73831E-07
PRPS2	1	2,76999E-07
DNA2	1	2,83878E-07
KLF10	4	2,92507E-07
PRDX5	1	2,92876E-07
MTG1	1	2,98026E-07
MYO6	1	3,02371E-07

IQCC	1	3,0306E-07
NKAPL	4	3,044E-07
VAT1	1	3,05004E-07
DNMBP	1	3,07444E-07
LMO1	1	3,35397E-07
ZNF296	2	3,40946E-07
CMTM8	1	3,45163E-07
SLC4A4	1	3,45667E-07
HPS3	1	3,49231E-07
PPM1K	4	3,78709E-07
NUP37	1	3,81705E-07
ZNF345	1	3,82427E-07
COLEC12	1	3,85007E-07
RPS29	4	3,94228E-07
CDK1	4	3,94532E-07
WDR55	4	3,94541E-07
RALYL	1	3,96782E-07
METTL12	4	3,99785E-07
MRPL43	3	4,00801E-07
TNFSF12	3	4,02026E-07
PAXBP1	4	4,11458E-07
MRPL14	1	4,141E-07
GABPB1	1	4,17339E-07
CDK20	2	4,17835E-07
PHLDB1	1	4,2678E-07
PSMG1	1	4,30733E-07
MTMR3	1	4,315E-07
VWA9	1	4,33378E-07
NIPA2	4	4,39402E-07
MAP4K5	1	4,47833E-07
CNN2	3	4,60029E-07
SCP2	1	4,65729E-07
LSS	5	4,71869E-07
PARP1	1	4,75091E-07
HTRA2	1	4,79654E-07
PTGR2	1	4,96511E-07
PTGFR	4	5,0203E-07
OTUD7B	1	5,04926E-07
TMEM150A	3	5,06519E-07
TTK	1	5,07875E-07
CAD	4	5,08804E-07
TXNIP	1	5,1631E-07

NCBP2	4	5,17707E-07
LHFPL4	1	5,17797E-07
SYNRG	1	5,18043E-07
MCM5	1	5,23965E-07
PLEKHO1	1	5,2718E-07
JMJD6	4	5,27702E-07
MTFMT	1	5,28842E-07
CNKSR1	3	5,31184E-07
TMEM50B	1	5,64758E-07
TMEM219	3	5,6551E-07
ZAR1	1	5,68072E-07
LOC100848703	1	5,71233E-07
VWF	1	5,7866E-07
BMPR1B	1	5,9483E-07
ALG14	3	6,00511E-07
TRAF3IP1	1	6,06093E-07
BCKDK	1	6,12594E-07
RAPGEF4	1	6,25979E-07
ATIC	1	6,32902E-07
ZNF395	3	6,64882E-07
METTL14	1	6,682E-07
RIC3	1	6,82601E-07
CLHC1	1	6,83469E-07
BRI3	3	6,93051E-07
RIIAD1	3	6,93933E-07
SUV39H2	1	7,02516E-07
TBC1D19	3	7,06088E-07
CEP44	1	7,13511E-07
BFAR	1	7,28502E-07
PCDH8	4	7,31367E-07
SNX2	1	7,46102E-07
UBASH3A	1	7,50187E-07
HVCN1	1	7,60446E-07
CEP41	3	7,80115E-07
MGC148714	3	7,81972E-07
MZB1	1	8,3339E-07
SYNM	1	8,34288E-07
EBPL	1	8,44408E-07
FAM213A	1	8,46266E-07
LCP1	3	8,47368E-07
KCNJ3	1	8,63353E-07
TMIGD1	1	8,70335E-07

ORC4	1	8,71025E-07
VPS25	1	8,74117E-07
RPL6	4	8,87859E-07
SCML2	1	8,88442E-07
MID1	1	9,07332E-07
GALK2	1	9,11876E-07
SPATA22	1	9,14146E-07
CRIM1	1	9,59028E-07
PRDX3	1	9,73771E-07
TMEM266	1	9,96732E-07
RCOR2	3	1,00105E-06
C5H12orf66	1	1,00882E-06
METTL6	1	1,08636E-06
TMEM242	1	1,09852E-06
NRBP1	5	1,1007E-06
CSRNP2	4	1,1011E-06
BUB1B	1	1,10361E-06
FKBP3	4	1,11614E-06
POLI	1	1,1225E-06
DNAJC15	3	1,16074E-06
CYSTM1	3	1,17542E-06
CROT	5	1,17551E-06
TMEM50A	3	1,19121E-06
KCTD3	1	1,21883E-06
RNASEH2C	4	1,21895E-06
ETS1	1	1,22399E-06
COQ2	1	1,23982E-06
B3GALNT2	1	1,24069E-06
ARPC4	1	1,24126E-06
GLS2	1	1,24845E-06
GABPA	4	1,25357E-06
PLEKHA8	1	1,26671E-06
SOCS2	5	1,27634E-06
ABCG5	1	1,27779E-06
TBCEL	1	1,27792E-06
ZMYM1	4	1,30548E-06
EML5	1	1,30915E-06
ATXN7L1	1	1,32038E-06
LYRM7	1	1,33738E-06
UROS	1	1,348E-06
TDRD7	1	1,36378E-06
NT5E	1	1,42406E-06

ZNF548	1	1,43437E-06
CNPPD1	1	1,44183E-06
RPL37	4	1,46989E-06
MOV10	1	1,47934E-06
PLEKHM3	1	1,52716E-06
SORBS1	1	1,53572E-06
NSMCE1	1	1,54571E-06
SKAP2	1	1,54988E-06
BBS5	1	1,56712E-06
ACSL3	1	1,56976E-06
TJP2	1	1,57783E-06
FTH1	3	1,62537E-06
NUDT22	1	1,64212E-06
EPC1	3	1,64954E-06
QTRT2	1	1,65619E-06
BCL2L12	4	1,66841E-06
CBR1	1	1,67579E-06
PON2	1	1,71989E-06
IMPDH1	4	1,72543E-06
KTI12	4	1,74985E-06
IRF6	1	1,78807E-06
DPPA2	4	1,81746E-06
FBN1	3	1,83043E-06
AKR1A1	1	1,84347E-06
DLD	4	1,84585E-06
PPP4R3A	4	1,8684E-06
PLXDC2	1	1,87219E-06
FAM21A	5	1,87242E-06
CHMP2B	1	1,88247E-06
ANO5	1	1,88358E-06
LRRC6	1	1,90753E-06
DENND2C	4	1,98051E-06
ARHGAP26	1	1,99784E-06
FRS3	1	2,02602E-06
IL1R1	1	2,02944E-06
GPR1	1	2,05102E-06
C7H5orf45	1	2,08935E-06
SGCE	1	2,08935E-06
SRSF6	2	2,10295E-06
MSMO1	1	2,10667E-06
SERP2	3	2,10823E-06
RTN2	4	2,12321E-06

CRYZL1	1	2,1279E-06
RPE	4	2,13889E-06
EHMT1	1	2,16692E-06
TFAM	4	2,18344E-06
ACSL5	5	2,18653E-06
MICU1	4	2,19154E-06
ZNF438	1	2,19212E-06
NAB1	1	2,22477E-06
ZNF35	1	2,22748E-06
SEC22B	1	2,24992E-06
HAGH	1	2,2993E-06
UBA3	1	2,30854E-06
AP1S1	1	2,32773E-06
TMEM167B	1	2,34635E-06
LOC789175	4	2,35248E-06
MANF	4	2,35281E-06
PARK2	1	2,36339E-06
MBIP	4	2,40168E-06
CDK5RAP1	1	2,42124E-06
ZNF713	1	2,43167E-06
UQCRFS1	4	2,45005E-06
PRSS23	3	2,45429E-06
COX20	1	2,50766E-06
AMN1	1	2,50846E-06
LZTFL1	1	2,51824E-06
EPS15L1	1	2,54296E-06
HILPDA	1	2,55432E-06
SLC38A8	3	2,57296E-06
GSTA2	4	2,57331E-06
DNAJC11	3	2,61057E-06
TMEM186	4	2,62176E-06
ODF4	1	2,63147E-06
TUBGCP4	1	2,63358E-06
DLST	1	2,64865E-06
NOL6	4	2,67074E-06
CXADR	4	2,69602E-06
RBMX	4	2,69724E-06
FZD3	1	2,70677E-06
TOB1	4	2,71252E-06
PTPRF	1	2,73373E-06
ORC6	1	2,74575E-06
CYCT	4	2,76467E-06

PSMD6	1	2,7934E-06
TM9SF1	1	2,79637E-06
SLC25A31	3	2,81898E-06
SLC24A2	1	2,83562E-06
ALKBH3	1	2,8471E-06
COQ8A	3	2,91578E-06
ZNF22	1	2,92361E-06
EFTUD2	1	2,94302E-06
GJD2	1	3,03497E-06
TMEM168	1	3,03497E-06
SH2B1	1	3,05681E-06
YPEL3	3	3,09345E-06
TMEM101	1	3,10296E-06
ATG4D	4	3,10811E-06
TMEM161A	1	3,1191E-06
SUPV3L1	1	3,17727E-06
DNAJB4	1	3,20085E-06
APOO	1	3,2178E-06
ROBO1	1	3,23037E-06
KLHDC2	1	3,24824E-06
PREP	1	3,29614E-06
SOX30	1	3,3045E-06
CCT4	4	3,38417E-06
EED	4	3,4271E-06
SOCS7	3	3,44729E-06
MPV17L2	1	3,45434E-06
F11R	4	3,49833E-06
ALDH1A1	1	3,51421E-06
MTM1	1	3,5155E-06
TXNDC5	1	3,55539E-06
PRPF3	1	3,58658E-06
MEDAG	4	3,66654E-06
CAB39	1	3,68164E-06
SNX19	3	3,69942E-06
MESDC1	4	3,79639E-06
RTN4	2	3,79775E-06
RNF44	4	3,80896E-06
MYL12B	1	3,81013E-06
UTP18	5	3,85036E-06
ZBTB6	1	3,86509E-06
C15H11orf74	1	3,90326E-06
DPH2	1	3,91133E-06

SDF2L1	1	3,91263E-06
PSMB7	1	3,91926E-06
PMPCB	1	3,92406E-06
LACC1	1	3,93926E-06
FAM72A	1	3,94538E-06
TSC22D1	4	3,94864E-06
FAM76B	1	3,99972E-06
UBE2L6	1	4,02458E-06
SIPA1L2	1	4,13407E-06
CLCC1	3	4,15782E-06
HDGF	3	4,17356E-06
C20H5orf47	1	4,26233E-06
FAM45A	4	4,3261E-06
TMEM39A	3	4,36023E-06
ZNF692	1	4,42323E-06
CASP2	1	4,45322E-06
NR2F2	4	4,50962E-06
PPAT	4	4,5709E-06
UFL1	1	4,61169E-06
SPATA2L	3	4,61693E-06
SCCPDH	3	4,68562E-06
LSM8	4	4,70706E-06
TTC4	1	4,7889E-06
IFT88	1	4,81228E-06
PLEKHJ1	4	4,92065E-06
HARS	1	4,99265E-06
JUN	1	5,00038E-06
COPRS	1	5,02396E-06
ZNF184	1	5,08874E-06
PDPN	1	5,10833E-06
ELMOD2	1	5,18102E-06
SNAPC5	4	5,19944E-06
RTKN2	1	5,20383E-06
TMX4	1	5,21588E-06
NDUFS4	1	5,2671E-06
NPC1	5	5,35579E-06
SRI	1	5,43197E-06
SLC16A13	1	5,51399E-06
MAP4	3	5,53716E-06
LUZP2	1	5,54525E-06
PEX3	1	5,58656E-06
RUNDC1	1	5,60636E-06

SIRT1	4	5,61216E-06
RAB3GAP1	5	5,61261E-06
C14H8orf59	4	5,63431E-06
QARS	4	5,64074E-06
RDH12	1	5,6642E-06
RPL13A	4	5,67315E-06
ZNRF1	4	5,70061E-06
CDH7	1	5,72375E-06
SASS6	1	5,73426E-06
DCTN3	1	5,7818E-06
TMX3	1	5,79351E-06
NSMCE2	1	5,8117E-06
DDRGK1	1	5,88662E-06
PMS1	1	6,01496E-06
C11H2orf49	3	6,19342E-06
EIF2B3	3	6,1981E-06
IDE	1	6,29635E-06
TMEM100	1	6,36518E-06
NRBF2	4	6,38535E-06
SEMA4A	1	6,45739E-06
PCYT1B	1	6,51251E-06
SYT11	4	6,51582E-06
NOL8	4	6,59123E-06
TRAPPC13	4	6,66253E-06
ANKRD50	4	6,73795E-06
ZAK	1	6,75989E-06
TGFBRAP1	1	6,82721E-06
PRKG1	3	6,89694E-06
NCAPH	1	7,03305E-06
NECAP1	4	7,06405E-06
STXBP5	1	7,07236E-06
TSTD3	1	7,13407E-06
MFSD13A	1	7,26535E-06
TMEM45A	1	7,28436E-06
ITGA2B	4	7,34353E-06
NKX2-2	1	7,34353E-06
RDH14	1	7,40151E-06
GPATCH1	3	7,68982E-06
PXMP4	1	7,73642E-06
TAF11	4	7,79406E-06
NFKBIB	4	7,86984E-06
RNF219	1	7,96974E-06

CDCA7	1	7,97139E-06
MRPS35	1	8,03397E-06
SPATA24	1	8,06356E-06
LTBR	1	8,06982E-06
TIMELESS	1	8,13859E-06
WDFY2	3	8,25045E-06
ALG8	1	8,32588E-06
ZCCHC7	1	8,34476E-06
MCC	1	8,366E-06
GPATCH2	1	8,37165E-06
TIFA	1	8,38114E-06
UNC50	1	8,41033E-06
SPON1	1	8,47038E-06
CCDC91	1	8,48912E-06
ATP6V0C	1	8,58808E-06
FBXO10	3	8,6654E-06
CRYM	4	8,6823E-06
VPS26A	1	8,69839E-06
MRAP2	1	8,75973E-06
COMMD2	1	8,76027E-06
TIMM17B	1	8,82549E-06
ARHGEF12	1	8,9861E-06
MAP2K1	1	9,00534E-06
PLCL2	3	9,01535E-06
MYC	4	9,07149E-06
NSG1	1	9,08039E-06
COL4A3BP	5	9,2755E-06
DYRK3	5	9,38731E-06
AKAP6	1	9,55267E-06
DICER1	1	9,61043E-06
PCDH10	4	9,66191E-06
TMEM86A	1	9,77883E-06
RPAP1	1	9,78134E-06
ILDR1	3	9,79006E-06
RARG	1	9,83356E-06
LMX1A	1	9,92271E-06
NADK2	1	9,97423E-06
LMOD3	1	1,00436E-05
IFT52	1	1,0077E-05
MED9	4	1,00804E-05
JMJD1C	1	1,04827E-05
ADAMTS1	2	1,0565E-05

ATP5G2	1	1,06575E-05
MIER3	1	1,06926E-05
PUS7L	1	1,0705E-05
ZW10	1	1,07317E-05
BLZF1	1	1,0798E-05
KIAA0754	1	1,08573E-05
ACAD11	1	1,08614E-05
ARHGEF39	1	1,08927E-05
TRIM59	3	1,09276E-05
FEN1	4	1,09481E-05
NFKBIE	1	1,09952E-05
DUSP5	1	1,10414E-05
ATP10D	1	1,1058E-05
DSTYK	1	1,11329E-05
PRKCI	1	1,11409E-05
P4HA3	1	1,14299E-05
DNAL4	3	1,14546E-05
SEC16B	3	1,14954E-05
BSDC1	1	1,15298E-05
ADAMTS9	1	1,16223E-05
SLC40A1	1	1,16306E-05
MRPL33	1	1,18592E-05
OSBPL11	1	1,19738E-05
GLOD4	1	1,2015E-05
NUPL2	4	1,20451E-05
RNASEH1	4	1,22028E-05
C1H21orf33	1	1,22155E-05
GAB1	1	1,22716E-05
THUMPD3	1	1,2357E-05
DCTN1	1	1,24104E-05
PFKFB3	1	1,24168E-05
TBC1D2	4	1,26374E-05
GADD45B	1	1,2878E-05
SORCS3	1	1,28791E-05
CHD8	4	1,29631E-05
PPP3R1	1	1,31934E-05
OVOL1	1	1,32976E-05
LOC100847759	4	1,34232E-05
TMEM184B	1	1,34451E-05
ENO1	1	1,34486E-05
MECP2	3	1,34486E-05
WDR61	1	1,3523E-05

MRPL3	1	1,36781E-05
MTIF2	1	1,3816E-05
ATP5A1	1	1,40596E-05
MDGA1	1	1,40927E-05
STAP2	1	1,42219E-05
TAF13	4	1,42329E-05
ITGB4	1	1,44699E-05
PPP1R21	1	1,4487E-05
RBAK	4	1,45591E-05
UCHL5	1	1,46931E-05
STX17	1	1,47249E-05
CCDC50	3	1,47413E-05
RECQL	1	1,49872E-05
SOD2	1	1,53397E-05
PGAM5	3	1,53576E-05
FANCM	1	1,53623E-05
NDUFAF7	1	1,54785E-05
FAM76A	1	1,54969E-05
SLC9A9	1	1,5578E-05
ZNF135	1	1,56296E-05
ETFDH	1	1,56638E-05
PRDX6	3	1,56801E-05
WDPCP	1	1,58926E-05
MND1	1	1,59629E-05
RPAIN	1	1,59726E-05
C10H14orf1	1	1,60382E-05
MAPK1IP1L	4	1,60611E-05
CLIP1	6	1,62183E-05
RAD52	3	1,63089E-05
TMA16	1	1,66118E-05
SLC17A5	1	1,66737E-05
ZNF419	1	1,6825E-05
PIH1D2	1	1,69865E-05
ZMAT3	1	1,71195E-05
UIMC1	1	1,71248E-05
RNF130	1	1,72359E-05
PCCB	1	1,7262E-05
NDUFA12	3	1,7304E-05
MTMR14	4	1,73783E-05
SLC25A15	1	1,7383E-05
ANKRD39	3	1,75236E-05
ARHGAP1	4	1,75408E-05

CISD2	1	1,75963E-05
LOC613444	4	1,77128E-05
FBXO11	5	1,773E-05
DPP6	1	1,77348E-05
ST5	1	1,7836E-05
IGFBP3	1	1,78818E-05
ARFIP2	1	1,80335E-05
OIP5	1	1,8098E-05
PATJ	1	1,81588E-05
ARNTL	3	1,82145E-05
GFPT2	1	1,82807E-05
MRPS15	3	1,85354E-05
C4H7orf25	3	1,85897E-05
SNX4	1	1,86337E-05
BAMBI	4	1,86485E-05
NIPAL1	4	1,86921E-05
KATNBL1	3	1,86925E-05
CAPN14	1	1,9019E-05
CPB2	1	1,91098E-05
SCG3	1	1,91971E-05
IPP	1	1,94646E-05
NDUFB3	4	1,94994E-05
DDA1	1	1,96373E-05
FLAD1	1	1,9839E-05
DTX2	1	1,99508E-05
COQ7	1	2,01552E-05
ST7L	1	2,03921E-05
LUC7L	4	2,05431E-05
ATP23	4	2,07907E-05
GHDC	3	2,11914E-05
ODZ3	1	2,1772E-05
HAUS4	1	2,23576E-05
TRIM52	1	2,24358E-05
PIH1D1	4	2,28904E-05
ARL4D	2	2,30246E-05
MAGOHB	1	2,30367E-05
RAB6B	1	2,34365E-05
TTF2	1	2,34689E-05
SSSCA1	4	2,34999E-05
DTX1	1	2,36564E-05
SNX11	1	2,37992E-05
HACE1	1	2,38917E-05

HKDC1	1	2,39252E-05
ZBTB40	1	2,39857E-05
YTHDF1	1	2,41698E-05
DIRC2	1	2,43405E-05
GTF2I	1	2,48933E-05
CPSF6	4	2,51672E-05
SDHAF3	1	2,51786E-05
TMEM110	1	2,5349E-05
TCIRG1	1	2,53495E-05
SMAD3	1	2,5524E-05
CXXC1	1	2,57434E-05
ELK3	1	2,59572E-05
OMA1	1	2,60376E-05
PDSS2	1	2,6088E-05
USP3	4	2,61972E-05
CDK14	1	2,68195E-05
METTL3	1	2,71201E-05
UBXN1	1	2,71549E-05
RNF181	1	2,7684E-05
PEX5	1	2,80148E-05
FBXO3	1	2,81177E-05
WDR74	4	2,82611E-05
TTLL4	1	2,86623E-05
CAT	1	2,86709E-05
TSPYL4	1	2,89684E-05
WDR48	1	2,91989E-05
IP6K1	1	2,9309E-05
PRRG2	4	2,95881E-05
ZNF397	1	2,9772E-05
EXOSC9	1	3,02059E-05
LSM12	3	3,0481E-05
CPNE1	3	3,04999E-05
EIF3D	4	3,05051E-05
WIF1	1	3,06313E-05
PJA2	1	3,07504E-05
MTHFD2	3	3,12791E-05
SLC39A12	3	3,15183E-05
SSX2IP	5	3,19114E-05
C18H16orf87	4	3,19196E-05
C3H1orf123	3	3,22518E-05
UBXN4	5	3,22534E-05
SHISA2	1	3,22696E-05

AP1AR	1	3,24269E-05
FAM89B	4	3,2465E-05
AXIN1	1	3,25789E-05
ECI2	1	3,30119E-05
MFSD1	1	3,3027E-05
RNF167	4	3,31544E-05
MGEA5	4	3,36687E-05
ZNF326	4	3,38222E-05
TRIM25	1	3,38782E-05
ZBED8	1	3,3913E-05
TNFAIP8L1	2	3,40834E-05
KCNN4	3	3,41182E-05
MED31	4	3,43803E-05
APBA3	1	3,44894E-05
INSIG1	3	3,49925E-05
SLC20A1	1	3,50108E-05
PYM1	1	3,51026E-05
AHSA2	1	3,51027E-05
FXN	1	3,53063E-05
AARSD1	1	3,54248E-05
GFI1	1	3,56239E-05
MGP	4	3,57649E-05
RHBDL2	1	3,57649E-05
OPA1	1	3,58235E-05
METTL22	3	3,62608E-05
SPINK5	1	3,63403E-05
ETV1	1	3,67809E-05
KLHDC1	1	3,68188E-05
S100B	1	3,73137E-05
TRPS1	1	3,77641E-05
GUCY2C	4	3,83616E-05
MRPL19	1	3,92947E-05
NKAIN2	1	3,96311E-05
MRVI1	1	3,96693E-05
NEGR1	1	3,98281E-05
FHIT	3	3,98401E-05
CREB5	1	4,02096E-05
GTF2H3	1	4,05024E-05
ATXN3	1	4,05458E-05
RGS3	1	4,0651E-05
SLC22A5	3	4,06733E-05
CMTM7	3	4,07465E-05

MYOF	1	4,08808E-05
CHEK1	5	4,1628E-05
GRAP2	1	4,19055E-05
AMT	4	4,19643E-05
ACAT1	1	4,20804E-05
PDIA5	3	4,22524E-05
HIKESHI	1	4,23337E-05
TXN2	4	4,23348E-05
DHX35	1	4,25184E-05
SHOX2	3	4,33918E-05
MFSD14A	1	4,35623E-05
IL1R2	1	4,35753E-05
EDF1	3	4,36043E-05
EFNB1	1	4,36964E-05
CAPN7	1	4,4098E-05
PAFAH1B2	3	4,42322E-05
NBR1	5	4,45557E-05
NCOA4	1	4,4556E-05
MYH2	1	4,47136E-05
LOC615809	4	4,47421E-05
ASAH1	1	4,50313E-05
ZNF34	1	4,53759E-05
PATZ1	3	4,55005E-05
MYH8	1	4,64381E-05
GSDMC	1	4,64973E-05
TIMMDC1	4	4,67141E-05
KIF15	1	4,67368E-05
LOC534742	3	4,67483E-05
KCNK1	1	4,6785E-05
WTIP	1	4,7181E-05
CCNH	3	4,74782E-05
CPNE8	4	4,76346E-05
MDM4	1	4,76521E-05
GNA14	1	4,80132E-05
RARS2	1	4,80132E-05
ETFA	1	4,82717E-05
PIGP	1	4,83491E-05
SLC10A7	1	4,84919E-05
POLR2F	4	4,88082E-05
ZFAND3	1	4,88964E-05
USP38	4	4,89607E-05
CHAC1	3	4,91663E-05

BMS1	4	4,92266E-05
LMO3	1	4,92386E-05
CCNB1IP1	1	4,96539E-05
SHROOM3	1	4,96843E-05
ANAPC11	3	5,02037E-05
NOL4	1	5,0853E-05
MTERF4	1	5,08575E-05
NIPSNAP3A	4	5,10771E-05
GNA11	3	5,11095E-05
FANCI	1	5,11539E-05
HACD2	1	5,15094E-05
FBXO21	3	5,16816E-05
RCSD1	4	5,22947E-05
TBC1D14	1	5,25303E-05
HACD3	1	5,27998E-05
GRK3	1	5,28331E-05
TAOK3	3	5,30428E-05
TUFT1	4	5,33506E-05
RMI2	1	5,34715E-05
PSME4	4	5,4057E-05
ACTL6A	4	5,41157E-05
RCN2	1	5,4174E-05
ACTR6	1	5,42763E-05
MACROD2	1	5,4389E-05
PEX11A	1	5,52055E-05
MTHFSD	1	5,57685E-05
RTN4IP1	1	5,59546E-05
NCF2	1	5,59672E-05
UBE3A	5	5,60771E-05
GNAI1	1	5,61839E-05
DARS	1	5,63164E-05
CCDC93	1	5,67131E-05
LRIG2	1	5,67293E-05
SMDT1	4	5,67543E-05
MRS2	4	5,67923E-05
SLC25A14	1	5,72771E-05
DGKB	3	5,72975E-05
SPATA5L1	4	5,7398E-05
DSP	1	5,83171E-05
BTBD1	4	5,84223E-05
C14H8orf76	3	5,84478E-05
CCDC65	1	5,87803E-05

CHD6	1	5,89582E-05
VTI1B	1	5,93493E-05
LRRIQ4	1	5,95457E-05
TMUB2	4	6,03038E-05
MRPL1	4	6,09225E-05
LRSAM1	1	6,1556E-05
XPA	3	6,1556E-05
SNTA1	1	6,15577E-05
GPRC5D	1	6,20985E-05
HORMAD1	4	6,2119E-05
SHFM1	4	6,2119E-05
GPR39	1	6,25365E-05
KATNAL1	1	6,2556E-05
CARD19	4	6,25606E-05
XRN1	1	6,26179E-05
HIBADH	1	6,28453E-05
AK6	4	6,34037E-05
MALSU1	4	6,34037E-05
RBP4	1	6,34282E-05
LCT	1	6,34817E-05
SPR	1	6,3973E-05
MTO1	1	6,4051E-05
DDX4	1	6,41119E-05
DPCD	1	6,43957E-05
NR4A1	1	6,48777E-05
CHGA	1	6,52986E-05
UBE2S	2	6,53191E-05
SYNJ2BP	1	6,54964E-05
FERMT1	1	6,57465E-05
BSP5	1	6,58392E-05
BTBD9	3	6,60431E-05
GCC1	1	6,81535E-05
ANXA11	1	6,86996E-05
RAF1	1	6,9112E-05
BPHL	1	7,00806E-05
NUAK2	1	7,02791E-05
ATOX1	1	7,0604E-05
RSPO3	1	7,13815E-05
TCHP	1	7,14718E-05
LAS1L	5	7,29709E-05
NDUFB6	1	7,30707E-05
AIMP1	4	7,35503E-05

EFR3A	1	7,36856E-05
BCL10	1	7,40049E-05
NUBPL	1	7,40841E-05
TOB2	4	7,41736E-05
PTGS2	1	7,42133E-05
TMEM230	1	7,50639E-05
CD63	1	7,54435E-05
SLC38A9	1	7,5725E-05
CD247	1	7,61744E-05
EPB41L4A	1	7,64138E-05
SERTAD1	4	7,65315E-05
GALNT1	1	7,70498E-05
ZIM2	1	7,73761E-05
PAN2	1	7,75566E-05
ANKRD46	1	7,77539E-05
CYBRD1	3	7,7805E-05
DDHD1	1	7,84788E-05
RBM46	1	7,88053E-05
DNAJC12	4	7,90329E-05
ACOT7	1	7,9201E-05
WDR83	4	7,9652E-05
LRRC8E	3	8,04857E-05
MARCH11	1	8,09861E-05
POLL	1	8,10231E-05
GPD1L	4	8,19719E-05
OSBPL3	1	8,28703E-05
PLEKHA3	1	8,35395E-05
ADCY6	1	8,35554E-05
C3H1orf50	1	8,35554E-05
PLEKHA1	1	8,51409E-05
FBXO15	1	8,67911E-05
DENND1A	1	8,75373E-05
LNX1	1	8,77264E-05
SPRY1	1	8,79353E-05
POLR2D	4	8,8046E-05
CFAP97	3	8,9237E-05
GCNT1	1	8,96606E-05
CCAR1	4	9,0549E-05
ADRM1	1	9,0841E-05
KIZ	1	9,24523E-05
HRASLS	1	9,26339E-05
TCEA1	1	9,28069E-05

TIMM9	3	9,28627E-05
RGS10	3	9,29226E-05
PLPP2	1	9,32008E-05
PPP3CC	1	9,34404E-05
SNAPC3	4	9,35019E-05
SLC35B2	1	9,36344E-05
TBCD	1	9,38685E-05
FAAP24	1	9,38953E-05
PHACTR3	3	9,39886E-05
PEX14	1	9,46228E-05
ABCD4	1	9,49744E-05
CXHXorf36	1	9,54592E-05
MOB1A	4	9,5845E-05
BEND4	1	9,62964E-05
CORO6	3	9,65013E-05
ATL3	1	9,71092E-05
TFDP1	1	9,73957E-05
SLC23A2	1	9,75596E-05
TEX9	1	9,79474E-05
NEIL1	3	9,82469E-05
ELK4	1	9,87328E-05
CIRBP	1	9,87641E-05
CTDSPL2	1	9,87641E-05
SNRNP40	3	9,88412E-05
SPINK2	3	9,88732E-05
THOP1	3	9,90959E-05
DDB2	1	9,93511E-05
NPHS2	1	9,95011E-05
GRAMD1A	1	0,000100031
SURF4	3	0,00010076
ATG3	4	0,000100795
PPP2R2B	1	0,000101066
CDIP1	3	0,000101271
DNTTIP1	1	0,000101499
EXOSC8	3	0,000102142
FBXO48	1	0,000102267
NCAPG2	1	0,000102342
C15H11orf49	1	0,00010339
TERF2	1	0,000103474
APLF	5	0,000103495
WFIKKN2	1	0,000103538
ETFRF1	1	0,000103804

TMCC1	3	0,000103962
WDTC1	1	0,000104196
PSMD10	1	0,000105365
GSTA4	1	0,000105475
ZDHHC17	4	0,00010583
HNF1B	3	0,000106689
SLC11A2	1	0,000107772
MSRB2	1	0,000107991
DSC3	4	0,000108241
ICE2	1	0,000108531
PLEKHG3	1	0,000109019
RWDD3	1	0,000109474
MKKS	1	0,00010978
TLE3	1	0,000109969
DPP8	1	0,000110936
SPAST	1	0,000112074
GFM2	1	0,000112911
GFER	3	0,000113018
DDIT4	3	0,000113652
MRE11A	1	0,000114259
CLDN10	1	0,000114278
ZNF277	1	0,000115275
G2E3	4	0,000115582
TIMM10	4	0,000115749
NDUFAF6	3	0,000116252
POLD1	1	0,000116431
IMPA2	1	0,000116597
LAMTOR2	3	0,000116597
CHD1	4	0,000117408
TXNL4A	3	0,000117649
TIPRL	1	0,000118591
RNF115	1	0,000118726
SFT2D1	3	0,000119965
CENPH	1	0,000120045
NELL2	4	0,000120282
ELL	3	0,000120763
SNX15	1	0,000121012
SMARCA1	1	0,000122549
LRRTM2	1	0,000123008
RPA1	3	0,000124099
UTP4	4	0,000124195
XKRX	1	0,00012435

HSPA1A	1	0,000124573
XXYLT1	1	0,000124629
EMC10	4	0,00012487
CRY1	1	0,000124906
FAM96B	1	0,000124939
CAPRIN1	4	0,000126645
NPR2	1	0,000126717
SPIRE2	1	0,000126853
CHM	5	0,000127393
PACSIN2	3	0,000128399
C25H16orf91	4	0,000129527
NFKB2	3	0,00012987
ACYP1	3	0,00013031
CAMKK2	3	0,000130594
PNPO	5	0,000131489
TRAPPC9	1	0,000132492
RRP8	1	0,000133203
METTL13	1	0,00013552
SLC18A2	1	0,000136892
SCMH1	3	0,000139035
SOX5	1	0,000140433
KIFAP3	1	0,000141193
TRIM3	3	0,000142091
TOMM5	4	0,000142137
AQR	1	0,000142985
TIMM22	4	0,000143397
CMYA5	1	0,000143633
ACAP2	1	0,000143895
LARP4B	1	0,000143921
VPS11	1	0,000144701
CTCFL	1	0,000144846
TMEFF1	1	0,000145908
PGM2	4	0,000146537
RNF170	1	0,00014858
ZFYVE26	1	0,000148912
HEATR4	1	0,000149954
IFIT3	1	0,000150066
SH3GLB2	3	0,000150093
SLC9A3R1	3	0,00015021
TRIM21	3	0,000151803
PIP5K1C	3	0,000153109
GIGYF1	1	0,0001539

UBE2M	1	0,000154735
ZNF33B	1	0,000154841
MCU	1	0,000155465
PSPH	1	0,000156003
SLC25A3	4	0,000159395
SMN2	1	0,000159652
NFKB1	1	0,000162282
UEVLD	1	0,000162282
PIN1	4	0,000163103
HDHD2	3	0,000163603
NFKBIA	1	0,000164227
CASP6	1	0,000164597
TIMD4	1	0,000165293
MBNL3	1	0,000165321
MSANTD3	1	0,000165634
SLC39A1	1	0,000165964
PLPP1	1	0,00016648
ERCC4	1	0,00016758
GABRG1	1	0,000167611
CFAP43	1	0,0001681
AAMP	4	0,000168748
YIPF6	1	0,000170307
STXBP6	1	0,000170597
PEX7	1	0,000170971
PTPRK	3	0,000170971
DOCK10	1	0,000171594
ADGRG1	1	0,000171696
FAM234A	1	0,000172714
CLVS2	1	0,000174809
RNASEH2A	1	0,000175113
TSPAN13	1	0,000176046
YPEL4	3	0,000176265
CLGN	1	0,000176975
AIDA	1	0,000179424
XRCC3	1	0,000179437
FGR	1	0,000181451
TSEN15	1	0,000182154
NRIP3	3	0,000183325
ZNF3	1	0,000183339
CDK5	1	0,000185423
BRWD1	1	0,000185801
CDKN1A	1	0,000186007

CCNE1	2	0,000186054
ELMOD1	1	0,000186825
RCHY1	1	0,000187107
LIN28A	1	0,000187658
SLC35A1	1	0,00018825
PRDM1	1	0,000189574
MOB1B	1	0,000190102
REL	1	0,000191623
PPTC7	1	0,000191944
ERCC5	1	0,000192413
FOSL1	1	0,000193373
MADD	1	0,00019387
ARHGEF4	1	0,000195015
PDIA3	2	0,000195352
HOXB7	1	0,000195442
BACE2	1	0,000195524
RTEL1	1	0,000195723
PCDHGC3	1	0,000196135
GTF2H1	4	0,000196848
NOP58	4	0,000197242
PRKAA2	1	0,000197652
RRAGD	1	0,000199719
PCP4	1	0,000202346
GAD1	1	0,000203553
LRRC59	1	0,000204438
MED18	1	0,000204722
UBA5	1	0,000205172
MRPL22	4	0,000206049
CDKL1	1	0,0002061
SLC35B1	3	0,00020741
CHD9	1	0,000209251
ZNF512	1	0,00020978
POLR2M	1	0,00020998
MASTL	3	0,000209986
PIM2	1	0,000210201
RUNDC3B	1	0,00021025
UQCR10	4	0,00021025
CPSF4	1	0,000210817
RIPK1	1	0,000211149
ATG12	4	0,000211583
RRP1	1	0,000213644
NEK9	1	0,00021425

PFDN4	1	0,00021425
PURB	4	0,000216134
SNRNP70	4	0,000216372
RILPL1	3	0,000217957
PEX19	1	0,000218977
CHMP3	1	0,000220351
TNIP1	3	0,000222294
ZNF394	4	0,00022395
ABCB11	1	0,000225492
TXNRD1	1	0,000225807
CENPO	1	0,000226768
LAMC1	1	0,000226804
BTG3	4	0,000227267
CLDN11	1	0,000227349
MAP4K3	1	0,000230297
PPM1B	5	0,000231736
AQP11	4	0,000235544
CTNNA2	1	0,000235617
HIST1H2AC	4	0,000238401
MED26	2	0,000239025
ERC1	1	0,000239541
CACNA1D	1	0,000240435
USP4	1	0,000240638
SUPT7L	1	0,000240823
ERLIN2	4	0,000241727
SF3A2	4	0,000242072
FOXN1	1	0,000242941
FLOT1	1	0,00024317
DHX16	4	0,000246087
STXBP4	1	0,000246231
KLK5	4	0,000246821
ZMYM2	1	0,000247866
HPS5	1	0,000248207
LEF1	1	0,000249467
BIVM	1	0,000249544
ATP6V1D	3	0,000250811
ZNF638	5	0,000254715
VPS39	1	0,000256582
NR1I2	1	0,000257252
ACBD4	1	0,000258758
SLC25A17	1	0,000258983
ARL15	1	0,00025936

CYB561A3	1	0,000261776
SKIL	4	0,00026302
TNK2	2	0,000264448
PTPN18	3	0,000268104
NOS2	3	0,000268699
DNMT3A	1	0,000268773
PSTPIP2	1	0,000271213
RHOG	3	0,00027384
DDC	1	0,000274945
LOC513767	1	0,000275213
PRKDC	1	0,00027556
EXOC3L1	1	0,000276507
MCM8	1	0,00027676
FLNB	1	0,00027693
RCC1	1	0,000277835
GABRG2	3	0,000279614
CPQ	1	0,00028001
NFIB	1	0,000281306
PRKG2	1	0,000281428
LEAP2	1	0,000281702
TMEM147	1	0,000284296
BCAR1	1	0,000286942
SH3GL2	1	0,000287426
LEPROT	1	0,000293434
RNF166	3	0,000293444
PLEK2	1	0,000293945
FAM84B	4	0,00029675
ZMAT4	2	0,000297496
MPDZ	1	0,000297529
C2H2orf76	1	0,000298242
SMARCD2	2	0,000298348
C7H19orf52	3	0,000298418
ACVR1	1	0,000298498
TSFM	3	0,00029891
DHX36	4	0,000299492
LBH	3	0,00029982
FUBP3	3	0,000301086
PDXDC1	1	0,000304578
APBA1	1	0,000304873
AFAP1L2	1	0,000310333
LYSMD3	1	0,000313597
STX6	1	0,000314644

CD3E	1	0,000317256
TWIST1	3	0,000319705
DENND4A	1	0,000320487
CC2D1A	3	0,000320958
TRIM27	4	0,000321588
REEP2	1	0,000322009
F2R	1	0,000322509
DNAJC10	4	0,000323441
FARSA	1	0,000326794
POLR3C	1	0,000328299
PSMD12	1	0,000328866
PDCD10	4	0,000329542
HINT1	3	0,000330337
CITED2	3	0,000330372
GLIPR2	4	0,000333292
LHX4	1	0,000333883
TTC27	1	0,000334101
DLG3	1	0,000334169
MYH10	1	0,000334831
DMAP1	1	0,000335113
KLHL42	1	0,000335113
SLC39A14	1	0,000335481
DYRK1B	1	0,000336631
VPS33A	1	0,000336854
STAR	3	0,000338742
MUTYH	1	0,000342625
CHPF2	1	0,000343627
CPN1	1	0,000343798
EIF3G	4	0,000344292
CCBL1	1	0,000346089
GMIP	1	0,000346875
BCL6B	1	0,000350495
CELF2	1	0,000352499
ZNF181	1	0,000354178
TM9SF2	3	0,000354732
PLS3	4	0,000356349
SPDYA	1	0,000357819
PUM1	4	0,000359711
ZNF451	1	0,000361054
ARHGEF2	1	0,000361596
BTD	1	0,00036272
TP53I3	1	0,000368459

CHMP4B	1	0,000370188
DEPTOR	1	0,000370919
HPS1	1	0,000371906
IP6K2	3	0,000375104
ACO1	3	0,000375764
DNAJC7	1	0,00037638
RB1	1	0,000379739
PDZD8	4	0,000382253
ESPL1	4	0,000382693
DNMT3B	1	0,000382884
SNCA	1	0,000383932
LIG4	1	0,000385396
RPL12	4	0,000386973
DDX3Y	4	0,000391242
CSNK1A1	5	0,000391538
ARCN1	1	0,000391842
LIG3	5	0,000392389
NES	1	0,000394242
AP1B1	1	0,000394792
PBK	1	0,000399423
MMAA	1	0,000399968
PACRGL	1	0,000400941
C6H4orf17	1	0,000401225
FEZ1	3	0,000402357
TUBE1	1	0,000404028
ZNF652	1	0,000406773
ATF7IP2	1	0,000406962
FAN1	1	0,000407619
TRAF4	3	0,00041091
FAM19A1	1	0,000411637
MRPL52	3	0,000411753
IBSP	1	0,000412778
PKM	1	0,00041317
ITGB1	1	0,000413962
ATF3	4	0,000414403
ATP2B1	1	0,000414713
NDUFS2	1	0,000414713
CCDC28B	1	0,000418751
SCFD1	1	0,000423575
STXBP5L	3	0,000423575
HYOU1	3	0,000423934
ARHGEF28	1	0,000424276

MXD1	1	0,000428454
STX18	1	0,000428593
TMEM115	1	0,000430229
HEXA	1	0,000430838
FAR1	4	0,000433064
SPRY2	1	0,000433432
KCNH1	3	0,000438327
NCR3LG1	1	0,000438386
ZNF148	4	0,00043842
TMED3	1	0,000439648
HMG20B	4	0,000443129
NUMA1	4	0,000444124
SARS2	1	0,000444448
PBXIP1	1	0,000447191
DIS3L	4	0,000448074
NDUFB5	1	0,000450421
BNIP3	2	0,000451035
THTPA	1	0,000451659
OXA1L	1	0,000453791
ZMPSTE24	1	0,000455244
VRK3	1	0,000455297
ZSWIM8	1	0,00045554
SMARCD1	1	0,000456556
PARP11	3	0,0004581
PEX2	3	0,00045904
DRC7	1	0,000461797
INIP	3	0,000463815
FXYD6	1	0,000466195
SERINC3	1	0,000466238
AS3MT	3	0,000471135
ATP6V1C1	3	0,000475792
SLC9A1	3	0,000476183
HID1	1	0,000477643
ASNS	1	0,000478559
EXOSC6	1	0,000480679
ANXA2	1	0,000481853
NSMCE4A	1	0,00048342
TBK1	1	0,000484349
JAM2	4	0,000488578
SEPT8	1	0,000490657
PPCS	1	0,000492257
EMC6	5	0,000493051

CBR4	1	0,000502653
NHS	1	0,000504278
STRAP	1	0,000504278
HSPB11	1	0,000505772
MRPL35	1	0,000506827
MYOM1	1	0,000509774
ADCY9	1	0,000515693
CEP135	1	0,00051857
EBF1	1	0,000521424
ABCC1	1	0,000523378
SDCCAG3	1	0,000524931
TPI1	1	0,000525274
DRG1	4	0,000525621
SNX27	1	0,000526143
METTL8	1	0,000528564
UNC5D	1	0,000530857
EEPD1	1	0,000532056
OCRL	1	0,000532497
UCP3	1	0,000535031
OCEL1	1	0,000536409
MINA	1	0,00053714
PLCG1	1	0,00053757
DCTN5	1	0,00054036
RND3	4	0,00054046
CAND1	4	0,000545091
VPS26B	1	0,000546898
CDK7	3	0,000551151
SEC22A	1	0,000558088
SUMO3	1	0,000561782
GNG4	1	0,00056234
CSPG5	2	0,000562945
CERS2	1	0,000564855
CREB3L2	3	0,000572122
CDH3	1	0,000572802
ARFGAP1	1	0,000575445
KLHL24	4	0,000581618
CD320	1	0,000582112
PANX1	1	0,000583163
TJAP1	1	0,000585372
ARPC1B	3	0,000585376
SLC41A2	1	0,000588025
RAD23A	3	0,000592331

CLSTN3	1	0,000593918
FREM1	1	0,000597638
COX19	1	0,000599185
TMEM59	4	0,000599185
ALG6	1	0,000599251
DTWD2	1	0,000599891
ZNF576	4	0,000602584
LRR1	1	0,000604464
ANAPC10	1	0,000604731
SPATA20	1	0,000606699
SGPL1	1	0,000610604
MED29	4	0,000611633
RASGEF1B	1	0,000611633
PAK3	1	0,000612241
COMMD6	3	0,000614368
VSIG1	1	0,000617052
PARK7	3	0,000618975
GABARAPL1	4	0,000620931
PLEKHH3	3	0,000620931
CDK5RAP2	1	0,000621599
LENG8	2	0,000625219
C8B	1	0,000627186
FKBP7	1	0,000627513
C26H10orf2	1	0,000627942
C7H19orf43	4	0,000628179
POC5	1	0,000628256
NSUN5	1	0,00063006
GOLM1	1	0,000639362
ASAP3	1	0,000639832
PALM2	1	0,000640652
DNAJB2	3	0,000643854
DPM2	3	0,000645625
C7H19orf24	4	0,000648972
STK19	4	0,000649401
EVI5L	1	0,000651512
SNX24	1	0,000657759
WDR89	4	0,000658722
EFEMP1	1	0,000665177
KCNA5	1	0,000665745
GJB4	1	0,000667669
FANCG	1	0,000668613
CREB1	3	0,000670215

PTPN3	1	0,000679465
MRPL58	3	0,000681868
MYL6B	3	0,000681868
BORCS5	3	0,000682494
ABTB1	4	0,00068612
ALAD	1	0,000688875
ADA	1	0,000691958
TFAP2B	1	0,000693144
NKD1	1	0,000700079
PROSC	4	0,000701712
NRF1	2	0,000703584
SLC35G1	1	0,000704667
FBLN5	1	0,000705818
SGSH	1	0,000712001
IRAK2	3	0,000719436
ST3GAL6	1	0,000726132
OTUD4	1	0,000731288
DHX32	1	0,000738355
ACOT8	1	0,000741256
TUBGCP5	1	0,000741795
MANBAL	1	0,000743638
GRB7	1	0,000747258
ITGA2	1	0,000748213
EMC8	3	0,00075419
HEY2	1	0,000756241
PCCA	3	0,000756324
GCHFR	4	0,000760013
OLFML1	1	0,000760013
GPS2	1	0,000762547
CCZ1	1	0,000763911
MED19	4	0,000766242
TANK	1	0,00077751
CDA	1	0,000782059
ERCC8	4	0,000782059
TAF6	1	0,000782059
PTPRB	1	0,000782544
GMCL1	1	0,000786218
MAP1B	1	0,000787971
AP1M2	1	0,000789005
TSG101	3	0,000790462
SESN2	1	0,000794723
TRIM13	3	0,000797137

ADCYAP1	5	0,000798986
FRMD3	1	0,000799709
LPGAT1	1	0,000799709
OSGEPL1	3	0,000801124
PRRG4	1	0,000804678
DNAJC21	1	0,000817104
UQCC	1	0,000827418
SDR42E1	1	0,00083575
MID1IP1	4	0,000837384
RASGRP2	1	0,000843978
PTBP2	1	0,000846781
CARS2	1	0,000848226
PTRH2	4	0,000848226
MTRR	1	0,000849417
MANBA	3	0,000852963
CD59	1	0,000855825
TMEM198	1	0,000866779
TRPV6	1	0,000870343
KIN	3	0,000871312
CETN3	1	0,000877933
FUT8	1	0,000881102
RTCB	1	0,000884315
S100A10	4	0,000885473
CLN5	3	0,00088637
MAPKAPK3	3	0,000889291
CA6	1	0,000893865
FGFR2	1	0,000893865
ATP1B3	4	0,000898234
CSTB	1	0,000898345
DGKA	1	0,000898902
CTNS	1	0,000899376
RAD54B	4	0,000901399
NUDT9	3	0,000904429
NDRG3	1	0,000907073
ITFG1	1	0,000907872
EIF4E3	1	0,000909339
MAK	4	0,000912199
KIAA0907	4	0,000914352
FBXO22	1	0,000918224
CRHBP	3	0,000924886
DTNB	1	0,000927969
CCS	2	0,000931689

PIK3CB	1	0,000932506
SSFA2	1	0,000944654
PRMT2	1	0,000953444
MRPL57	4	0,000957841
XAB2	1	0,000969506
GTF3C1	1	0,000973503
DPP10	3	0,000977004
CACNA1E	1	0,000983639
LAMP1	5	0,000983733
DTD1	1	0,000987627
CDKN1B	1	0,000989167
BHMT	1	0,000991396
TBX18	1	0,000991396
ACTC1	1	0,000992509
ACCS	1	0,000993645
LRRC45	1	0,000995538
LOC788142	1	0,000997921
NSUN6	3	0,001003067
EFHB	3	0,001005563
KCNK5	4	0,001011774
PGGT1B	1	0,00101807
C2H2orf47	1	0,001019056
BBS7	1	0,001021438
DDX28	1	0,00103224
UBE2G2	1	0,00103588
PTPN5	1	0,00103812
CMBL	1	0,001039467
KANSL2	4	0,001040723
PNOC	1	0,001049103
DHRS4	1	0,001053172
EXOG	1	0,001059754
MORN2	3	0,001069831
VMP1	4	0,001075127
SUN2	1	0,001083258
GLCE	1	0,001085248
PFN1	3	0,001097303
ERLIN1	1	0,001104823
KPNB1	1	0,001105711
PRRC1	1	0,001113334
LETMD1	3	0,001115626
SERGEF	1	0,001120244
PPP1R1A	1	0,001122844

HIP1	1	0,0011238
ARFIP1	1	0,00112506
HYKK	1	0,001129048
C20H5orf22	1	0,001129659
LOC512899	1	0,001132368
CNGA3	1	0,001134978
BDH1	4	0,001137132
LOC534913	3	0,001140105
RAD1	1	0,00114752
POR	1	0,001148283
FAM13A	1	0,001152642
ATP6V1C2	1	0,001154022
POLR1B	1	0,001156099
TMCC2	3	0,001161699
SFXN4	1	0,001164924
P4HA1	1	0,001166141
GPR179	1	0,001171625
APIP	1	0,001173245
SMYD3	3	0,001175321
PTCD3	1	0,00118411
FERMT3	1	0,001184243
NOS1AP	1	0,001185229
ARPC3	1	0,001187666
SOCS4	4	0,001187666
DYNC1I1	1	0,001189114
TSKU	1	0,001190236
KLHDC9	1	0,001209096
POLR2I	4	0,001212211
LIX1L	3	0,00121915
BCAT1	3	0,001221185
P2RX1	1	0,001230863
ARFGAP2	1	0,001235998
RPS19BP1	4	0,001236847
STK3	5	0,001240878
SF3B3	4	0,001241507
LDLR	1	0,001246172
JAK1	1	0,001263167
MSX2	1	0,00127546
FGFR1OP2	4	0,001276471
NEK3	1	0,001283079
SFRP1	1	0,001285736
KLHDC10	1	0,001287066

SDHAF2	1	0,001289409
ZNF341	1	0,001289409
ILDR2	1	0,001289996
BLOC1S6	3	0,001291581
PPP2CB	4	0,001292312
ABHD6	1	0,001296917
BTRC	3	0,001296917
IFT81	1	0,001297461
PTN	1	0,001301648
NAP1L4	1	0,001302145
IQSEC1	3	0,001302516
SGCB	1	0,001310702
PSMD3	1	0,001315518
STIM1	1	0,001316926
GABPB2	1	0,001322149
CLCN4	1	0,001322389
LOC616319	1	0,001323658
WNT2B	1	0,001327094
ZKSCAN8	4	0,001330252
NHEDC1	1	0,001331468
IDI1	1	0,001356693
SCLY	4	0,001369267
BICDL2	3	0,001370153
TNPO3	4	0,00137056
DOLK	3	0,001375957
ADGRL3	1	0,001378666
CTU1	4	0,001391189
LATS1	1	0,001399899
TTC21B	1	0,001401645
GAN	4	0,001401712
MAPKAP1	1	0,001402318
WDR70	5	0,001411445
CPTP	3	0,001416147
GPC5	1	0,00141667
EHD4	1	0,001443884
HMG20A	1	0,001453555
UMPS	4	0,001456429
SAR1B	1	0,001471159
NDUFA5	1	0,001475525
SLC39A7	1	0,00148448
CUX2	3	0,001485206
FNDC3A	1	0,001486772

HSPBAP1	1	0,001495812
USO1	1	0,001499125
MMACHC	4	0,001500755
LAMTOR5	1	0,001504046
CASC1	1	0,001505699
PCBD1	1	0,001541544
PTPRR	1	0,001542787
FNTB	1	0,001543277
ZHX2	1	0,001561492
NAV3	1	0,001562455
LRRFIP1	1	0,001574612
SLC5A6	4	0,0015859
CNEP1R1	3	0,0015873
ZNF445	1	0,0015873
RASGEF1A	3	0,001603422
UBE2D4	1	0,001619135
MRPS2	3	0,001630016
RFX5	3	0,001632001
AK3	1	0,00163607
HMMR	1	0,00163607
ARL2BP	1	0,001647093
SPIN1	4	0,001663772
HARBI1	1	0,001673252
MSI1	1	0,00167601
RWDD2A	1	0,00167601
SIGMAR1	1	0,00167601
CNOT10	3	0,001676741
SULF2	1	0,001676987
FARS2	1	0,001678171
HSPA1L	1	0,001692895
CMTR1	1	0,00170005
TLR2	5	0,001701931
MRPL48	1	0,001708364
TBL2	1	0,001709682
GCNT3	1	0,001711203
FBXL14	1	0,001713199
MGAT4B	3	0,001715447
ACACA	1	0,001720605
PPP3CB	1	0,001723207
ZFYVE27	4	0,001729542
EXTL3	1	0,001731609
C5	1	0,00173381

FAM92A1	3	0,00174717
GATB	3	0,001771756
FAT1	1	0,001772161
MCTP1	3	0,00177239
RNF7	1	0,001773873
ATP5B	4	0,001775351
PPP1R1B	1	0,001780863
SLC31A2	1	0,001789812
ULK3	1	0,001813118
GTSE1	1	0,001817496
MGAT4A	1	0,001820852
TPPP3	1	0,001836349
SPCS1	3	0,001846298
VIPAS39	1	0,001847185
WLS	3	0,001863281
PHC2	1	0,001863821
GOLGA7B	3	0,001876497
EIF2S1	1	0,00187794
DNM3	1	0,001882042
HSPD1	1	0,00188868
SNX22	1	0,00188868
ANKRD1	3	0,001891488
EMG1	4	0,001899242
TMEM126A	1	0,001900033
ASL	1	0,001903363
ALDH3A2	1	0,001906221
GPX8	1	0,001906221
FRZB	1	0,001923991
MRPS9	3	0,001923991
USP44	1	0,001935283
ITPA	3	0,001936121
PTGER4	4	0,001941848
TFB1M	1	0,001954803
MRPS28	3	0,001992206
PDE12	4	0,002000459
TMEM127	1	0,002012563
PNPLA6	1	0,002013716
POLR3F	4	0,002017029
DYM	3	0,002035929
RPL7L1	4	0,002046128
NUP155	4	0,002047426
ZSWIM7	1	0,002052313

GET4	1	0,002056397
VRK2	1	0,002056397
BAHD1	3	0,002059231
HESX1	1	0,002059231
RAB28	1	0,002059231
ZSCAN26	1	0,002069557
OGDHL	1	0,002093648
JAG1	1	0,002099358
PPM1L	3	0,002106886
YARS	4	0,002106886
ACRV1	1	0,002116778
BANP	3	0,002116778
ORAI1	1	0,002116778
ZNF774	1	0,002117173
PORCN	3	0,002118503
SUGP1	4	0,002119984
FBXO18	1	0,002130756
SYT4	3	0,002160627
MAPK9	1	0,002170669
TRAPPC3	1	0,002175536
ADORA2B	1	0,002186329
H1F0	1	0,002198201
KIAA2012	1	0,002199535
KCNMA1	1	0,002202221
FXR2	1	0,002202783
B4GALT6	1	0,002214889
C7H5orf24	1	0,002215002
TMEM41A	3	0,002237782
COPS5	3	0,002239304
DEUP1	1	0,002243772
UBE3D	1	0,002243987
EIF2B1	1	0,002252515
ZNF621	1	0,002267501
BROX	4	0,002280057
LOC788201	1	0,002289312
CDC42BPG	1	0,002293615
ARL8B	1	0,00229451
FBF1	3	0,00230526
MICAL1	1	0,002309884
TDRKH	1	0,0023118
SNX3	1	0,00231542
RFWD2	1	0,002317541

CMPK1	1	0,002324502
RPL18	4	0,002330531
CDC7	1	0,002330644
PKIG	1	0,002330644
MLF1	1	0,002331154
SLC46A1	1	0,002337003
GTF2E1	4	0,002339682
LRIG3	1	0,002346632
CBLB	1	0,002346836
ANKRD27	1	0,002348237
EMILIN2	3	0,002355818
NAE1	1	0,002367687
DIP2B	1	0,002369921
EMC7	1	0,002369921
RHPN2	4	0,002369921
ARSB	1	0,002370004
PTMS	3	0,002373189
ABCA4	1	0,002383933
BCL7C	3	0,002387085
BLOC1S5	3	0,002387085
MRGPRX2	4	0,002387115
STMN1	3	0,002387115
ITGA6	1	0,002397557
BRIX1	1	0,002413713
C7H19orf66	1	0,002413713
RASD2	3	0,002414695
UXS1	3	0,002419785
IMPA1	3	0,002424157
CECR5	1	0,00242905
MTERF3	6	0,002435834
NDUFA7	1	0,00244509
HHEX	1	0,002467904
RAB3C	3	0,002473661
ATP6V0A1	1	0,002479199
INPP5K	4	0,002481063
LOC515736	1	0,002496922
DVL1	1	0,00249924
AIM1L	1	0,002519286
CSTF2T	4	0,002522574
C9H6orf203	1	0,002528452
GPR84	3	0,002533141
TUBGCP3	3	0,002533141

NAIF1	4	0,002542512
PPT1	1	0,002542512
GFRA3	4	0,002544483
SLC3A2	1	0,002551391
C10H14orf37	1	0,002556731
DECR1	1	0,002590619
TMEM55B	3	0,002601897
MLN	3	0,002608544
RARRES1	3	0,002616015
FARP1	1	0,002625609
ZNF384	2	0,002633626
USP15	5	0,002642667
KCNH5	1	0,00266065
CSK	1	0,002670467
UNC93B1	3	0,002677155
NAA60	3	0,002678542
MAN2A1	1	0,002692364
BLOC1S1	3	0,002693075
APOBEC2	3	0,002698753
ECHS1	1	0,002707442
COMMD7	1	0,002722133
CNKSR3	1	0,002723949
ZNF689	3	0,002725352
ATG7	1	0,002725926
ZCCHC4	1	0,002730235
NDUFA9	1	0,002741827
C16H1orf27	1	0,002761189
SFXN1	1	0,002762926
TAB1	3	0,002765929
TEK	1	0,002780371
ZDHHC13	1	0,002789557
CCDC115	4	0,002794578
SOX2	3	0,002796215
NAAA	3	0,002797539
SUPT3H	1	0,00281543
CALCOCO2	1	0,002823739
ADPRM	4	0,002832946
PPP1R3F	3	0,002838523
PNRC2	3	0,002841993
ERP44	1	0,002844677
MIOS	1	0,002852477
SLC8B1	1	0,002853963

WDR54	1	0,002859461
PPIP5K1	1	0,002862093
PIP4K2B	1	0,002864164
MRPS27	1	0,002869858
GPN3	4	0,00287423
DAPK1	1	0,00290186
SRSF9	3	0,00290186
IGFLR1	4	0,002906477
LMO2	5	0,002922058
EPN2	1	0,002936998
SMIM14	1	0,002954828
TRIM32	1	0,002964788
PSMB6	4	0,002967296
RPS6KC1	1	0,002969075
TRPC6	1	0,002970809
PHLPP2	1	0,002981126
LETM1	3	0,00298344
CHRNA7	1	0,002993913
MTMR10	1	0,003008076
TUBB6	1	0,003021367
ABR	3	0,003024952
ACSS1	4	0,003028142
SIAE	1	0,003035456
KIF4A	5	0,003072853
TDP2	1	0,003075672
CPNE3	1	0,003086111
SYN3	3	0,003160119
CALB2	1	0,003164618
METTL18	1	0,003171404
COX10	1	0,003171513
CSNK1E	3	0,003171513
SPCS3	4	0,003185127
RPA2	1	0,003189359
RFC3	3	0,003211983
HSPB1	3	0,003228392
OGDH	1	0,003234315
CCAR2	1	0,003265077
TRMT12	3	0,003270534
DONSON	1	0,003278974
MRPL47	3	0,003298548
NCAPD2	4	0,00330789
CDK16	1	0,003342163

OGFR	1	0,003382965
RNF121	3	0,003393082
NCSTN	3	0,003394624
CDC42EP4	1	0,003420978
LTA4H	3	0,003423215
NQO2	1	0,003425797
NUCKS1	3	0,003431093
ECD	1	0,00345243
ADAMTS12	1	0,003452449
TMED5	4	0,003452449
PKN2	1	0,003458495
KIF3B	3	0,003458929
UBE2D1	1	0,003507763
CASC3	1	0,003508257
RPAP2	1	0,003508257
GTF2A1L	1	0,003513407
TTL	1	0,003517372
KLHL20	1	0,003539308
LYRM9	1	0,003548049
AGO3	4	0,003553701
VCAN	3	0,003557973
QDPR	3	0,003580778
PIGM	4	0,003582393
LOC533308	1	0,003599048
DDX6	1	0,003613049
CKMT2	3	0,003633953
TSR3	3	0,00364131
SCG5	1	0,003656384
PAQR7	3	0,003660115
ATP5G1	1	0,003678582
MRPL46	1	0,003705062
STAT1	1	0,003707165
WDR77	4	0,003708953
TMCO3	3	0,003714449
ZBTB11	5	0,003716877
SUMF1	1	0,003753354
UTP6	4	0,003756592
BCAR3	1	0,003762176
PCGF5	1	0,003762176
VAPB	3	0,003772599
BID	1	0,003773977
IER2	4	0,003775639

CTDSPL	1	0,003781034
SNX5	4	0,003824179
MYD88	1	0,003851229
ZC4H2	3	0,003874484
FAM81B	1	0,003884988
RNF128	4	0,003894887
IVD	1	0,003897645
TBC1D9B	3	0,003898072
RILPL2	1	0,003932757
TMEM106B	3	0,003937765
PITPNA	1	0,00394235
C1GALT1	4	0,00394665
HLF	3	0,00394665
SNX30	1	0,003948709
RUFY3	1	0,003953793
PIK3R1	1	0,003963108
SLC44A3	1	0,003981263
TMEM206	1	0,003981263
FAF2	1	0,004013911
ZNF705A	3	0,004015428
RAD9A	1	0,004019672
HECTD2	1	0,004023016
HAT1	4	0,004029957
CPOX	1	0,004035896
EPB41L3	1	0,004035896
CIDEA	1	0,004043
NUDT16	1	0,004050245
PSTK	1	0,004058357
GCAT	1	0,004063879
ZSCAN31	1	0,004087927
EIF2A	4	0,004096651
ETV5	1	0,004096651
SYTL4	3	0,004109118
CSNK2A2	3	0,004117196
SMG5	4	0,00411936
NXT1	1	0,004122344
TRAT1	3	0,004131262
NOSTRIN	1	0,00413377
AARS	4	0,004183632
PHF1	3	0,004185119
EXOSC4	1	0,004218751
CLASP2	1	0,004237858

UXT	4	0,004269979
BSP3	1	0,004271747
PSMG2	3	0,004288392
STRN3	5	0,004295918
SLA2	1	0,004323241
RNF138	4	0,004354793
HINFP	4	0,004355642
HIST3H2A	1	0,004363319
ARRDC4	1	0,004406088
HDDC3	1	0,004407276
MRPS5	1	0,004420822
DEF8	1	0,004425203
CLN8	3	0,004432803
HMBOX1	1	0,004438646
B4GALT3	5	0,00444504
POLR2C	1	0,004459415
TMEM35	3	0,00447635
UBALD1	4	0,004501876
PFKFB2	1	0,004509682
BUD13	3	0,004580206
SORCS1	1	0,004580982
STC1	3	0,004580982
RPL14	4	0,004581392
LRRTM1	1	0,004585915
ORMDL3	2	0,004587156
TAOK2	1	0,004587156
RNF123	3	0,004610083
NKIRAS2	1	0,004613137
CARD14	4	0,004614853
LRCH4	1	0,004630865
COQ3	4	0,004640492
EIF2B2	4	0,004663528
WDR91	1	0,004666358
DBT	1	0,004668487
ADGRE5	1	0,0047068
GAS7	1	0,004714886
NXN	3	0,004717503
MEST	1	0,004722657
FAM210B	3	0,00473322
PRIM2	1	0,004748879
PDE6A	1	0,004753185
HEATR6	1	0,004769451

C14H8orf33	4	0,004779259
IL17RB	1	0,004779259
BDNF	1	0,004822306
DIS3L2	1	0,004832182
CNST	1	0,004865929
PPP2R3C	1	0,00486836
TOR2A	1	0,004875266
CYCS	1	0,004908616
TUBA4A	4	0,004918124
BCKDHB	1	0,004918712
NOL12	1	0,004939072
DPPA4	4	0,004966559
C15H11orf70	1	0,004966675
LRP10	4	0,004967348
TLE1	4	0,004982855
STK33	1	0,00499298
C7H5orf30	4	0,005001948
PRPF31	4	0,005003887
BARHL2	1	0,005063582
ENHO	1	0,005069613
TOR1AIP1	1	0,005069613
NUP188	1	0,005095838
RAB32	1	0,005099532
PLA2G16	1	0,005105095
TBC1D7	3	0,005105095
TMEM163	3	0,005105095
KCNE1	1	0,005106827
LOC534155	4	0,005112424
ISY1	3	0,005113543
PRPF4B	4	0,005174474
TBC1D20	3	0,005202385
FAM228B	1	0,005208985
HSPA2	5	0,005212466
PHPT1	1	0,005219872
PRMT7	1	0,005236894
ARRDC1	1	0,005240916
PIGS	1	0,005276172
CDX1	3	0,005282702
SLC35A5	3	0,005282702
LPCAT4	3	0,00529033
RAC3	1	0,005316631
STAM2	4	0,005322059

SARAF	1	0,005344972
POLA1	1	0,005402
TRAIP	1	0,005402
GRM1	1	0,005433269
SLC35F5	1	0,005433269
LYSMD4	1	0,005435278
STX8	2	0,005448837
TRPM7	1	0,005454134
DTNBP1	3	0,00546821
KRTCAP3	1	0,005579776
SEC14L1	1	0,005589311
CAPZB	1	0,005637545
GALNT2	1	0,005678233
SDCBP	3	0,005715446
TEX30	1	0,005744609
METTL21B	3	0,005803238
ADCY7	1	0,005812579
PIGW	4	0,005821165
TP63	3	0,005821165
DCK	3	0,005826727
ALG2	4	0,005839595
ORC2	1	0,005863028
DBN1	3	0,005866494
MEGF10	1	0,005867479
PDHX	1	0,005887593
CDX2	1	0,00590016
UBTD2	1	0,005905155
FH	1	0,005931983
HIRIP3	1	0,005948812
MRPL10	3	0,005951717
RNF214	3	0,005960119
WBP4	1	0,005974885
PATL1	5	0,006016422
RXRA	1	0,006079207
MRPS22	1	0,006095436
ZCCHC11	3	0,006097608
AIMP2	4	0,006108042
ACADS	1	0,006119905
AZIN2	3	0,006148145
GFI1B	1	0,006148145
TRMT11	1	0,006167192
NT5C3B	1	0,006176911

MFF	3	0,0061882
MED25	1	0,006212317
SQSTM1	1	0,006261512
MYL6	1	0,006320268
TRMT10B	3	0,006348766
SETDB2	4	0,006351109
ALDH5A1	3	0,006366306
TRIM37	1	0,00637258
ACOT13	1	0,006384032
MRRF	1	0,006393316
KIAA1551	4	0,006399854
PPRC1	4	0,006402607
GATA2	1	0,006429783
PSMC3IP	3	0,006450633
DPP3	3	0,006484501
DUSP4	2	0,006484501
SMYD2	1	0,006544242
MYCBP2	1	0,006571798
PCED1A	1	0,006580498
PLA2G4D	1	0,006589775
ANKRA2	1	0,006604496
PAFAH2	1	0,00660695
RBFOX1	1	0,006625548
HSF2BP	1	0,006659799
ING2	2	0,006671385
KRAS	1	0,006679518
MTMR7	1	0,006679518
NENF	3	0,006753953
TRAPPC11	1	0,006781487
CAPNS1	4	0,006790189
CHCHD6	1	0,006799349
NAGK	1	0,006854768
MBOAT1	1	0,006897043
PDCL2	3	0,006904875
C5H12orf4	1	0,00690507
CCR8	1	0,006920098
ZPR1	4	0,006931019
MSN	1	0,006936196
RBMX2	1	0,006953672
MIP	1	0,006979838
CTNNA3	3	0,006984334
MIS12	4	0,007002246

ZDHHC21	1	0,007019107
C11H9orf16	4	0,007019127
RNF185	4	0,007092415
CDKN2AIP	4	0,007143869
PIK3C3	1	0,007146646
CAST	2	0,00714819
GARS	1	0,007153285
CPA1	1	0,007163567
RALGPS2	3	0,007168215
DUSP11	4	0,007171553
GMPR	1	0,007178558
RLIM	4	0,007191088
WDR19	1	0,007195182
DGUOK	3	0,007219138
EXOC1	1	0,007236437
LIPT2	1	0,007260711
RAB26	3	0,007260711
ZMYM3	1	0,007279177
FRMD5	1	0,007401861
KMT5A	4	0,007410414
RIOK2	1	0,007412675
URB1	4	0,007416699
SMCHD1	4	0,007417914
ZC3H4	1	0,007442828
ABCF3	4	0,007452537
MAN1A1	1	0,007473662
CSTF2	1	0,007473845
ZNF570	1	0,007514198
ZBED5	1	0,007569151
GCLC	1	0,007581257
NPRL2	1	0,00763053
MAB21L1	1	0,00765764
ATG4C	4	0,00767663
MUM1	3	0,007677033
TEFM	1	0,007710682
C21H14orf2	3	0,007731225
TTYH1	3	0,007764028
GRK2	1	0,007862783
LIX1	1	0,007877377
ELN	3	0,007941771
NSFL1C	1	0,007941771
FEM1A	4	0,007970337

CHPF	1	0,007997016
ITPRIP	4	0,008027605
HK1	2	0,008072913
RNF122	1	0,008074664
POLA2	1	0,008142728
TRAPPC10	3	0,008157375
LIN7B	1	0,008172137
MSH6	4	0,008182419
CDYL	1	0,008190213
PYURF	3	0,008229837
RNF43	1	0,00824559
PPP1R13L	1	0,008263941
FGF16	1	0,008344226
NADK	1	0,00837861
ARIH2	3	0,008411697
CTPS1	1	0,008411697
PI4K2B	1	0,008429291
NT5DC1	3	0,008447511
IQCD	4	0,008488485
EIF4EBP2	5	0,008548759
C24H18orf25	1	0,008562681
IL2RA	1	0,008562681
PSAT1	1	0,008568754
TSPAN33	1	0,00858584
DNAJC18	1	0,008618209
RPRD1B	4	0,00864536
NCKIPSD	1	0,008670522
COPS6	1	0,008683954
FAT2	1	0,008746286
SRF	3	0,008761545
TRAP1	3	0,008781144
GNG12	1	0,008811502
RPF2	1	0,008888981
WDR6	4	0,008916522
UBL4A	1	0,008925377
IAH1	1	0,008949835
NDUFS8	3	0,008994069
MBTD1	5	0,009023039
TMX1	4	0,009023039
UPP2	1	0,009069447
CPE	1	0,009103802
IL2RG	4	0,009160343

ACACB	1	0,009180295
ZNF329	1	0,009195134
FECH	1	0,009258712
RAD51B	1	0,009307576
DCLRE1C	1	0,009313812
CCDC36	1	0,009345922
RGL1	1	0,009398127
RND2	1	0,009436791
VPS50	1	0,009540973
DFNA5	1	0,009551717
FCF1	3	0,009551717
MRPL41	4	0,009551717
DNASE1	4	0,009572089
ODF2L	1	0,009585034
NUDT11	3	0,009603152
MCRS1	4	0,009605893
ARHGEF37	1	0,00961075
C9H6orf118	3	0,009614828
PRKACA	3	0,009622304
TNFSF8	1	0,0096315
SNX29	1	0,009667983
CMTM4	1	0,009687578
ARHGEF16	1	0,009704424
TUG1	4	0,009735821
PRKCE	1	0,00974598
SMIM12	4	0,009763965
PARVG	1	0,009767631
PDSS1	1	0,009779268
GLDC	1	0,009803759
MRPL16	4	0,009843099
NPAS2	1	0,009848027
RPS6KA3	1	0,009848027
EOGT	1	0,009917712
SMG6	1	0,00997363
RPTOR	1	0,009990719

Supplementary Table S2. 2,494 differentially abundant levels of transcripts (DAT) with $p < 0.01$ were identified by using SC3 pipeline.

Gene Name	adjusted p-value	AUROC	Cluster (K)
C8H9orf64	5,78322E-11	0,868639668	1
COG2	3,18661E-10	0,860159225	1
DPP4	1,09151E-10	0,859813084	1
F3	1,01963E-10	0,871408792	1
NETO1	5,25661E-11	0,857995846	1
RUFY2	5,26725E-10	0,859813084	1
TIGAR	2,2572E-10	0,864053306	1
TMEM128	5,35744E-10	0,859640014	1
TPMT	1,85153E-11	0,869505019	1
UCHL1	4,81329E-10	0,853409484	1
XRCC2	1,12258E-11	0,858428522	1
ZNF75A	4,96539E-10	0,857130495	1
RHEBL1	8,21539E-06	0,855979644	2
AMIGO2	8,57864E-06	0,865198711	4
AMT	1,35901E-05	0,85754565	4
ARFGAP3	3,34991E-07	0,895005371	4
ARHGAP1	6,1081E-06	0,866272825	4
ARMT1	4,12503E-07	0,888829216	4
ATF7IP	4,1745E-06	0,872180451	4
C14H8orf59	1,60997E-07	0,900912997	4
C1D	6,31323E-07	0,889366273	4
C3H1orf52	1,0613E-05	0,863050483	4
CAD	1,32611E-08	0,918367347	4
CCDC126	8,25557E-07	0,886949517	4
CCT4	5,17188E-06	0,870032223	4
CDK1	9,85311E-06	0,863856069	4
CDKN2C	1,95214E-05	0,851638024	4
CXADR	3,19081E-05	0,851235231	4
DESI2	2,11316E-07	0,889500537	4
DLD	3,41191E-05	0,851235231	4
EIF3D	1,54396E-05	0,859291085	4
EIF6	5,42133E-07	0,891245972	4
EXOSC1	5,09899E-06	0,870032223	4
FAM207A	7,47777E-08	0,886815252	4
FAM89A	1,14757E-06	0,880773362	4
FOLR1	3,65359E-08	0,914607948	4
GART	5,55874E-06	0,868689581	4
HAX1	5,46665E-07	0,890708915	4
HIST1H2BD	7,6562E-09	0,926154672	4
IL18	1,33071E-07	0,89943609	4

IMP3	1,28889E-07	0,90386681	4
IPMK	1,66538E-05	0,852712137	4
ISG20L2	8,56319E-08	0,892722879	4
ITM2B	3,01123E-08	0,900778733	4
KLF3	5,76141E-06	0,859828142	4
KLF5	5,61358E-07	0,888426423	4
LARP4	5,79018E-06	0,86895811	4
LOC782781	1,24401E-07	0,901718582	4
LRRC40	2,1534E-06	0,87755102	4
LSM8	3,8289E-06	0,871911923	4
MANF	7,06591E-06	0,855263158	4
MBIP	6,54952E-06	0,867883996	4
MED31	1,98476E-05	0,856068743	4
MRPL17	1,98026E-07	0,90037594	4
MTHFD1L	2,35239E-07	0,895542427	4
NAA11	9,59681E-07	0,883458647	4
NANOG	2,21636E-06	0,861976369	4
NCBP2	8,23006E-07	0,887486574	4
NDUFB2	1,39641E-06	0,882384533	4
NDUFB3	3,04196E-06	0,870435016	4
NKAPL	6,17809E-07	0,88990333	4
NOL6	1,26957E-06	0,883190118	4
NOP16	1,00822E-06	0,883458647	4
PARP14	8,49937E-07	0,87150913	4
PDCD10	1,04396E-05	0,863050483	4
PHF5A	1,90154E-05	0,855397422	4
PIP5K1A	2,52619E-05	0,853383459	4
PLEKHJ1	1,42305E-05	0,857411386	4
PPAT	9,59053E-06	0,863990333	4
PPIL1	3,90162E-06	0,855934479	4
PRPS1	2,5436E-05	0,853920516	4
PSMA1	3,08411E-06	0,862916219	4
PYCR2	2,77566E-05	0,853383459	4
RACK1	4,44504E-06	0,871643394	4
RNF11	7,78745E-07	0,888023631	4
RPL26	2,97325E-06	0,875402793	4
RPL36AL	4,45686E-06	0,871643394	4
RPL37	6,89829E-07	0,888560687	4
RPL38	7,635E-06	0,866272825	4
RPS19	3,95417E-08	0,91433942	4
RPS27	3,00288E-07	0,896616541	4
RPS29	6,74663E-07	0,889366273	4

RPS4Y1	7,33016E-07	0,888560687	4
RPS9	3,75967E-06	0,87244898	4
SCO1	3,90642E-06	0,862379162	4
SLC27A1	1,8594E-05	0,852577873	4
SLC33A1	2,57437E-08	0,90829753	4
SNHG12	3,3282E-07	0,887218045	4
SNRPB	5,43696E-06	0,869495166	4
SYT11	2,96711E-05	0,852846402	4
TAF11	8,12336E-06	0,86546724	4
TCEB2	1,32201E-06	0,882384533	4
TIMM10B	1,75964E-07	0,885606874	4
TMEM41B	2,86018E-05	0,852309345	4
TSC22D1	3,20347E-05	0,852040816	4
TSEN54	5,12698E-06	0,866004296	4
TTC14	7,33487E-07	0,888292159	4
TYW3	3,5239E-06	0,865601504	4
UQCRFS1	1,66106E-06	0,878625134	4
ZBTB9	1,69814E-06	0,880504834	4
ZNRF1	1,66365E-06	0,879699248	4
GRO1	4,91E-006	0,860767991	5

Supplementary Table S3. Cluster specific marker genes identified using SC3 pipeline with a threshold of the adjusted p-value < 0.01 and the area under the ROC curve (AUROC) > 0.85.

GO ID	GO Term	Corrected P-Value	Nr. Genes
GO:0042254	ribosome biogenesis	2,90E-06	9
GO:0042255	ribosome assembly	2,90E-03	3
GO:0042273	ribosomal large subunit biogenesis	3,60E-03	3
GO:0046112	nucleobase biosynthetic process	4,20E-03	3
GO:0006414	translational elongation	4,60E-03	3
GO:0008652	cellular amino acid biosynthetic process	5,40E-03	3

Supplementary Table S4. GO terms related to the six topics identified by using SC3 tool.

Topic	GO ID	GO Term	Term pValue corrected	No. Genes
1	GO:0006412	translation	1,50E-06	286
1	GO:0051301	cell division	2,20E-06	151
2	GO:0006412	translation	4,10E-18	286
2	GO:0006446	regulation of translational initiation	1,30E-08	29
2	GO:0000398	mRNA splicing, via spliceosome	1,70E-07	79
2	GO:0002181	cytoplasmic translation	5,60E-07	22
2	GO:0006364	rRNA processing	3,10E-06	74
2	GO:0000245	spliceosomal complex assembly	5,20E-06	14
2	GO:0048025	negative regulation of mRNA splicing, via spliceosome	5,60E-06	8
2	GO:0051301	cell division	1,10E-05	151
2	GO:0000381	regulation of alternative mRNA splicing, via spliceosome	1,90E-05	16
3	GO:0006412	translation	2,20E-06	286
4	GO:0015986	ATP synthesis coupled proton transport	7,10E-04	18
5	GO:0070125	mitochondrial translational elongation	6,50E-05	74
6	GO:0015850	organic hydroxy compound transport	3,00E-04	20

Supplementary Table S5. GO terms of the different topics, obtained by using CellTree tool.

Supplementary Figures

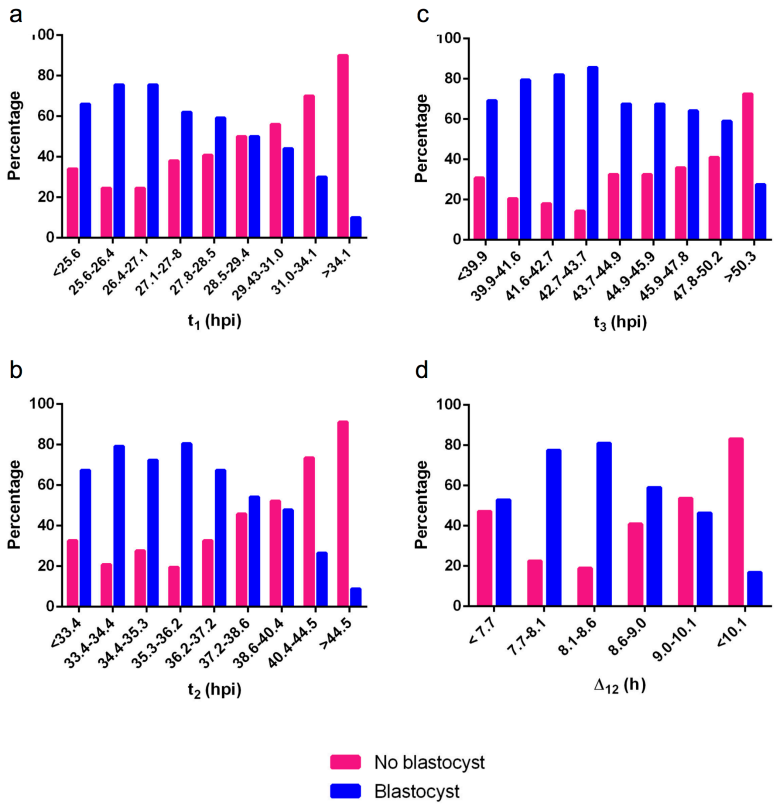

Supplementary Figure S1. (a) Early timing of the first cleavage had a positive effect on the blastocyst rate (optimal time range: 25.6-27.1 hpf) **(b)** Early timing of the second cleavage had a positive effect on the blastocyst rate (optimal time range: 33.4-36.2 hpf) **(c)** Early timing of the third cleavage had a positive effect on the blastocyst rate (optimal time range: 34.0-43.7 hpf). **(d)** Very short and very long time between the first and second cleavage had a negative effect on the blastocyst rate (optimal time range: 7.7-8.6 hpf). hpf = hours post fertilization.

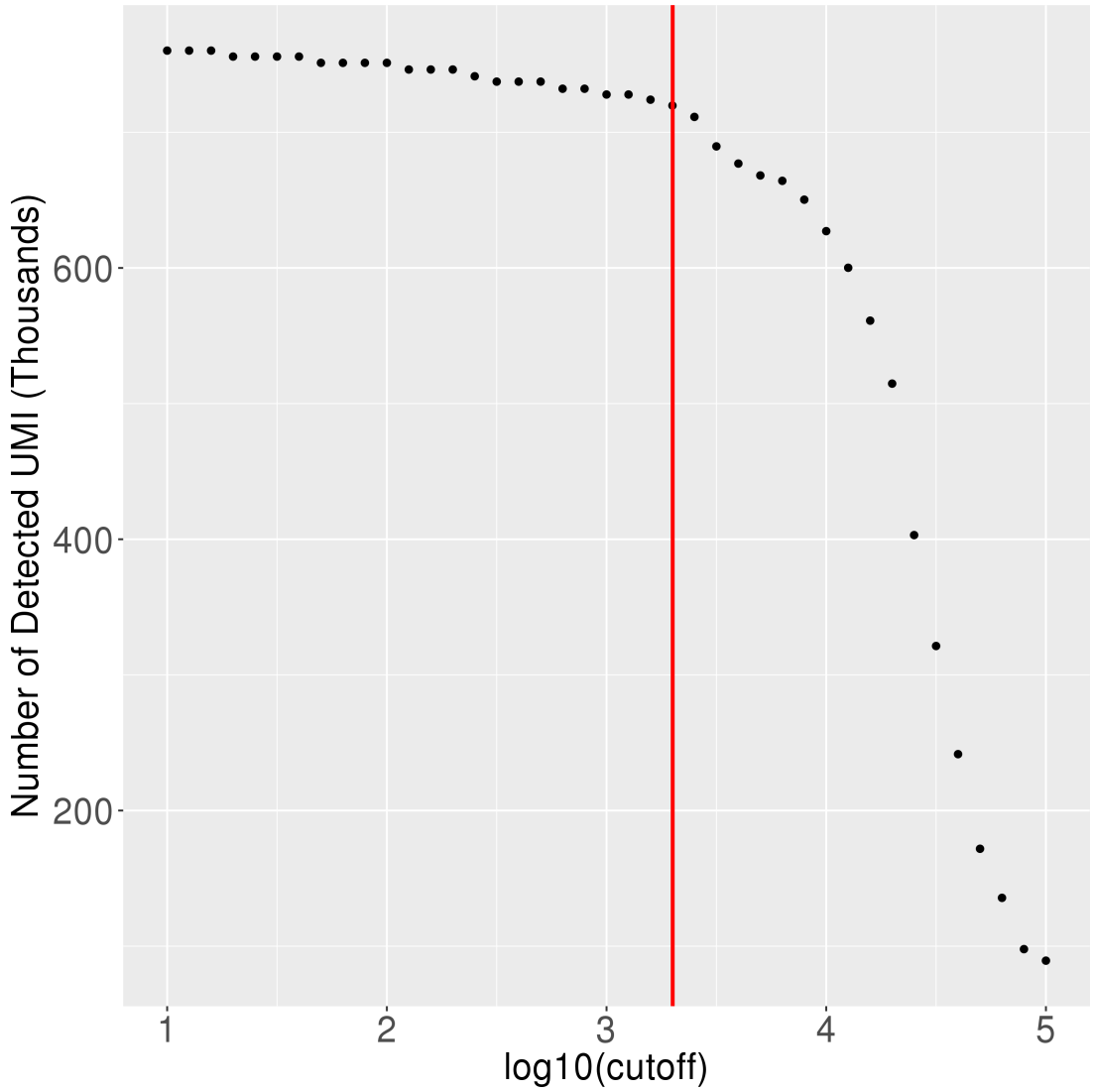

Supplementary Figure S2. Sum of the number of UMI counts detected across all cells with respect to the total UMI cut-off. The UMI cut-off is represented in log10 scale. The cut-off is set to 3.4 (~ 2,000 UMI).

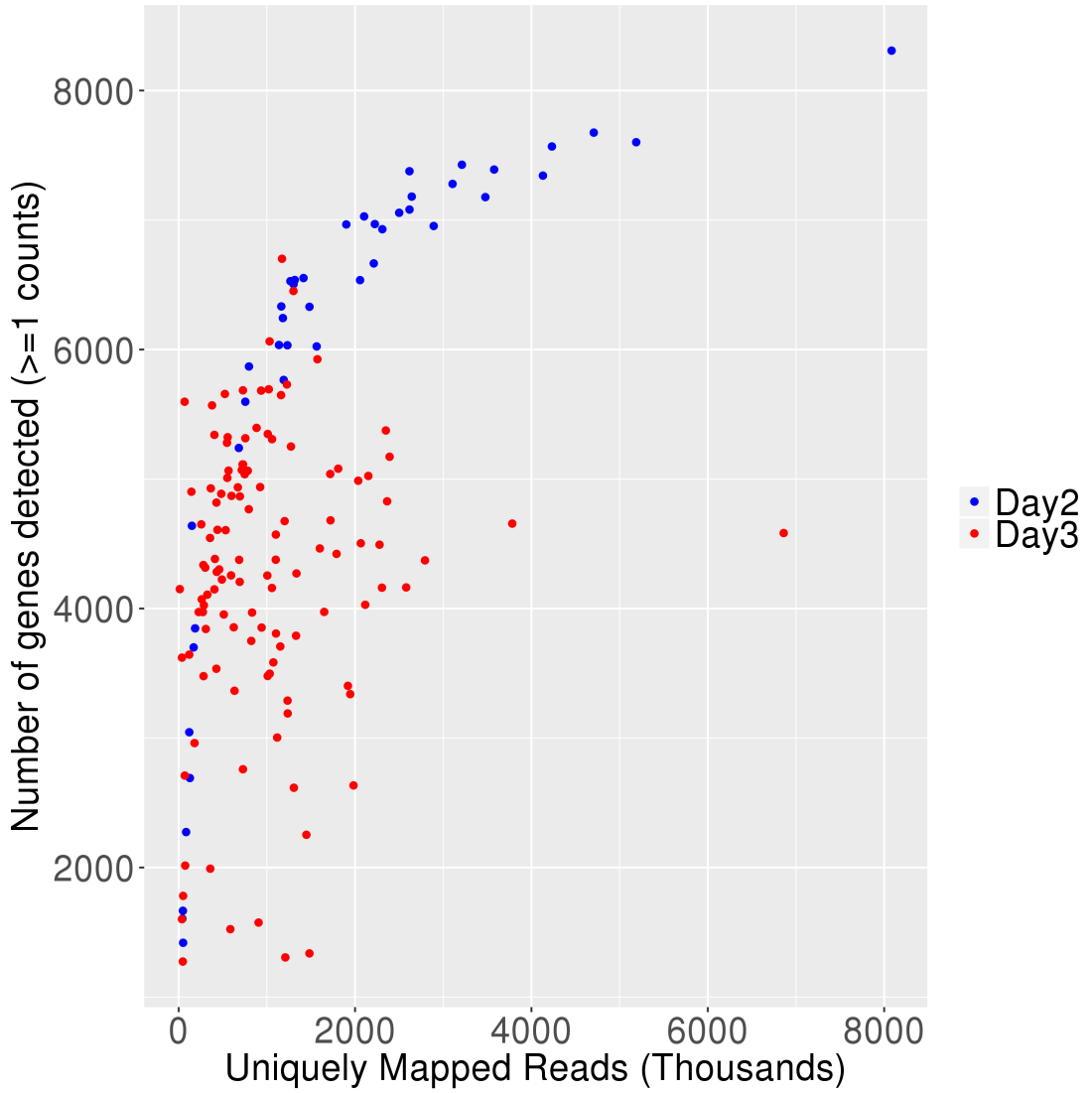

Supplementary Figure S3. Saturation Plot. Number of uniquely mapped reads vs number of genes with detected transcripts (>=1 counts). Data points are represented in blue for cells collected in Day 2 and in red for cells collected in Day 3.

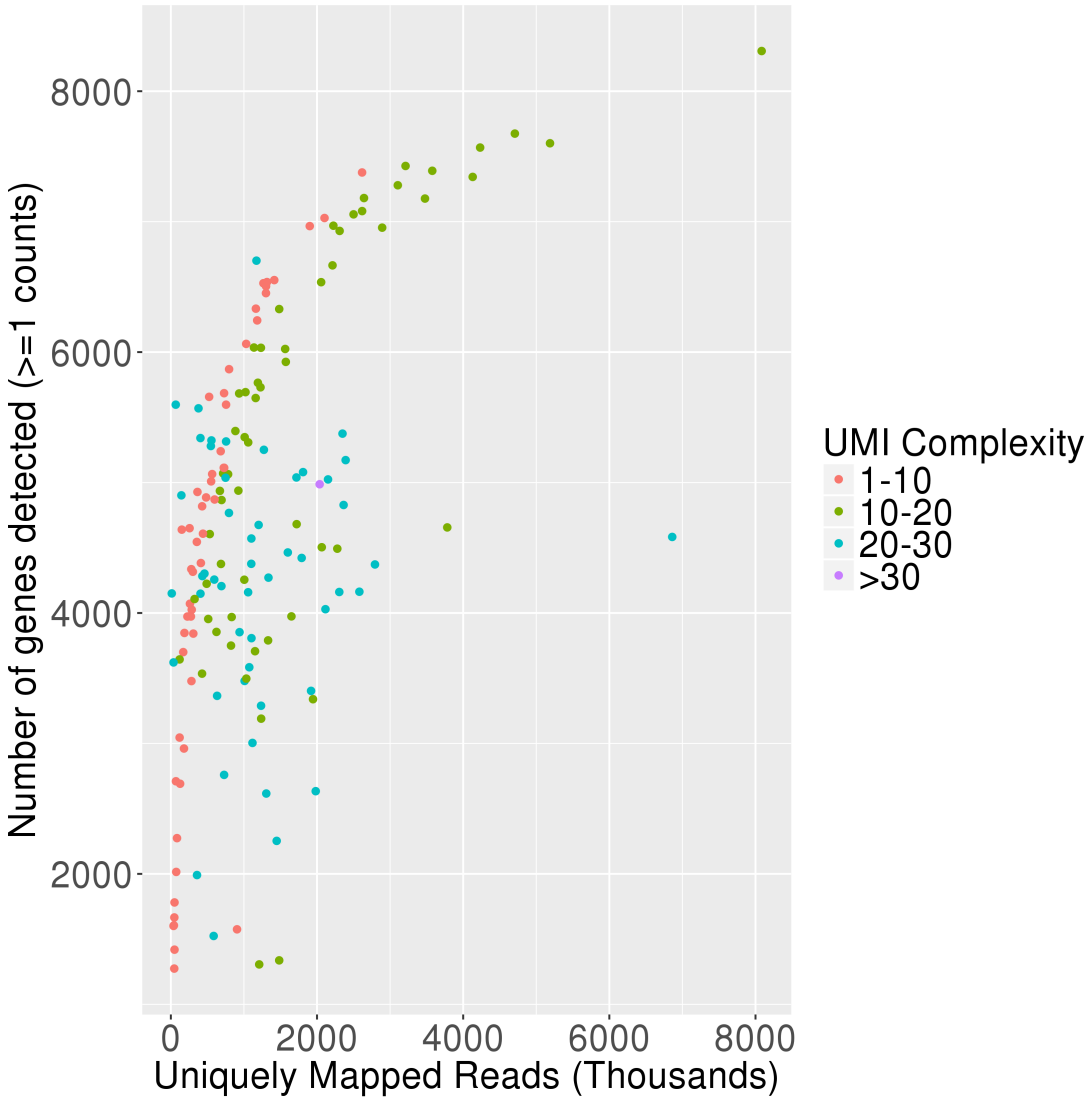

Supplementary Figure S4. Saturation Plot. Number of uniquely mapped reads vs number of genes detected (>=1 counts). Data points are represented in different colours according to the UMI complexity. The UMI complexity corresponds to the ratio between all counted molecular identifiers (MIs) and the number of unique molecular identifiers (UMIs).

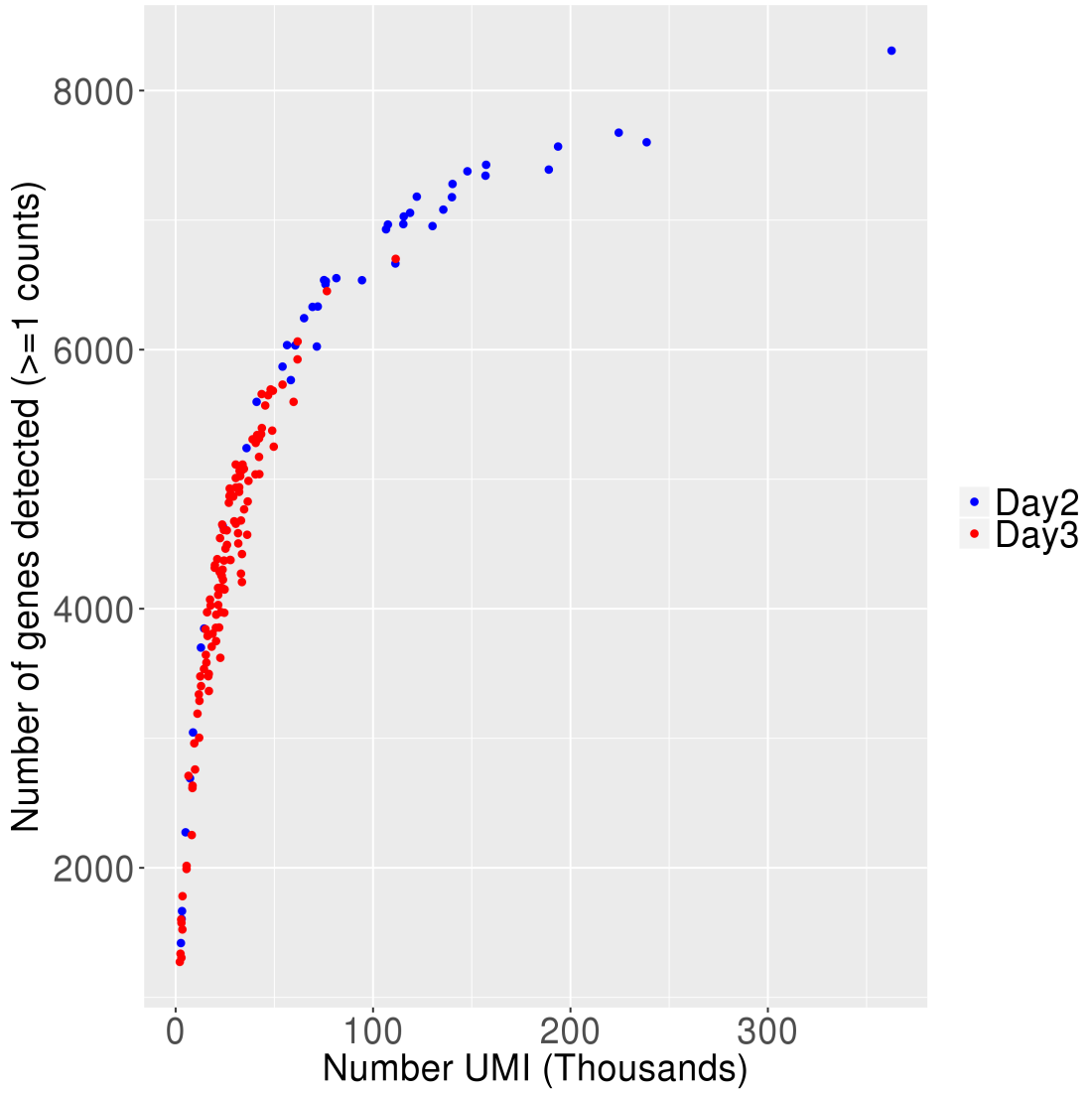

Supplementary Figure S5. Saturation Plot. Number of UMI vs number of genes with detected transcripts (>=1 counts). Data points are represented in blue for cells collected in Day 2 and in red for cells collected in Day 3.

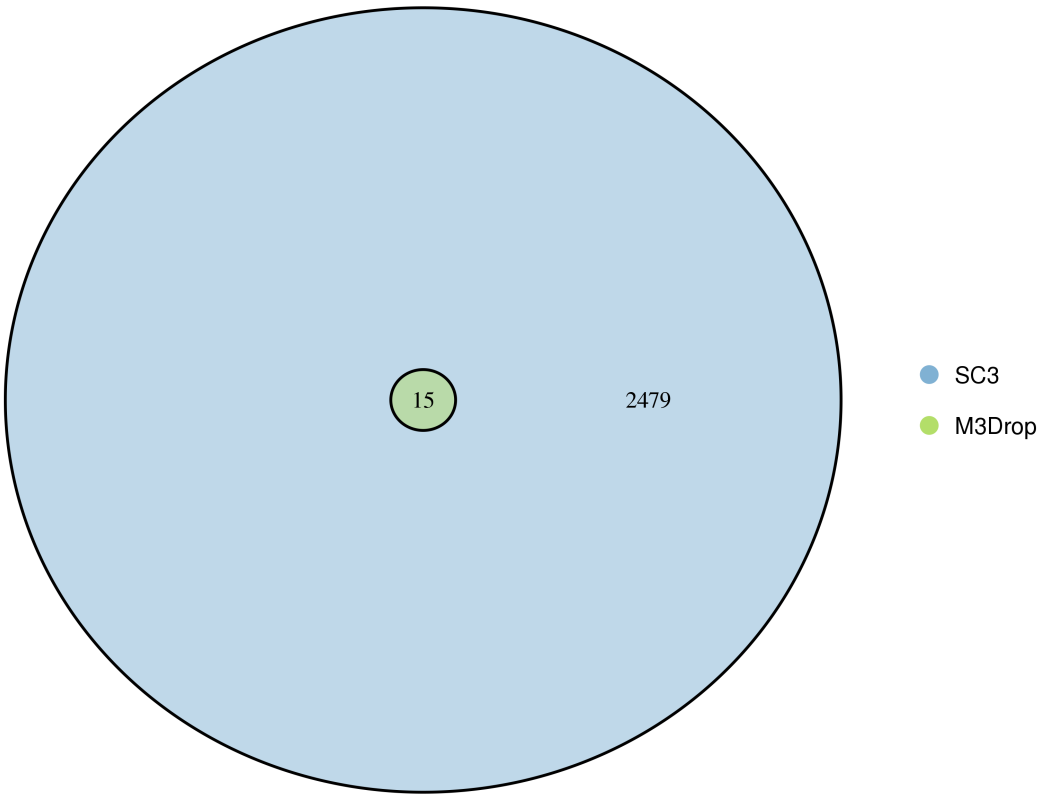

Supplementary Figure S6. Venn diagram comparing the 2,494 DATs, obtained by using SC3 pipeline, with the 15 genes not affected by drop-outs, obtained by using M3Drop approach.

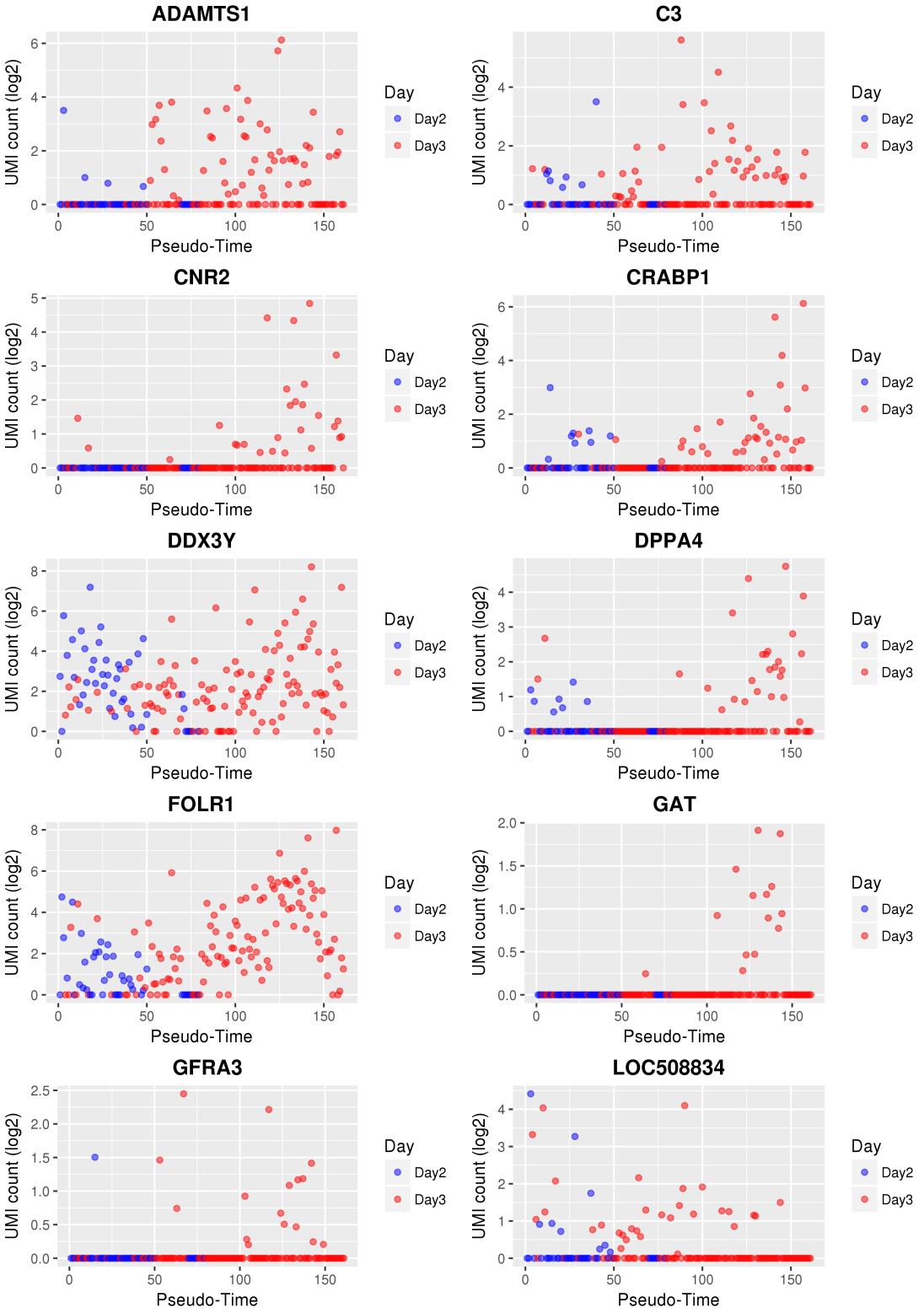
ADAMTS1
C3
CNR2
CRABP1
DDX3Y
DPPA4
FOLR1
GAT
GFRA3
LOC508834
UMI count (log2)
Pseudo-Time
Day
Day2
Day3

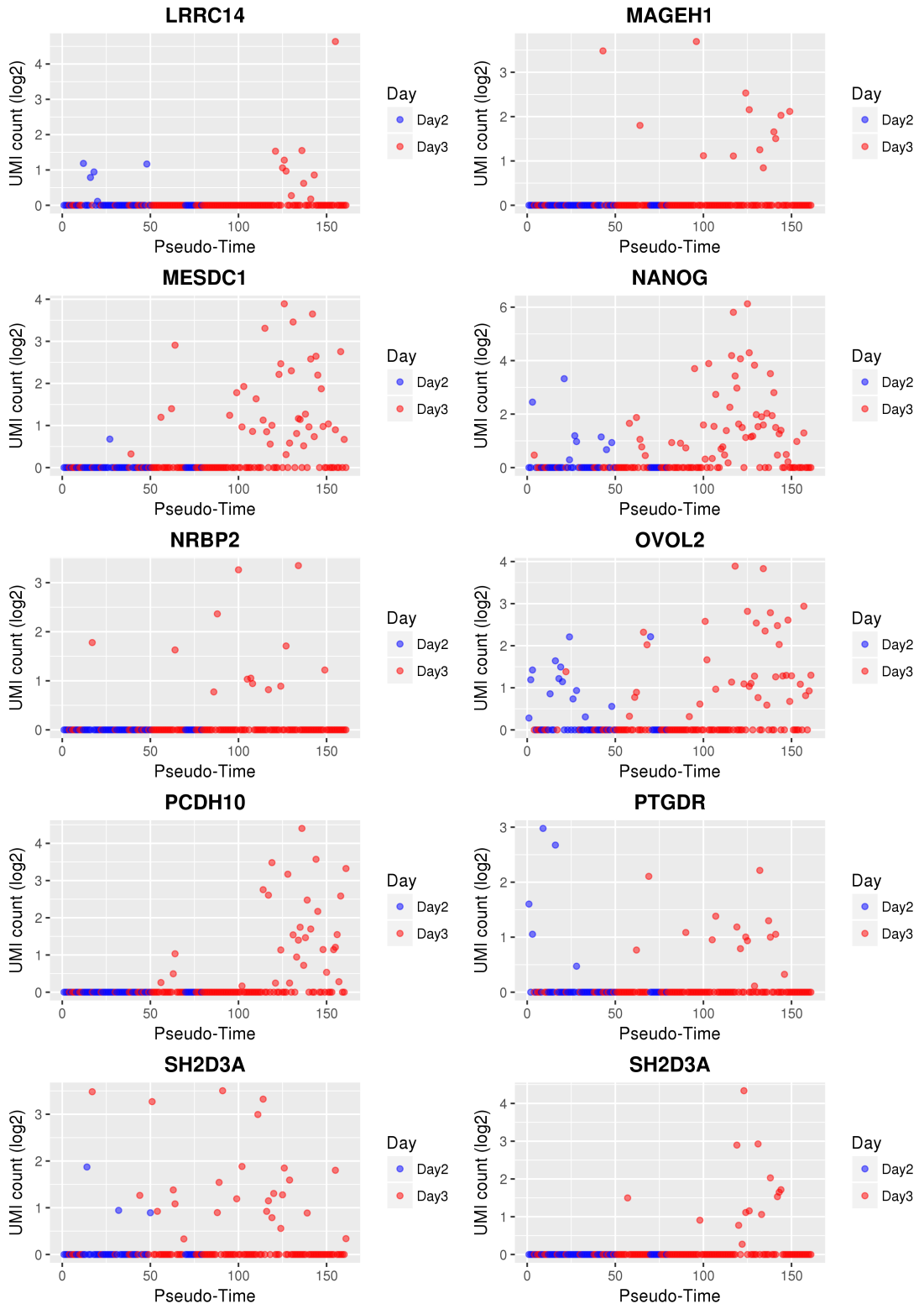

Supplementary Figure S7. Transcript abundance of the genes first actively transcribed at the major Embryonic Genome Activation (EGA), in all single cells. The single cells are aligned according to the pseudo-time line.

References

1. Tadros, W. & Lipshitz, H.D. The maternal-to-zygotic transition: a play in two acts. *Development* **136**, 3033-3042 (2009).
2. Sirard, M.A. Factors affecting oocyte and embryo transcriptomes. *Reprod Domest Anim* **47 Suppl 4**, 148-155 (2012).
3. Sepulveda-Rincon, L.P. *et al.* Random Allocation of Blastomere Descendants to the Trophectoderm and ICM of the Bovine Blastocyst. *Biol Reprod* **95**, 123 (2016).
4. Biase, F.H., Cao, X. & Zhong, S. Cell fate inclination within 2-cell and 4-cell mouse embryos revealed by single-cell RNA sequencing. *Genome research* **24**, 1787-1796 (2014).
5. Guo, G. *et al.* Resolution of cell fate decisions revealed by single-cell gene expression analysis from zygote to blastocyst. *Developmental cell* **18**, 675-685 (2010).
6. Blakeley, P. *et al.* Defining the three cell lineages of the human blastocyst by single-cell RNA-seq. *Development* **142**, 3613 (2015).
7. Petropoulos, S. *et al.* Single-Cell RNA-Seq Reveals Lineage and X Chromosome Dynamics in Human Preimplantation Embryos. *Cell* **167**, 285 (2016).
8. Yan, L. *et al.* Single-cell RNA-Seq profiling of human preimplantation embryos and embryonic stem cells. *Nature structural & molecular biology* **20**, 1131-1139 (2013).
9. Chitwood, J.L., Rincon, G., Kaiser, G.G., Medrano, J.F. & Ross, P.J. RNA-seq analysis of single bovine blastocysts. *BMC genomics* **14**, 350 (2013).
10. Graf, A. *et al.* Fine mapping of genome activation in bovine embryos by RNA sequencing. *Proceedings of the National Academy of Sciences of the United States of America* **111**, 4139-4144 (2014).
11. Negron-Perez, V.M., Zhang, Y. & Hansen, P.J. Single-cell gene expression of the bovine blastocyst. *Reproduction (Cambridge, England)* **154**, 627-644 (2017).
12. Wei, Q., et al. Bovine lineage specification revealed by single-cell gene expression analysis from zygote to blastocyst. *Biology of Reproduction* (2017).
13. Sugimura, S. *et al.* Promising system for selecting healthy in vitro-fertilized embryos in cattle. *PloS one* **7**, e36627 (2012).
14. Beck, A. (Universitätsbibliothek der Ludwig-Maximilians-Universität, München; 2014).
15. Soumillon, M., Cacchiarelli, D., Semrau, S., van Oudenaarden, A. & Mikkelsen, T.S. Characterization of directed differentiation by high-throughput single-cell RNA-Seq. *bioRxiv* (2014).
16. Kiselev, V.Y. *et al.* SC3: consensus clustering of single-cell RNA-seq data. *Nature methods* **14**, 483-486 (2017).
17. Tracy, C.A. & Widom, H. Level spacing distributions and the Bessel kernel. *Communications in Mathematical Physics* **161**, 289-309 (1994).
18. Andrews, T.S. & Hemberg, M. Modelling dropouts allows for unbiased identification of marker genes in scRNASeq experiments. *bioRxiv* (2016).

19. Goorden, S.M. *et al.* Rheb is essential for murine development. *Molecular and cellular biology* **31**, 1672-1678 (2011).
20. Khan, D.R. *et al.* Expression of pluripotency master regulators during two key developmental transitions: EGA and early lineage specification in the bovine embryo. *PloS one* **7**, e34110 (2012).
21. Kooistra, M., Trasler, J.M. & Baltz, J.M. Folate transport in mouse cumulus-oocyte complexes and preimplantation embryos. *Biol Reprod* **89**, 63 (2013).
22. Parisi, S. *et al.* Klf5 is involved in self-renewal of mouse embryonic stem cells. *Journal of cell science* **121**, 2629-2634 (2008).
23. Bindea, G. *et al.* ClueGO: a Cytoscape plug-in to decipher functionally grouped gene ontology and pathway annotation networks. *Bioinformatics (Oxford, England)* **25**, 1091-1093 (2009).
24. duVerle, D.A., Yotsukura, S., Nomura, S., Aburatani, H. & Tsuda, K. CellTree: an R/bioconductor package to infer the hierarchical structure of cell populations from single-cell RNA-seq data. *BMC bioinformatics* **17**, 363 (2016).
25. Carlson, M.R., Pages, H., Arora, S., Obenchain, V. & Morgan, M. Genomic Annotation Resources in R/Bioconductor. *Methods in molecular biology (Clifton, N.J.)* **1418**, 67-90 (2016).
26. Le Bin, G.C. *et al.* Oct4 is required for lineage priming in the developing inner cell mass of the mouse blastocyst. *Development (Cambridge, England)* **141**, 1001-1010 (2014).
27. Kirchhof, N. *et al.* Expression pattern of Oct-4 in preimplantation embryos of different species. *Biol Reprod* **63**, 1698-1705 (2000).
28. Simmet, K. *et al.* Bovine OCT4 (POU5F1) knockout embryos fail during the second lineage differentiation due to loss of NANOG. *Reproduction, Fertility and Development* **29**, 138-138 (2016).
29. Schiffmacher, A.T. & Keefer, C.L. CDX2 regulates multiple trophoblast genes in bovine trophectoderm CT-1 cells. *Molecular reproduction and development* **80**, 826-839 (2013).
30. Berg, D.K. *et al.* Trophectoderm Lineage Determination in Cattle. *Developmental cell* **20**, 244-255 (2011).
31. Kuijk, E.W. *et al.* Differences in early lineage segregation between mammals. *Developmental dynamics : an official publication of the American Association of Anatomists* **237**, 918-927 (2008).
32. Bai, H. *et al.* Expression and Potential Role of GATA6 in Ruminant Trophoblasts during Peri-Implantation Periods. *Journal of Mammalian Ova Research* **29**, 135-141 (2012).
33. Claveria, C., Giovinazzo, G., Sierra, R. & Torres, M. Myc-driven endogenous cell competition in the early mammalian embryo. *Nature* **500**, 39-44 (2013).
34. Zhang, P., Andrianakos, R., Yang, Y., Liu, C. & Lu, W. Kruppel-like factor 4 (Klf4) prevents embryonic stem (ES) cell differentiation by regulating Nanog gene expression. *The Journal of biological chemistry* **285**, 9180-9189 (2010).

35. Katz, J.P. *et al.* The zinc-finger transcription factor Klf4 is required for terminal differentiation of goblet cells in the colon. *Development* **129**, 2619-2628 (2002).
36. Zhang, J. *et al.* Sall4 modulates embryonic stem cell pluripotency and early embryonic development by the transcriptional regulation of Pou5f1. *Nat Cell Biol* **8**, 1114-1123 (2006).
37. Karantzali, E. *et al.* Sall1 regulates embryonic stem cell differentiation in association with nanog. *The Journal of biological chemistry* **286**, 1037-1045 (2011).
38. Kent, L.N., Rumi, M.A., Kubota, K., Lee, D.S. & Soares, M.J. FOSL1 is integral to establishing the maternal-fetal interface. *Molecular and cellular biology* **31**, 4801-4813 (2011).
39. Nagatomo, H. *et al.* Transcriptional wiring for establishing cell lineage specification at the blastocyst stage in cattle. *Biol Reprod* **88**, 158 (2013).
40. Wong, C.C. *et al.* Non-invasive imaging of human embryos before embryonic genome activation predicts development to the blastocyst stage. *Nature biotechnology* **28**, 1115-1121 (2010).
41. Dobin, A. *et al.* STAR: ultrafast universal RNA-seq aligner. *Bioinformatics (Oxford, England)* **29**, 15-21 (2013).
42. Tung, P.Y. *et al.* Batch effects and the effective design of single-cell gene expression studies. *Scientific reports* **7**, 39921 (2017).
43. Kivioja, T. *et al.* Counting absolute numbers of molecules using unique molecular identifiers. *Nature methods* **9**, 72-74 (2011).
44. Buettner, F. *et al.* Computational analysis of cell-to-cell heterogeneity in single-cell RNA-sequencing data reveals hidden subpopulations of cells. *Nature biotechnology* **33**, 155-160 (2015).
45. McDavid, A., Finak, G. & Gottardo, R. The contribution of cell cycle to heterogeneity in single-cell RNA-seq data. *Nature biotechnology* **34**, 591-593 (2016).
46. Knott, J.G. & Paul, S. Transcriptional regulators of the trophoblast lineage in mammals with hemochorial placentation. *Reproduction (Cambridge, England)* **148**, R121-136 (2014).
47. Arnold, S.J. & Robertson, E.J. Making a commitment: cell lineage allocation and axis patterning in the early mouse embryo. *Nature Reviews Molecular Cell Biology* **10**, 91 (2009).
48. Bruce, A.W. & Zernicka-Goetz, M. in Current Opinion in Genetics & Development, Vol. 20 485-491 (2010).
49. Reichenbach, M. *et al.* Germ-line transmission of lentiviral PGK-EGFP integrants in transgenic cattle: new perspectives for experimental embryology. *Transgenic research* **19**, 549-556 (2010).
50. Kurome, M., Kessler, B., Wuensch, A., Nagashima, H. & Wolf, E. Nuclear transfer and transgenesis in the pig. *Methods in molecular biology (Clifton, N.J.)* **1222**, 37-59 (2015).
51. Simmet, K., Reichenbach, M., Reichenbach, H.D. & Wolf, E. Phytohemagglutinin facilitates the aggregation of blastomere pairs from Day 5 donor

embryos with Day 4 host embryos for chimeric bovine embryo multiplication. *Theriogenology* **84**, 1603-1610 (2015).
52. Macosko, E.Z. *et al.* Highly Parallel Genome-wide Expression Profiling of Individual Cells Using Nanoliter Droplets. *Cell* **161**, 1202-1214 (2015).

Discussion

The aim of the project was to study blastomere development during and right after the major embryonic genome activation in bovine embryos, by evaluation of transcriptome profiles at single cell level. These profiles had been generated by single-cell RNA-sequencing of eight- to 16-cell stage *in vitro* fertilized bovine embryos. Eight-cell stage embryos were collected at Day 2 post fertilization, while 16-cell stage embryos were collected at Day 3 post fertilization. For this purpose, Single Cell RNA-Barcode Sequencing (SCRB-seq) sequencing libraries were constructed, with polyA+ of adequate size selection. These transcriptome profiles were evaluated by tailored bioinformatics approaches in order to gain new insights into the transcriptome dynamics of developing blastomeres in bovine embryos from eight- to 16-cell stage.

The technology of Single-cell RNA sequencing

Single-cell RNA sequencing (scRNA-seq) offers new possibilities to address specific biological questions as it enables transcriptomic analysis of cell states and dynamics [24].

A characteristic of this technology is the very low amount of starting material. For bulk RNA-seq the starting material is ~100 ng, while for scRNA-seq the amount of starting RNA is ~10 pg [25]. This implies that for scRNA-seq amplification plays a crucial role and that for this technology avoiding PCR duplicates is fundamental [26]. In order to avoid PCR duplicates, Unique Molecular Identifiers (UMIs), molecular tags used to identify unique mRNA transcripts, can be used [25].

Diverse scRNA-seq protocols with specificities are available to researchers (e.g. Drop-seq, SCRB-seq, Smart-seq). For the purpose of our study, we decided to carry out the experiment with SCRB-seq protocol because it enables UMIs usage (necessary to exclude duplicates originating from PCR amplification) and 3' specific through polyA+ selection [27]. The SCRB-seq protocol does not involve the full-length sequencing, thus reducing the cost. SCRB-seq protocol was also observed to provide high complexity of mRNA-molecules and good sensitivity and accuracy when compared to CEL-seq2, Drop-seq, MARS-seq, Smart-seq, and Smart-seq2 [28]. These features offered us the opportunity to conduct good scientific research at lower cost.

From Raw to Processed Data

scRNA-seq data present the feature of a high proportion of zero reads because of both biological (e.g. subpopulation of cells or transient states where a gene is not expressed) and technical reasons (e.g. drop-out, where a gene in expressed but not detected) [24]. Therefore many assumptions done for bulk RNA-seq do not apply to scRNA-seq and specific pipelines for data processing are necessary in order to avoid

misleading data interpretation [29]. This paragraph describes the pipeline for obtaining the processed data that were used for the subsequent downstream analyses.
After sequencing, cDNA reads were mapped to the bovine genome reference btau7 (UCSC) with the STAR tool [30]. SCRB-seq allowed us the usage of UMIs [26] instead of read count in order to exclude duplicates due to PCR amplification.
Subsequently, data were normalized to account for differences in efficiency of transcript recovery between wells. In order to perform normalization gene specific UMI counts were divided by the total number of UMI counts per blastomere and then multiplied by the median of total UMI counts across all blastomeres. Soumillon et al. [27] had carried out this procedure for normalization. Normalization was indeed performed without using exogenous spike-ins, because technical variations do not affect spike-ins and endogenous transcripts uniformly, thus causing poorly normalized data [31].
In order to remove the blastomeres with low quality data, a threshold for the minimum number of UMI per library was set to 2,000 UMI, as suggested by Soumillon et al. [27]. In order to ensure a correct value for the threshold, this was also empirically estimated on our dataset by plotting the sum of the number of UMI counts detected across all cells with respect to the total UMI cut-off. The empirical threshold value estimation confirmed the value of 2,000 UMIs per library and nine out of 170 cells, having a lower amount of UMI, were not included in the following downstream analyses.
In single-cell transcriptome analysis genes involved in cell cycle are sometimes omitted from downstream analyses because they are believed to constitute a substantial proportion of the variability in single-cell gene expression (>30%) [32]. However, this has been object of debate in the scientific community [33] and for our dataset genes involved in cell cycle were not excluded.

Cell Population Characterization Based on Transcriptome Profiles

Single-cell RNA-seq (scRNA-seq), acquiring the whole transcriptome of individual cells, enables a quantitative cell population characterization. Due to the large variability in gene expression and the presence of drop-outs (zero read counts for certain genes, due to failure of the reverse transcription or low read counts), identifying cell populations based on the transcription profiles is a challenging task. The Single-Cell Consensus Clustering (SC3) tool [34] achieves high accuracy and robustness by integrating different clustering solutions through a consensus approach. The number of clusters to assign to the unsupervised clustering tool was determined by using the Tracy-Widom test [35]. This finding suggests the presence of six cell populations during the development between eight- and 16-cell stages. Three out of six clusters contained cells from both Day 2 and Day 3 embryos, hinting that at least some blastomeres of an embryo evolve independently. Among these six clusters, 2,494 differentially abundant transcripts (DATs) were found. This number is comparable to the number of 2,940 DATs described by Graf, et al. [10] in pools of ten of eight- to 16-cell stage embryos. For four out of six clusters, cluster specific (also

called “marker”) genes were identified. Interestingly, *NANOG*, a gene involved in the maintenance of pluripotency, was found as one of the 86 marker genes in cluster 4.
In order to investigate the drop-outs present in our dataset, we also used Michaelis-Menten Modelling of Dropouts (M3Drop) tool [36] and found that only 15 not dropout-affected genes. However this approach cannot distinguish between technically caused drop-outs and stage specific mRNA species that are thus degraded over the time. These findings suggest the presence of transient states, where some genes are not expressed. This data interpretation correlates well with the linear structure of the backbone tree (discussed in the paragraph “Pseudo-time of Blastomeres”), thus excluding the presence of cell-types at these developmental stages.

Pseudo-time of Blastomeres

In order to better understand the biological processes occurring during the development, another approach focusing on the different positions of the blastomeres in the developmental line was used. The individual blastomeres were aligned according to their *in silico* chronological order (also called “pseudo-time”) and a backbone tree taking into account such order was constructed by using the CellTree tool [37]. Along the pseudo-time line, some embryos had their blastomeres either located in close vicinity or distributed over a broad range. This finding hints individual development of each blastomere within an embryo. Furthermore, the not-branched but linear structure of the backbone tree suggests the first lineage differentiation towards inner cell mass and trophectoderm has not occurred yet, and that it is a temporal continuity of the development. Along the pseudo-time line, different over-represented GO terms were identified. Their order suggests organized on-going biological processes and hints that initially “translation” and “cell division” are the most over-represented GO terms, the “cell division” GO term then gradually disappears being replaced first by the “translation” GO term and later by “translation” and terms involved in “RNA processing” GO terms. The over-representation of the “translation” GO term along the pseudo-time line can be explained by the fact that many transcripts involved in translation were activated at the four-cell stage or before [38].

Embryonic Genome Activation in each Blastomere

In order to study the major Embryonic Genome Activation (EGA) at single cell level, we investigated the abundance of 20 detected transcripts (out of a total of 129) that are known to be first detected at the eight-cell stage [10]. Seven of the 161 analyzed cells did not have detectable levels of any of these transcripts and were collected at both Day 2 and Day 3 post fertilization. In the other cells we observed individual transcript abundances of these 20 genes and could not find significant high correlation among their transcript levels. In addition, blastomeres of individual embryos showed different transcript abundances. These results showed that the major EGA events occur individually and in individual blastomeres of embryos. This corroborates the

findings of the stochastic gene expression detected in single-cell RNA sequencing data. Stochasticity has been explained as a result of histone modifications modulating transcription, thus having impact on the probability of differentiation in embryonic stem cells [39].

Genes inducing or Reflecting Cell Fate Decisions

In order to shed light on cell lineage inclination events, we investigated a selected set of genes known to be involved in early cell fate decision. As *CDX2*, *POU5F1/OCT4*, *GATA6* and *NANOG* are the key genes involved during the first and second lineage segregation in mouse embryos [40], they were selected for further investigated.

In the bovine embryo *CDX2* is known to be the marker gene of trophectoderm. However a key gene involved in differentiation towards inner cell mass (ICM) has not been identified in bovine embryos yet [40]. *POU5F1*/*OCT4* and *CDX2* transcripts were revealed in 74% and 53% of the Day 2 blastomeres, while these proportions decreased to 50% and 12% in the Day 3 blastomeres, respectively. This is most likely due to degradation of maternal RNA that is apparently more pronounced for *CDX2* than for *POU5F1*/*OCT4*. The relatively high mRNA levels of *CDX2* in a proportion of the Day 3 blastomeres may hint to lineage inclination towards trophectoderm, although this was not evident from the backbone tree generated by the CellTree tool. An alternative explanation would be impaired maternal RNA degradation in a proportion of the blastomeres. It is known that *CDX2* down-regulates *POU5F1/OCT4* levels [41], without suppressing its expression [42]. However statistical analyses did not identify a significant correlation between the transcript abundance of *CDX2* and *POU5F1*/*OCT4* at these stages, thus suggesting that at these stages *CDX2* does not play its regulatory role.

During the second lineage segregation, as well as in the mouse model, *GATA6* and *NANOG* are key regulators of primitive endoderm and pluripotent epiblast, respectively [40]. Transcripts of the primitive endoderm marker gene *GATA6* were not detected in our study. *NANOG* transcripts were detected in only 19% (8/43) of the Day 2 blastomeres, but in 43% (51/118) of the Day 3 blastomeres, reflecting a gradual and asynchronous activation of this gene in individual blastomeres. *NANOG* and *POU5F1/OCT4* were observed to be up-regulated in epiblast in bovine [43]. It is known that *POU5F1/OCT4* is required for *NANOG* expression in bovine blastocysts [44], however statistical analyses did not identify a significant correlation between the transcript abundances of these two genes, suggesting that the developmental stage is too premature for observing gene product interactions.

Other genes whose transcription was activated at the eight- or 16-cell stage were further investigated. Transcripts of *MYC* that is involved in selecting the epiblast cell pool are already present in the oocyte [10], but were detected in only one blastomere from a Day 2 embryo and in ~ 45% of the Day 3 blastomeres. This suggests rapid degradation of maternal *MYC* transcripts and embryonic activation of *MYC* towards the end of major EGA in about half of the blastomeres. *KLF4* (necessary for preventing differentiation) and *SALL4* (involved in maintenance of pluripotency) are

also present in oocytes and are thus detected before the eight-cell stage [10]. In the present study, blastomeres located at the end of the pseudo-time line showed higher transcript abundance of *KLF4,* suggesting increased embryonic transcription of this gene. The abundance levels of *SALL4* transcripts were high at the beginning and at the end of the pseudo-time line, but lower in the middle. This finding hints to initial degradation of maternal *SALL4* transcripts followed by active embryonic transcription of *SALL4*. Embryonic transcription of *SALL1* (involved in pluripotency) and *FOSL1* (involved in TE development) is known to start at the 16-cell stage, although maternal transcripts of these genes were detected at earlier stages [10]. This explains the higher abundance of transcripts of the *SALL1* and *FOSL1* at the beginning of the pseudo-time line. Compared to *FOSL1*, the abundance of *SALL1* transcripts was on average lower and detected in a smaller proportion of blastomeres. Blastomeres with detectable levels of both transcripts were frequently found at the beginning of the pseudo-time line. Interestingly, in mouse embryonic stem cells, over-expression of the *Sall1* gene was observed to positively regulate the *Nanog* expression and thus prevent differentiation [45]. *FOSL1* is known to be important for invasive placentation, e.g. in human and mouse [46]. In our study of bovine embryos, the abundance of *FOSL1* transcripts was highest at the beginning and decreased towards the end of the pseudo-time line, which may be related to the late implantation and non-invasive, synepitheliochorial placentation in ruminants.

The interesting finding of *PCDH10*

As the analysis showing the backbone tree suggested that first lineage segregation events do not occur at the major EGA (in bovine embryos between eight- to 16-cell stage), we investigated cell fate inclination events towards inner cell mass (ICM) or trophectoderm (TE). Similar studies revealed cell fate inclination between two- and four- cell stages in mouse embryos by using single-cell RNA-seq [47].

In order to answer this question, we investigated the abundance of *PCDH10* transcript. We selected this as candidate gene because it is known to be first detectable at the eight-cell stage [10] and predominantly expressed in ICM at the blastocyst stage [21]. In mice, PCDH10 protein was detected along axon fibers, but its role is still unclear (reviewed by [48]). In our study, *PCDH10* transcripts were detected in 30 blastomeres of 7 Day 3 embryos at the advanced end of the pseudo-time line, raising the possibility that these blastomeres may be determined towards ICM.

The comparison of the transcriptome profiles of the blastomeres expressing *PCDH10* with those ones not expressing *PCDH10* did not show significant results. This did not support the hypothesis that *PCDH10* is an indicator of cell fate inclination towards ICM. Furthermore, the non-branched backbone tree revealed by the CellTree analysis of our data set argues against major lineage inclination events at the developmental stages investigated. These results correlate well with elegant aggregation experiments of labelled TE cells with blastomeres from eight-cell embryos. These revealed that TE cells can contribute to the ICM and its derivatives [42], thus arguing against early lineage commitment in bovine embryos.

Summary

In this thesis, the transcriptome of bovine embryos is investigated at the single-cell level, at the eight- to 16-cell stage. Therefore, cells were collected from *in vitro* fertilized bovine embryos at the Day 2 and Day 3 post fertilization, which correspond to eight- to 16-cell stage. Subsequently, the libraries were performed using Single Cell RNA Barcode-Sequencing (SCRB-seq) protocol and 1,896,797 reads were obtained on average per library. After filtering and normalizing, the transcriptome data were used to cluster the cells and to *in silico* sort them in a time line and then build a backbone tree.

Hierarchical clustering analysis identified six different groups (cell populations) among the blastomeres collected from the eight- to 16-cell stage. Each cell population comprised blastomeres of different embryos and three of the six cell populations included blastomeres of embryos collected at a different day. This result suggested heterogeneity in the transcription pattern among the blastomeres. Furthermore, cells were *in silico* aligned according to their computed pseudo-time. In each embryo, blastomeres were located either in close vicinity or distributed over a broad range. This suggested asynchronous development of embryos and the individual development of each blastomere. In addition, the structure of the related backbone tree was not branched but linear, suggesting that the first lineage differentiation towards inner cell mass (ICM) or trophectoderm (TE) has not occurred yet, but that it is an on-going process.

To conclude, *PCDH10* was bioinformatically identified because its transcript is known to be firsts observed at the eight-cell stage [10] and because observed as predominantly expressed in ICM at the blastocyst stage [21]. However its role in bovine embryo development needs to be further investigated in order to assess if it is event inclination marker gene towards ICM.

In summary, this thesis sheds unprecedented light on blastomere transcriptome dynamics in bovine embryo, during and after the major embryonic genome activation. Blastomeres collected from eight- to 16-cell stage embryos showed heterogeneity in the transcriptome profiles and a continuity of the developmental process is visible.

Zusammenfassung

Analyse der Blastomeren boviner Embryonen im Zeitraum der Genomaktivierung anhand von Einzelzell-RNA-Sequenzierungsdaten

Ziel dieser Arbeit war zu klären, wie die Genomaktivierung in einzelnen Blastomeren von Rinderembryonen im 8- bis 16-Zellstadium abläuft, wie groß die Heterogenität der Transkriptome einzelner Blastomeren innerhalb eines Embryos sowie zwischen Embryonen des gleichen Stadiums ist und ob es bereits in diesen frühen Stadien Hinweise auf erste Differenzierungsprozesse im Embryo gibt.
Aus *in vitro* produzierten Embryonen wurden am Tag 2 und 3 nach der Befruchtung Zellen gesammelt, welche dem 8- bis 16-Zellen-Stadium entsprechen. Anschließend wurden die cDNA Bibliotheken für die Einzellzell-RNA-Sequenzierungsanalyse unter Verwendung des Einzelzell-RNA-Barcode-Sequenzierungs-(SCRB-seq)-Protokolls generiert. Im Durchschnitt wurden pro Bibliothek 1.896.797 reads erhalten. Nach dem Filtern und Normalisieren wurden die Transkriptomdaten verwendet, um die Zellen zu clustern. Danach wurden sie *in silico* mit Hilfe des Programms CellTree in einer Pseudo-Zeitlinie sortiert und in einem Baumdiagram angeordnet.
Die hierarchische Clusteranalyse identifizierte sechs verschiedene Gruppen (Zellpopulationen) unter den Blastomeren, die im 8- bis 16-Zellstadium gesammelt wurden. Jede Zellpopulation umfasste Blastomeren verschiedener Embryonen. Drei der sechs Zellpopulationen umfassten Blastomeren von Embryonen, die an einem anderen Tag gesammelt wurden. Dieses Ergebnis zeigt eine Heterogenität des Transkriptionsmusters der Blastomeren. Darüber hinaus wurden Zellen *in silico* entsprechend ihrer berechneten Pseudo-Zeit angeordnet. In jedem Embryo befanden sich Blastomeren entweder in enger Nachbarschaft oder weit verteilt auf der Pseudo-Zeitlinie. Dies suggerierte eine asynchrone Entwicklung von Embryonen und die individuelle Entwicklung jeder einzelnen Blastomere. Darüber hinaus war die Struktur des zugehörigen Baumdiagram nicht verzweigt, sondern linear, was darauf hindeutet, dass noch keine Differenzierung in Richtung Trophektoderm bzw. Innere Zellmasse stattgefunden hat. Trotzdem war in einigen Blastomeren im späteren Abschnitt der Pseudo-Zeitlinie eine vermehrte Expression des Gens *PCDH10* zu beobachten, das im Blastozystenstadium vor allem in der Inneren Zellmasse exprimiert ist [10,21].

Zusammenfassend liefert diese Arbeit einen Einblick in die Dynamik des Blastomerentranskriptoms in Rinderembryonen während Hauptwelle der embryonalen Genomaktivierung. Die gefundene Heterogenität der Blastomeren-Transkriptome weist auf ein Kontinuum des Entwicklungsprozesses hin.

References

1 Menezo, Y. J. & Herubel, F. Mouse and bovine models for human IVF. *Reproductive biomedicine online* **4**, 170-175 (2002).

2 Barnes, F. L. E., W.H. Early cleavage and the maternal zygotic transition in bovine embryos. *Theriogenology* **33**, 141-152 (1990).

3 Plante, L. & King, W. A. Light and electron microscopic analysis of bovine embryos derived by in vitro and in vivo fertilization. *Journal of assisted reproduction and genetics* **11**, 515-529 (1994).

4 Johnson, M. H. & McConnell, J. M. Lineage allocation and cell polarity during mouse embryogenesis. *Seminars in cell & developmental biology* **15**, 583-597, doi:10.1016/j.semcdb.2004.04.002 (2004).

5 Koyama, H., Suzuki, H., Yang, X., Jiang, S. & Foote, R. H. Analysis of polarity of bovine and rabbit embryos by scanning electron microscopy. *Biol Reprod* **50**, 163-170 (1994).

6 Laurincik, J. *et al.* Nucleolar proteins and nuclear ultrastructure in preimplantation bovine embryos produced in vitro. *Biol Reprod* **62**, 1024-1032 (2000).

7 Kopecny, V., Flechon, J. E., Camous, S. & Fulka, J., Jr. Nucleologenesis and the onset of transcription in the eight-cell bovine embryo: fine-structural autoradiographic study. *Molecular reproduction and development* **1**, 79-90, doi:10.1002/mrd.1080010202 (1989).

8 Tadros, W. & Lipshitz, H. D. The maternal-to-zygotic transition: a play in two acts. *Development* **136**, 3033-3042, doi:10.1242/dev.033183 (2009).

9 Sirard, M. A. Factors affecting oocyte and embryo transcriptomes. *Reprod Domest Anim* **47 Suppl 4**, 148-155, doi:10.1111/j.1439-0531.2012.02069.x (2012).

10 Graf, A. *et al.* Fine mapping of genome activation in bovine embryos by RNA sequencing. *Proceedings of the National Academy of Sciences of the United States of America* **111**, 4139-4144, doi:10.1073/pnas.1321569111 (2014).

11 Li, E. Chromatin modification and epigenetic reprogramming in mammalian development. *Nature reviews. Genetics* **3**, 662-673, doi:10.1038/nrg887 (2002).

12 Hemberger, M., Dean, W. & Reik, W. Epigenetic dynamics of stem cells and cell lineage commitment: digging Waddington's canal. *Nature reviews. Molecular cell biology* **10**, 526-537, doi:10.1038/nrm2727 (2009).

13 Fairburn, H. R., Young, L. E. & Hendrich, B. D. Epigenetic reprogramming: how now, cloned cow? *Current biology : CB* **12**, R68-70 (2002).

14 Kouzarides, T. Chromatin modifications and their function. *Cell* **128**, 693-705, doi:10.1016/j.cell.2007.02.005 (2007).

15 Bernstein, B. E., Meissner, A. & Lander, E. S. The mammalian epigenome. *Cell* **128**, 669-681, doi:10.1016/j.cell.2007.01.033 (2007).

16 Lepikhov, K. *et al.* Evidence for conserved DNA and histone H3 methylation reprogramming in mouse, bovine and rabbit zygotes. *Epigenetics & chromatin* **1**, 8, doi:10.1186/1756-8935-1-8 (2008).

17 Johnson, M. H. & Ziomek, C. A. The foundation of two distinct cell lineages within the mouse morula. *Cell* **24**, 71-80 (1981).

18 Watson, A. J. & Barcroft, L. C. Regulation of blastocyst formation. *Frontiers in bioscience : a journal and virtual library* **6**, D708-730 (2001).
19 Wang, H. & Dey, S. K. Roadmap to embryo implantation: clues from mouse models. *Nature reviews. Genetics* **7**, 185-199, doi:10.1038/nrg1808 (2006).
20 Ozawa, M. *et al.* Global gene expression of the inner cell mass and trophectoderm of the bovine blastocyst. *BMC Dev Biol* **12**, 33, doi:10.1186/1471-213X-12-33 (2012).
21 Nagatomo, H. *et al.* Transcriptional wiring for establishing cell lineage specification at the blastocyst stage in cattle. *Biol Reprod* **88**, 158, doi:10.1095/biolreprod.113.108993 (2013).
22 Sepulveda-Rincon, L. P. *et al.* Random Allocation of Blastomere Descendants to the Trophectoderm and ICM of the Bovine Blastocyst. *Biol Reprod* **95**, 123, doi:10.1095/biolreprod.116.141200 (2016).
23 Wei, Q., et al. . Bovine lineage specification revealed by single-cell gene expression analysis from zygote to blastocyst. *Biology of Reproduction* (2017).
24 Liu, S. & Trapnell, C. Single-cell transcriptome sequencing: recent advances and remaining challenges. *F1000Res* **5**, doi:10.12688/f1000research.7223.1 (2016).
25 Grun, D. & van Oudenaarden, A. Design and Analysis of Single-Cell Sequencing Experiments. *Cell* **163**, 799-810, doi:10.1016/j.cell.2015.10.039 (2015).
26 Kivioja, T. *et al.* Counting absolute numbers of molecules using unique molecular identifiers. *Nature methods* **9**, 72-74, doi:10.1038/nmeth.1778 (2011).
27 Soumillon, M., Cacchiarelli, D., Semrau, S., van Oudenaarden, A. & Mikkelsen, T. S. Characterization of directed differentiation by high-throughput single-cell RNA-Seq. *bioRxiv*, doi:10.1101/003236 (2014).
28 Ziegenhain, C. *et al.* Comparative Analysis of Single-Cell RNA Sequencing Methods. *Mol Cell* **65**, 631-643 e634, doi:10.1016/j.molcel.2017.01.023 (2017).
29 Vallejos, C. A., Risso, D., Scialdone, A., Dudoit, S. & Marioni, J. C. Normalizing single-cell RNA sequencing data: challenges and opportunities. *Nature methods* **14**, 565-571, doi:10.1038/nmeth.4292 (2017).
30 Dobin, A. *et al.* STAR: ultrafast universal RNA-seq aligner. *Bioinformatics (Oxford, England)* **29**, 15-21, doi:10.1093/bioinformatics/bts635 (2013).
31 Tung, P. Y. *et al.* Batch effects and the effective design of single-cell gene expression studies. *Scientific reports* **7**, 39921, doi:10.1038/srep39921 (2017).
32 Buettner, F. *et al.* Computational analysis of cell-to-cell heterogeneity in single-cell RNA-sequencing data reveals hidden subpopulations of cells. *Nature biotechnology* **33**, 155-160, doi:10.1038/nbt.3102 (2015).
33 McDavid, A., Finak, G. & Gottardo, R. The contribution of cell cycle to heterogeneity in single-cell RNA-seq data. *Nature biotechnology* **34**, 591-593, doi:10.1038/nbt.3498 (2016).
34 Kiselev, V. Y. *et al.* SC3: consensus clustering of single-cell RNA-seq data. *Nature methods* **14**, 483-486, doi:10.1038/nmeth.4236 (2017).
35 Tracy, C. A. & Widom, H. Level spacing distributions and the Bessel kernel. *Communications in Mathematical Physics* **161**, 289-309, doi:10.1007/BF02099779 (1994).
36 Andrews, T. S. & Hemberg, M. Modelling dropouts allows for unbiased identification of marker genes in scRNASeq experiments. *bioRxiv*, doi:10.1101/065094 (2016).

37 duVerle, D. A., Yotsukura, S., Nomura, S., Aburatani, H. & Tsuda, K. CellTree: an R/bioconductor package to infer the hierarchical structure of cell populations from single-cell RNA-seq data. *BMC bioinformatics* **17**, 363, doi:10.1186/s12859-016-1175-6 (2016).
38 Graf, A. *et al.* Genome activation in bovine embryos: review of the literature and new insights from RNA sequencing experiments. *Animal reproduction science* **149**, 46-58, doi:10.1016/j.anireprosci.2014.05.016 (2014).
39 Kim, J. K. & Marioni, J. C. Inferring the kinetics of stochastic gene expression from single-cell RNA-sequencing data. *Genome biology* **14**, R7, doi:10.1186/gb-2013-14-1-r7 (2013).
40 Kuijk, E. W. *et al.* Differences in early lineage segregation between mammals. *Developmental dynamics : an official publication of the American Association of Anatomists* **237**, 918-927, doi:10.1002/dvdy.21480 (2008).
41 Schiffmacher, A. T. & Keefer, C. L. CDX2 regulates multiple trophoblast genes in bovine trophectoderm CT-1 cells. *Molecular reproduction and development* **80**, 826-839, doi:10.1002/mrd.22212 (2013).
42 Berg, D. K. *et al.* Trophectoderm Lineage Determination in Cattle. *Developmental cell* **20**, 244-255, doi:10.1016/j.devcel.2011.01.003 (2011).
43 Negron-Perez, V. M., Zhang, Y. & Hansen, P. J. Single-cell gene expression of the bovine blastocyst. *Reproduction (Cambridge, England)* **154**, 627-644, doi:10.1530/rep-17-0345 (2017).
44 Simmet, K. *et al.* OCT4/POU5F1 is required for NANOG expression in bovine blastocysts. *Proceedings of the National Academy of Sciences of the United States of America*, doi:10.1073/pnas.1718833115 (2018).
45 Karantzali, E. *et al.* Sall1 regulates embryonic stem cell differentiation in association with nanog. *The Journal of biological chemistry* **286**, 1037-1045, doi:10.1074/jbc.M110.170050 (2011).
46 Knott, J. G. & Paul, S. Transcriptional regulators of the trophoblast lineage in mammals with hemochorial placentation. *Reproduction (Cambridge, England)* **148**, R121-136, doi:10.1530/rep-14-0072 (2014).
47 Biase, F. H., Cao, X. & Zhong, S. Cell fate inclination within 2-cell and 4-cell mouse embryos revealed by single-cell RNA sequencing. *Genome research* **24**, 1787-1796, doi:10.1101/gr.177725.114 (2014).
48 Hayashi, S. & Takeichi, M. Emerging roles of protocadherins: from self-avoidance to enhancement of motility. *Journal of cell science* **128**, 1455-1464, doi:10.1242/jcs.166306 (2015).